DEVELOPMENT OF A NOVEL OMEGA-6 FATTY ACID BASED TREATMENT STRATEGY FOR COLON CANCER BY KNOCKING DOWN DELTA-5-DESATURASE AND EXPLOITING HIGH COX-2 LEVELS IN CANCER CELLS/TUMORS

A Dissertation
Submitted to the Graduate Faculty
of the
North Dakota State University
of Agriculture and Applied Science

By

Yi Xu

In Partial Fulfillment of the Requirements
for the Degree of
DOCTOR OF PHILOSOPHY

Major Department:
Pharmaceutical Sciences

July 2017

Fargo, North Dakota

North Dakota State University
Graduate School

Title

DEVELOPMENT OF A NOVEL OMEGA-6 FATTY ACID BASED TREATMENT STRATEGY FOR COLON CANCER BY KNOCKING DOWN DELTA-5-DESATURASE AND EXPLOITING HIGH COX-2 LEVELS IN CANCER CELLS/TUMORS

By

Yi Xu

The Supervisory Committee certifies that this ***disquisition*** complies with North Dakota State University's regulations and meets the accepted standards for the degree of

DOCTOR OF PHILOSOPHY

SUPERVISORY COMMITTEE:

Dr. Steven Qian
Chair

Dr. Sanku Mallik

Dr. Estelle Leclerc

Dr. Katie Reindl

Approved:

09/15/2017
Date

Dr. Jagdish Singh
Department Chair

ABSTRACT

Colon cancer is the third most commonly diagnosed cancer in the world. Research showed that arachidonic acid, a downstream ω-6 fatty acid (ω-6), plays a role in colon cancer development by producing deleterious metabolites from its COX-2 catalyzed peroxidation. On the other hand, dihomo-γ-linolenic acid (DGLA), the immediate precursor of arachidonic acid, may represent an exceptional ω-6 associated with anti-cancer activities. However, the mechanism of DGLA's anti-cancer effect still remains unclear, and the rapid conversion of DGLA to arachidonic acid in human body by delta-5 desaturase (D5D) greatly restricts DGLA's availability. Recent work from Dr. Qian's group demonstrated that DGLA can undergo a unique pathway during COX-2-catalyzed peroxidation and produce distinct free radical byproducts. Here we proposed that (1) DGLA's anti-cancer activity is derived from its distinct byproduct, *e.g.*, 8-hydroxyoctanoic acid (8-HOA), from COX-2-catalyzed peroxidation, and (2) by knocking down cellular D5D expression, we can take advantage of the commonly overexpressed COX-2 in cancer cells to promote 8-HOA formation, inhibit colon cancer growth and migration, and develop a novel cancer therapy and a paradigm shift concept in contrast to classic COX-2 inhibition strategy in cancer treatment. Our results showed that 8-HOA, at physiological concentrations, could suppress human colon cancer cell growth and migration, by serving as a histone deacetylase inhibitor and DNA damage agents. Data also showed that knocking down D5D in colon cancer cells promoted endogenous formation of 8-HOA to a threshold level which then inhibited cancer cell growth and migration. Consistent with the *in vitro* data, knocking down D5D in human colon cancer cell-derived mice xenograft tumors along with DGLA supplementation promoted endogenous formation of 8-HOA *in vivo* and significantly suppressed tumor growth. In addition, direct supplementation and endogenous formation of 8-HOA from COX-2 catalyzed DGLA peroxidation were found to enhance the

efficacies of various chemotherapeutic drugs. In conclusion, we demonstrated that by taking advantage of commonly overexpressed COX-2 in cancer, D5D knockdown can promote the formation of 8-HOA from DGLA peroxidation to inhibit cancer growth and migration. Results from this work will lead us to develop a novel ω-6 based treatment strategy for colon cancer.

ACKNOWLEDGMENTS

It is a great pleasure to acknowledge my deepest gratitude to my Ph.D. supervisor, Dr. Steven Qian, who is a role model for me. He helped me a lot throughout the whole time since I joined his group, both in my research and personal life. He inspired me with his enthusiasm and immense knowledge, otherwise I couldn't have made it this far. Dr. Qian also provided encouragement and a lot of excellent advice during my thesis-writing. He is the reason that I would like to continue my research in this area.

I would like to express my sincere thanks to the members of my advisor committee, Dr. Sanku Mallik, Dr. Estelle Leclerc and Dr. Katie Reindl for their guidance during my Ph.D. work. With them in my advisor committee, I feel confident as I can always look for their help and advice no matter what difficulty I have to face.

I am grateful to Dr. Jagdish Singh for providing me with the opportunity to work in the wonderful department. I would like to thank Janet Krom, Jean Trautmann and Diana Kowalski, the secretaries in Department of Pharmaceutical Sciences, for assisting my daily work in many different ways. I am indebted to the whole department of Pharmaceutical Sciences for providing a caring, stimulating and fun environment in which I can learn and grow. I also want to thank my labmates and people who helped me with my experiments, Xiaoyu Yang, Lizhi Pang, Drs. Yan Gu and Qi Jin.

I would like to thank my friends for all their support, encouragement, and caring, they helped me get through the difficult times.

Lastly and most importantly, I wish to thank my parents, who bore me, raised me, supported me, and loved me. To them I dedicate this thesis.

TABLE OF CONTENTS

LIST OF TABLES

LIST OF FIGURES

LIST OF SCHEMES

LIST OF ABBREVIATIONS

AA	Arachidonic acid
AcH3	Acetyl histone H3
ALA	α-linolenic acid
APS	Ammonium persulfate
COX	Cyclooxygenase
DGLA	Dihomo-γ-linolenic acid
DHA	Docosahexaenoic acid
D5D	Delta-5 desaturase
D5D-*KD*	D5D-knockdown
D6D	Delta-6 desaturase
EPA	Eicosapentaenoic acid
ESR	Electron spin resonance
FBS	Fetal bovine serum
GC	Gas chromatography
GLA	Gamma-linolenic acid
HDAC	Histone deacetylase
HEX	1-hexanol
HPLC	High performance liquid chromotograpghy
HTA	Heptanoic acid
LA	Linoleic acid
MMP	Matrix metalloproteinase
MS	Mass spectrometry
MTS	[3-(4,5-dimethylthiazol-2-yl)-5-(3- carboxy methoxyphenyl)-2-(4-sulfophenyl)-2H-tetrazolium inner salt

Nc-si.....Non target negative siRNA transfected cells

Omega-3 (ω-3).....ω-3 polyunsaturated fatty acid

Omega-6 (ω-6).....ω-6 polyunsaturated fatty acid

PBS .....Phosphate buffered saline

PFB-Br.....Pentafluorobenzyl bromide

PGE1.....Prostaglandin E1

PGE2.....Prostaglandin E2

PI.....Propidium iodide

PUFA .....Polyunsaturated fatty acid

SDS .....Sodium dodecyl sulfate

TBS .....Tris buffered saline

TEMED.....Tetramethylethylenediamine

wt.....Wild type

5-FU 5-fluorouracil

8-HOA.....8-hydroxyoctanoic acid

1. INTRODUCTION

Colon cancer is the third most commonly diagnosed cancer in the world and the second leading cause of cancer deaths in United States [1]. A large body of evidence suggested that there is a substantial association between dietary fatty acid consumption and colon cancer incidence [2-11]. For instance, research showed that consumption of ω-3 fatty acids (ω-3s), such as docosahexaenoic acid (DHA) and eicosapentaenoic acid (EPA), which are mainly found in marine food products, may suppress colon cancer development, and also reverse drug resistance in cancer cells [3-7, 10]. On the other hand, arachidonic acid (AA), a downstream ω-6 fatty acid, could produce deleterious metabolites (*e.g.*, prostaglandin E2, PGE2) from cyclooxygenase-2 (COX-2) catalyzed peroxidation and play a role in colon cancer development [8-9, 11-18]. Given these observations, ω-3s have been extensively investigated for their anti-cancer activities, whereas ω-6s received much less research attention although they are the much more abundant in our daily food compared to ω-3s.

Recently, increasing evidence suggested that the immediate precursor of AA, *i.e.* dihomo-γ-linolenic acid (DGLA), may represent an exceptional ω-6 which was reported to associate with anti-proliferative activities against various types of cancer cells [19-24]. Therefore, considering the abundance of ω-6 fatty acids in our daily food, DGLA might be a promising dietary source for cancer prevention and treatment. However, the molecular mechanism of DGLA's anti-cancer activities has not been understood until the present study. In addition, the rapid conversion of DGLA to AA in the human body by delta-5-desaturase (D5D) greatly restricts DGLA's availability and activity.

Cyclooxygenase-2 is overexpressed in 85% of adenocarcinomas, and, it can promote colon cancer progression by catalyzing AA peroxidation to produce the deleterious metabolite PGE2

[25-28]. Therefore, COX-2 inhibition, which aims at limiting the COX-2/AA pathway, has been extensively studied as a conventional strategy for the treatment of cancers [29-30]. However, COX-2 can be induced rapidly in the cancer environment even with the presence of COX-2 inhibitors, which raises the question about the therapeutic efficacy from COX-2 inhibitors in cancer patients [31]. In addition, COX-2 inhibitors were found to induce GI injury and cardiovascular side effects in patients [30, 32-34]. Therefore, alternative treatment strategy targeting COX-2 peroxidation in colon cancer with safer and better therapeutic outcomes are urgently needed.

In the presenting study, for the first time, we discovered that, through COX-2 catalyzed peroxidation, DGLA can produce a distinct byproduct, 8-HOA, which serves as an HDAC inhibitor and inhibits colon cancer growth and migration. Based on this novel finding, we proposed and demonstrated that instead of inhibiting COX-2, we can take advantage of the high COX-2 expression in cancer cells to promote the formation of DGLA's beneficial byproduct 8-HOA to inhibit cancer cell growth and migration. This novel strategy will lead to a better therapeutic effect in colon cancer treatment due to its dual anti-cancer mechanisms, *i.e.* simultaneously promoting the anti-cancer effect from DGLA and limiting the pro-cancer effect from AA. Our strategy will also have fewer side effects *vs.* classic COX-2 inhibitors as normal tissues have less COX-2 expression and a lower fatty acids intake rate compared to cancer cells [25-28, 35]. In addition, our proposed strategy of making use the hallmark of cancer cell (*i.e.* the commonly overexpressed COX-2) to work against cancer cell itself would provide a novel insight into cancer therapy and challenge the current paradigm of COX-2 inhibition strategy in cancer treatment. Results from this study will lay down the foundation for further development of a ω-6 fatty acids-based diet care strategy for colon cancer prevention and treatment.

1.1. Polyunsaturated Fatty Acids

1.1.1. Polyunsaturated fatty acids: ω-6s *vs.* ω-3s

Polyunsaturated fatty acids (PUFAs) are fatty acids that contain more than one C=C double bonds in their backbone [36]. There are two important classes of dietary PUFAs, namely ω-6s and ω-3s, which are essential cellular components and possess diverse bioactivities in the human body [37-38]. These two types of PUFAs are classified according to the position of the first C=C double bond in their backbone. For example, ω-6 fatty acids, including linoleic acid (LA), gamma-linolenic acid (GLA), DGLA and AA, have their first double bond at the sixth carbon atom (ω-6 carbon) from the end of the carbon chain (**Scheme 1**). ω-3 fatty acids, on the other hand, have their first C=C double bond at the third carbon atom (ω-3 carbon) from the methyl end of the carbon chain (Scheme 1). The common ω-3s includes α-linolenic acid (ALA), EPA and DHA, *etc*.

ω-6s and ω-3s are important cellular components and are indispensable to maintain normal cellular functions [39-41]. However, the human body cannot synthesize them *de novo* due to a lack of the enzyme needed to introduce double bonds into fatty acids beyond carbons 9 and 10 from the carboxyl end [42]. Therefore, ω-6s and ω-3s are considered essential fatty acids which must be obtained from our daily diet. The dietary source varies for different ω-6s and ω-3s. For example, LA is the precursor and main source for ω-6s, it is widely present in vegetable oils including sunflower, safflower, corn and soybean oil [43]. GLA can be found in evening primrose oil, borage oil, black currant oil, and hemp seed oil [44]. A small amount of AA can be obtained from meat and egg yolks [45].

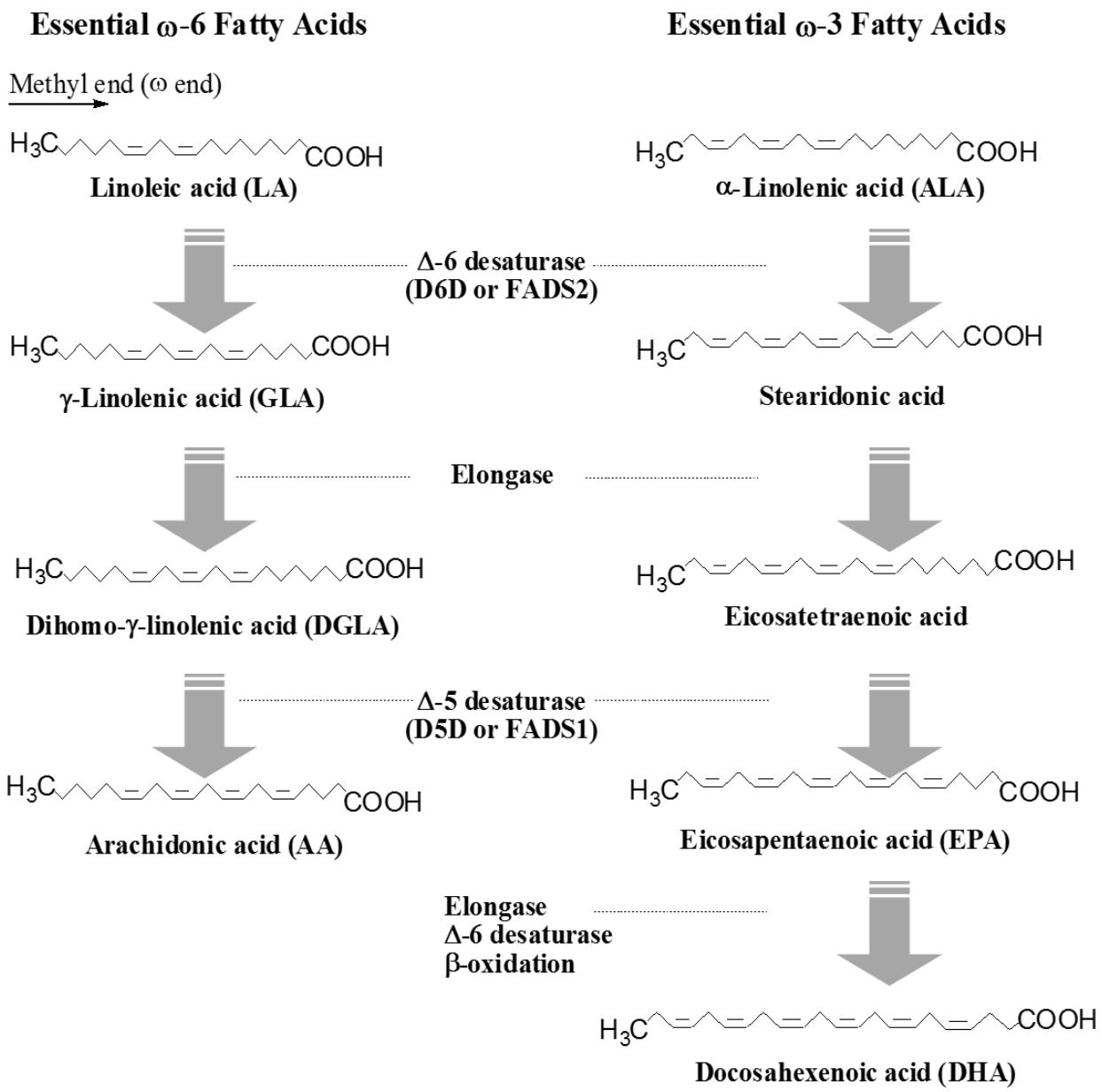

Scheme 1. Essential ω-6 and ω-3 fatty acids in the human body.
Upon uptake into the human body, LA and ALA, the parent ω-6 and ω-3 fatty acids, respectively, are converted to their corresponding downstream fatty acids under the catalysis of a series of fatty acid metabolism enzymes including delta-6 desaturase, elongase and delta-5 desaturase. Note, the ω-6 and ω-3 are not interconvertible in human bodies.

ALA is the parent fatty acid for the ω-3 family, and it is present in canola oil, perilla oil, flaxseed oil and walnuts [43]. EPA and DHA are mostly found in the oil from deep, cold water fish [56-57]. In the typical western diet, the ratio of daily intake of ω-6 to ω-3 is around 10:1 to 30:1 [48-51].

Although they cannot be synthesized *de novo*, the downstream ω-6s and ω-3s can be produced in the human body from their corresponding parent fatty acids, *i.e.* LA and ALA, respectively [52-56]. For instance, upon uptake into the human body, LA, the precursor of ω-6s, will be converted to GLA by delta-6 desaturase (D6D, also known as fatty acid desaturase 2 or FADS2) which introduces a new C=C double bond to the structure (Scheme 1). GLA will then be converted into DGLA by elongase which adds two additional carbon atoms. DGLA is further metabolized to arachidonic acid by delta-5 desaturase (also known as fatty acid desaturase 1 or FADS1) which adds another C=C double bond. In fact, the ω-6s in human tissues are mainly derived from dietary LA. Similarly, upon consumption, ALA, the precursor of ω-3s, can be metabolized *via* elongase, delta-6-desaturase and delta-5-desaturase to produce various downstream PUFAs including EPA and DHA (Scheme 1). However, the conversion of ALA to EPA and DHA is very limited, for example, only ~20% of dietary ALA is converted to EPA and less than 10% is converted to DHA in females, while only ~8% of ALA is converted to EPA and no conversion to DHA in males [54-56]. In addition, the conversion rate from ALA to EPA and DHA could be further reduced when ALA is consumed along with ω-6s, as they will compete for the same sets of fatty acids metabolizing enzymes.

1.1.2. Polyunsaturated fatty acids and human health

ω-6s and ω-3s possess diverse bioactivities and are both essential to maintain normal cellular functions [39-41]. For example, PUFAs can be incorporated into cell membranes and become important structural cellular components. Research showed that the fatty acids composition in the membrane lipid bilayers is critical for membrane fluidity, flexibility and normal function of membrane-bound enzymes [40-41, 57-63]. Animal studies indicated that the high level of DHA in the retina plays an important role in the normal development and function of the retina [64-65]. DHA and AA are involved in normal neurogenesis, neurotransmitter metabolism, and learning function [66-67]. In addition, ω-6s and ω-3s were also found to regulate gene expression by interacting with various transcription factors [68-69].

Besides directly exerting biological effects, the ω-6s and ω-3s in cells can also undergo enzymatic or non-enzymatic lipid peroxidation to produce various bioactive metabolites. For instance, through the actions of cyclooxygenase, lipoxygenase or cytochrome P450s, fatty acids such as DGLA, AA, EPA and DHA can be metabolized to produce various lipid-derived signaling molecules, including prostaglandins (PGs), prostacyclins, thromboxanes, leukotrienes, hydroxyeicosatetraenoic acids and epoxy eicosatrienoic acids, *etc* [70-73]. These lipid-derived metabolites act in an autocrine or paracrine manner to deliver diverse bioactivities in regulating platelet aggregation, blood vessel permeability, dilation and constriction, as well as modulating cell adhesion and chemotaxis [70-73]. Alternatively, fatty acids can also go through non-enzymatic lipid peroxidation to produce isoprostanes, isoleukotrienes, and other peroxidized fatty acid products which may also function as inflammatory mediators [74].

Although dietary intake of ω-3s and ω-6s are both essential for maintaining normal cellular functions, ω-3s and ω-6s supplementation could lead to contrasting biological consequences in the

human body. In general, it is widely accepted that ω-3s supplementation may result in many beneficial effects on human health, while arachidonic acid (a downstream ω-6) is associated with a deleterious outcome [2-11, 75-88]. For example, supplementation of ω-3s, especially EPA and DHA, has been shown to prevent incidence of cardiovascular disease, ameliorate the symptoms of chronic inflammation, improve cognitive function, and prevent cancer incidence [2-11, 75-86]. On the other hand, a large body of cellular, animal and epidemiological studies have suggested that the increased cellular level of arachidonic acid, mediated *via* its COX-catalyzed peroxidation, is associated with an increase in the incidence of diseases involving inflammatory processes, such as cardiovascular diseases, rheumatoid arthritis, inflammatory bowel diseases, and colon cancer [5, 8-9, 11, 86-88]. Given these facts, the bioactivities from ω-3s have been extensively studied for health improvement purposes, whereas the potential beneficial effects from ω-6s have received much less research attention.

1.2. COX-2 Catalyzed Fatty Acid Peroxidation and Its Association with Colon Cancer

After directly obtained from food or released from membrane phospholipids, ω-3 and ω-6 PUFAs will undergo enzymatic or non-enzymatic lipid peroxidation to produce various important lipid-derived signaling molecules with diverse bioactivities [70-73]. COX is one of the major lipid peroxidizing enzymes that metabolizes PUFAs such as AA and DGLA to produce prostaglandins (**Scheme 2**), which can be further converted to prostacyclins and thromboxane [70-73]. COX is a bi-functional enzyme containing a cyclooxygenase site and a peroxidase site, thus it metabolizes fatty acids by two reactions, *e.g.* its cyclooxygenase activity incorporates two oxygen molecules into fatty acids, and its peroxidase activity reduces them to their corresponding alcohol [89-91].

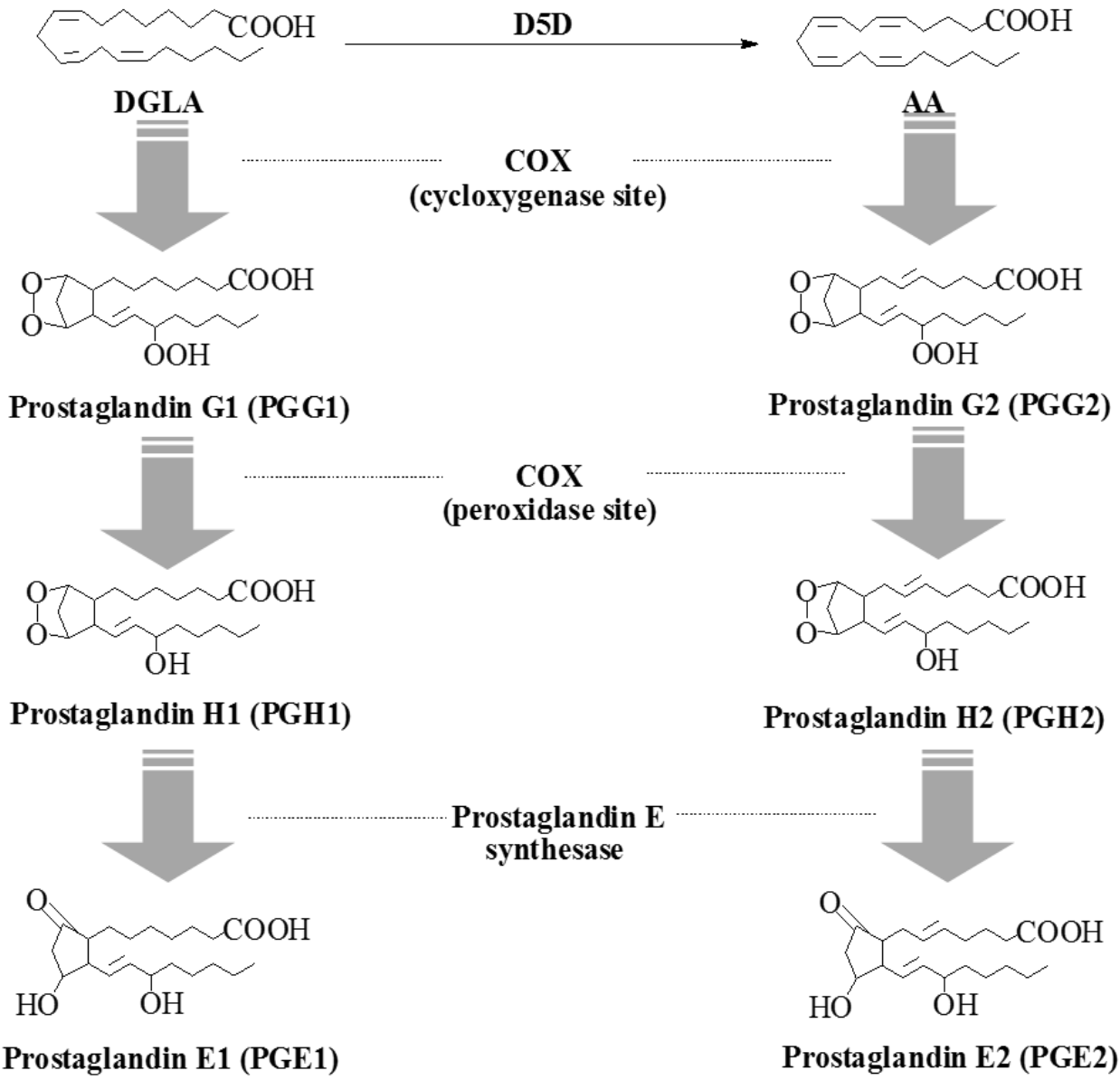

Scheme 2. COX catalyzed DGLA and AA peroxidation.
Mediated by the cyclooxygenase and peroxidase activities, COX metabolizes DGLA and AA to produce PGH1 and PGH2, respectively, which can be further converted to prostaglandin E1 and E2 (major bioactive metabolites from DGLA and AA), as well as various other products including 1 and 2 series prostaglandin D, prostaglandin F, prostacyclins and thromboxanes by corresponding enzymes.

There are two isoforms of COX, *i.e.* COX-1, the constitutive form which is expressed in most tissues, and COX-2, the inducible form that can be readily induced in response to various stimuli including stresses, cytokines, growth factors, pro-inflammatory signals as well as cancer promoters [91-94]. COX-1 and COX-2 contain 576 and 587 amino acids, respectively [95-97]. They are membrane bound proteins and located on the lumenal surfaces of the endoplasmic reticulum and nuclear membranes. The three-dimensional structures of both isoforms are nearly superimposable, both of them are homodimers with each subunit of the dimer consisting of three domains, *e.g*. the epidermal growth factor domain, the membrane binding domain and the catalytic domain [90-93]. COX-1 and COX-2 are encoded by different genes, and there is 60%-65% sequence identity between COX-1 and 2 from the same species and 85%-90% identity among individual isoforms from different mammalian species [94, 98]. COX-1 play a housekeeping role in normal physiological processes by providing immediate, pulsatile prostaglandins formation in various organs [99], while COX-2 is rapidly induced under pathological conditions and metabolizes PUFAs to produce lipid-derived molecules to mediate the inflammatory process.

It has been well established that COX-2-catalyzed arachidonic acid peroxidation is the major mechanism by which ω-6s are implicated in the carcinogenic process. Evidence showed that COX-2 is overexpressed in ~50% of human adenomas and ~85% of adenocarcinomas relative to normal mucosa, and is associated with worse survival among colon cancer patients [25-28]. It has also been commonly observed that the levels of PGE2 (the major metabolite from COX-2-catalyzed arachidonic acid peroxidation) as well as PGE2 receptors are elevated in colorectal cancers [100-103]. These observations suggested an association between the COX-2-catalyzed arachidonic acid signaling pathway and colorectal carcinogenesis. In fact, research showed that PGE2 can promote colon cancer cell survival and intestinal adenoma formation by indirectly

transactivating PPAR δ receptor through phosphoinositide 3-kinase and protein kinase B (PI3k/Akt) signaling [104]. PGE2 stimulation also led to the stabilization and nuclear translocation of β-catenin, thereby stimulating β-catenin-dependent gene expression and the aberrant growth of colon cancer cells [105-108]. In addition, PGE2, as a major pro-inflammatory mediator, plays an important role in chronic inflammation, while long term inflammatory bowel diseases, such as ulcerative colitis and Crohn's disease, are major risk factors for developing colon cancer [109-111].

Considering the implication of COX-2 catalyzed AA peroxidation in cancer, the COX enzymes have been studied extensively as a drug target in cancer treatment as well as in other inflammation-related diseases for over 100 years [112-115]. More recently, many selective COX-2 inhibitors have been developed and tested for clinical use, including celecoxib, etoricoxib and rofecoxib, *etc*, which are collectively known as non-steroidal anti-inflammatory drugs or NSAIDs [116-122].

COX-2 inhibitors have been widely tested and applied as adjuvant agents in combination with front-line chemo-therapy drugs for treatment of colon cancer [120-122]. However, COX-2 can be induced rapidly in the cancer environment even with the presence of COX-2 inhibitors, which raises the question about the therapeutic efficacy from COX-2 inhibitors in cancer patients [31]. In addition, it has been documented that COX-2 inhibitors can cause critical safety issues, including severe gastrointestinal tract injury and increased risk of cardiovascular diseases (*e.g.*, heart attacks and strokes), probably due to the impairment of the normal function of COX [30, 32-34]. Therefore, developing an alternative treatment strategy for colon cancer with safer and better therapeutic outcome is an urgent need.

1.3. Potential Anti-Cancer Activity from DGLA and Its COX-2 Mediated Byproducts

1.3.1. DGLA, an exceptional ω-6 fatty acid associated with potential anti-cancer activities

While arachidonic acid is associated with cancer incidence mainly due to its peroxidation by COX-2, DGLA, the immediate precursor of arachidonic acid, may represent an exceptional ω-6 by virtue of its potential anti-inflammatory and anti-cancer effects [19-24, 123-124]. For instance, dietary DGLA supplementation prevented atherosclerosis in ApoE-deficient mice, but this anti-atherosclerotic effect was attenuated by a COX inhibitor naproxen [123-124]. DGLA exerted cytotoxicity towards human cervical carcinoma cells *in vitro* and enhanced the susceptibility of cancer cells to chemo-drug, probably by improving drug uptake and reducing drug efflux [19, 22, 24]. In rats with 7, 12-dimethylbenz(α) anthracene-induced mammary tumors, the ratio of tumor-bearing rats to total number of rats was lowest in the DGLA treatment group compared to groups treated with GLA and corn oil [20]. More importantly, DGLA supplementation induced apoptosis in tumor cells associated with significant increase of free radicals and lipid peroxide formation, suggesting that DGLA-derived free radicals and lipid peroxides may be responsible for its anti-tumorigenic effect [19, 22, 24]. Further study showed that the COX inhibitor indomethacin as well as various anti-oxidants blocked the tumoricidal action of DGLA on human cervical carcinoma cells [22, 24]. This evidence together suggested that DGLA might represent an exceptional ω-6s with anti-cancer activity, and the free radical species generated from COX-2 catalyzed DGLA peroxidation may play a role in the anti-cancer effect of DGLA. However, the molecular mechanism of DGLA derived anti-cancer activities has not been understood until the present study.

1.3.2. Identification of distinct free radical byproducts produced from COX-2 catalyzed DGLA peroxidation

COX-2-catalyzed fatty acid peroxidation is a well-known free radical chain reaction during which a variety of free radical intermediates are produced [125-128]. Initially, the tyrosyl radical in the COX enzyme is activated and abstracts H at the bis-allylic methylene position of a lipid molecule, which leads to the formation of a carbon-centered lipid radical. The lipid radical will then react with O_2 to form peroxyl radical, which can further attack other lipid molecules during the propagation process. The peroxyl radical can also be converted into other types of free radicals through Fenton-type reactions and β-scission [127-128]. Identification of these highly reactive free radical intermediates may advance our understanding of the biological implications of PUFAs in many diseases, especially in the inflammatory disorders and cancer. However, due to their extremely short half-life, these free radical intermediates were not characterized until recent work from Dr. Qian's group [129-134].

Previous work from Dr. Qian's group developed and refined a novel HPLC/ESR (spin-trapping)/MS combined technique, in which spin-trapped free radicals with different structures are separated by an HPLC column according to their distinct chromatographic behavior, followed by ESR monitoring for radical confirmation and MS detection for structural identification [135]. This novel technique enabled us to successfully identify and characterize both common and exclusive free radical byproducts from COX-2 catalyzed DGLA and arachidonic acid peroxidation [136-138]. Dr. Qian's research demonstrated that, due to the common structural moiety in arachidonic acid and DGLA, COX-2 can catalyze their peroxidation through the same C-15 oxygenation pathway to form two common C=C centered free radical metabolites (**Scheme 3**). These free radicals are converted to their corresponding stable forms in a cellular reducing environment, *i.e.*

pentane and 1-hexanol (HEX), which accumulate overtime [136-138]. On the other hand, the different structural moiety in DGLA leads to a unique C-8 oxygenation and consequently the formation of two distinct free radical derived byproducts, *i.e.* heptanoic acid (HTA) and 8-hydroxyoctanoic acid (8-HOA, **Scheme 4**) [136-138].

Inspired by these novel findings, we proposed that the distinct free radical pathway and byproducts, *i.e.* 8-HOA, from COX peroxidation may be responsible for DGLA's anti-cancer activity. Therefore, in the present study, we investigated the potential anti-cancer effect from DGLA's free radical byproducts as well as possible molecular mechanisms. The study is expected to provide the first detailed data of the biological effects from COX-2-mediated free radical byproducts in colon cancer. The outcome of our study will allow us to manipulate ω-6 peroxidation to promote the anti-cancer benefits from DGLA for colon cancer treatment.

We proposed that DGLA's anti-cancer activity may be derived from its COX-2 peroxidation, which leads to a possibility that instead of inhibiting COX-2, one can take advantage of the high COX-2 expression in cancer cells to promote formation of 8-HOA to control cancer cell growth. As COX-2 is commonly overexpressed in colon cancers, our innovative idea of using a cancer cell hallmark to work against a cancer cell itself may provide a novel insight into cancer therapy, and challenge the classic paradigm of COX-2 inhibition strategy in cancer treatment.

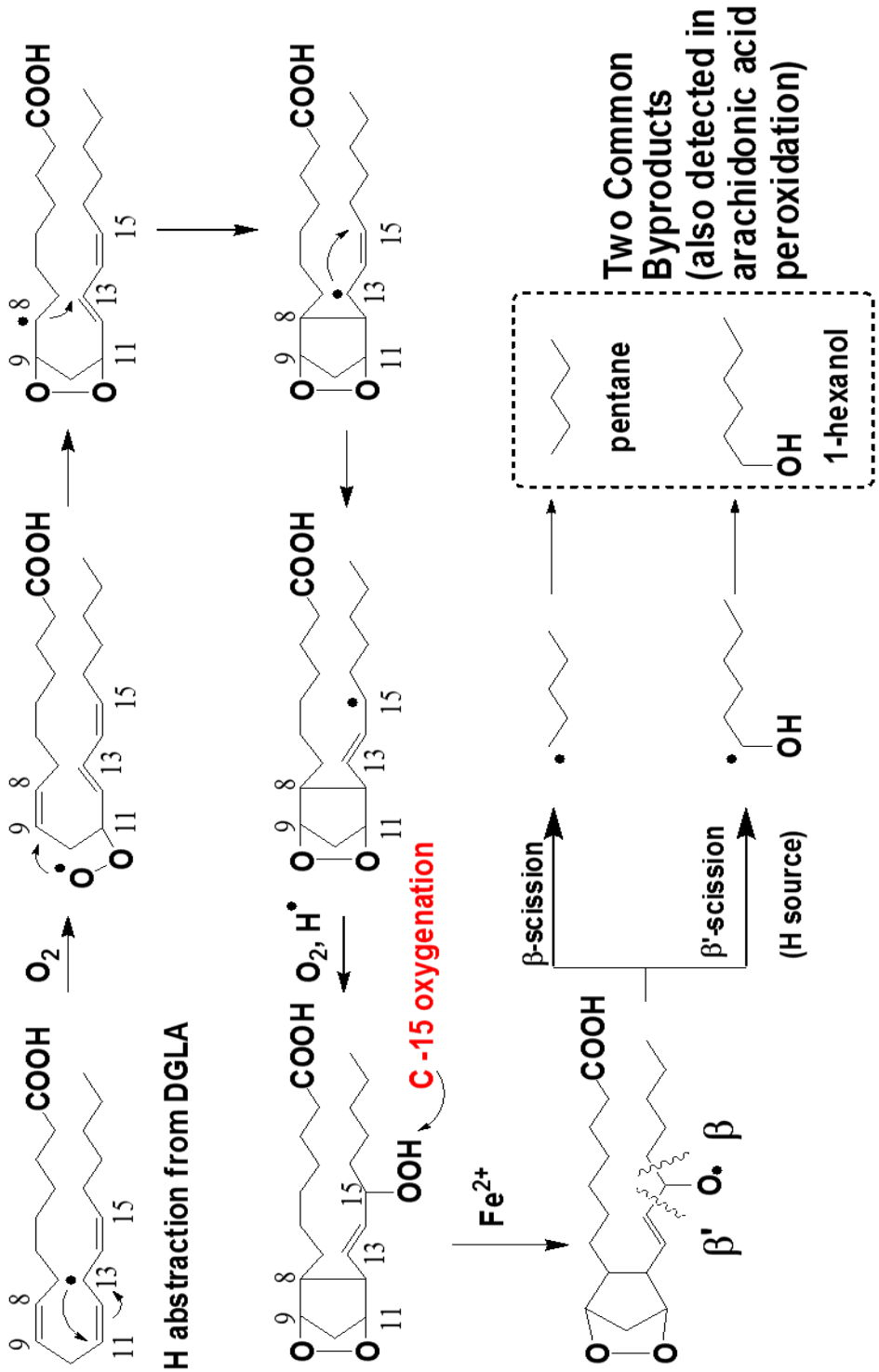

Scheme 3. Pathway of COX-2 catalyzed DGLA C-15 peroxidation.
Due to the common structural moiety in arachidonic acid and DGLA, both of them can go through the same C-15 oxygenation pathway and produce two common free radical byproducts, *e.g.* pentane and 1-hexanol [136-138].

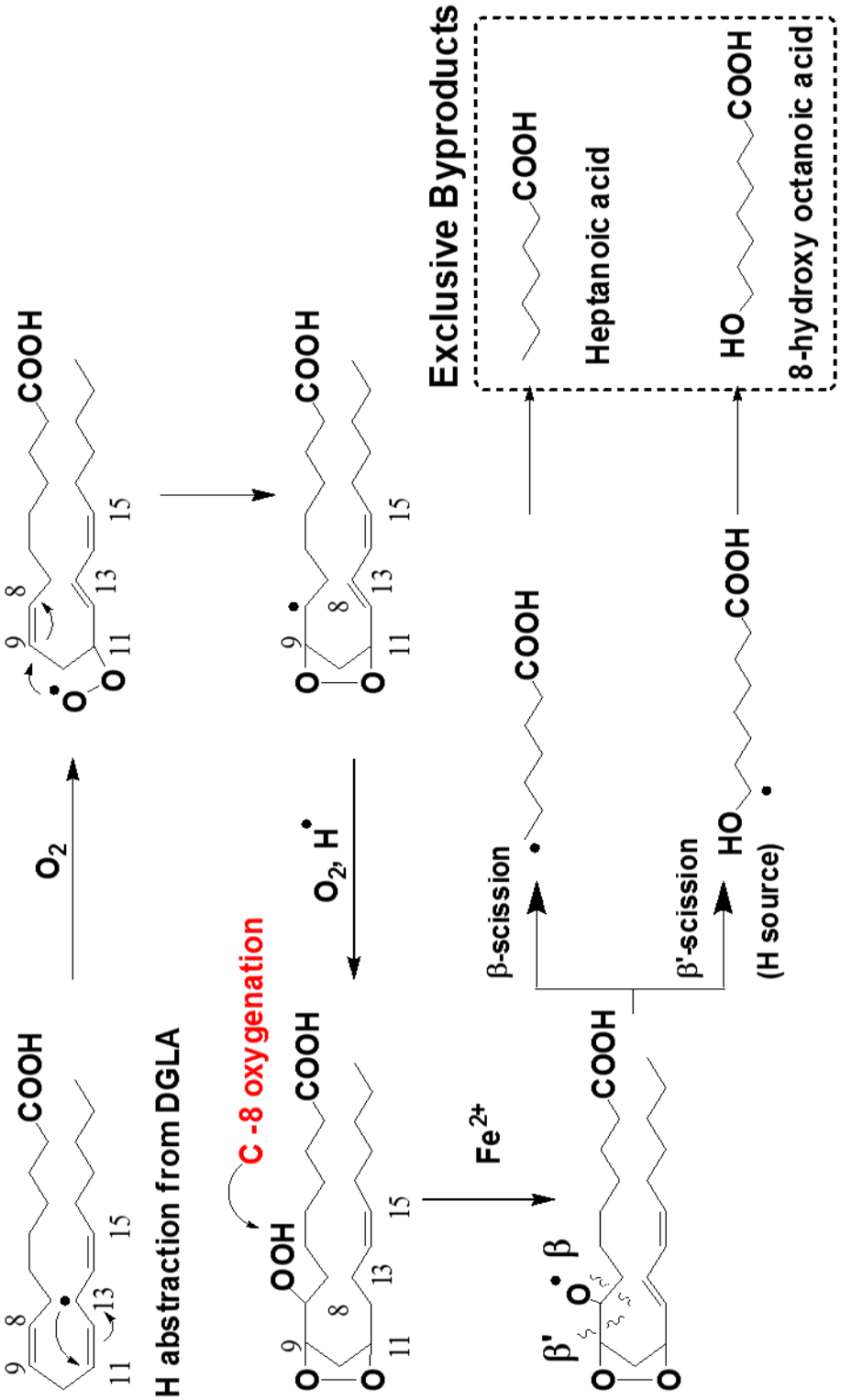

Scheme 4. Pathway of COX-2 catalyzed DGLA C-8 peroxidation.
The different structural moiety in DGLA leads to a unique C-8 oxygenation and consequently the formation of distinct free radical byproducts, *e.g.* heptanoic acid and 8-hydroxyoctanoic acid [136-138].

1.4. D5D Represents a Novel Target for Colon Cancer Treatment

DGLA is associated with potential anti-cancer activity, however, the rapid conversion of DGLA to AA in human body by D5D greatly restricts DGLA's availability and activity [139-148]. For example, it was reported that dietary supplementation of DGLA as ethyl esters or triglycerides leads to only a small increase in DGLA content in cell membrane lipids, while accompanied by a very significant increase in AA content [139]. Other *in vitro* and *in vivo* studies also showed that even after enrichment with DGLA, the cellular content of AA was still 2.5 to 3 fold higher than DGLA due to effective desaturation of DGLA [139-141].

Therefore, inhibiting D5D will be an effective way to limit the conversion of DGLA to AA and promote potential anti-cancer effect from DGLA's distinct byproducts (*e.g.* 8-HOA). In fact, some natural and synthesized compounds such as sesame, curcumin and CP-24879 have been reported to own certain inhibitory effect against D5D activity [139, 149-153]. For exampl curcumin inhibited rat liver microsomal delta-5 and delta-6 desaturases, and led to a 2 fold increase of mycelial DGLA levels in fungus with a concomitant decrease in AA levels [150]. Results obtained in experiments with both a cell-free extract of the fungus and with rat liver microsomes demonstrated that (+)-sesamin specifically inhibits D5D at low concentrations, resulting in increased DGLA content [151]. CP-24879, a mixed D6D/D5D inhibitor, was shown to increase cellular DGLA content in cultured lung carcinoma cells and decrease AA content both *in vitro* and *in vivo* [139, 152-153].

Although D5D inhibition was studied to modify the ratio between DGLA and AA (as well as their corresponding metabolites), D5D was not investigated specifically related to any major diseases including cancer. In this study, we proposed that D5D is a novel drug target for colon

cancer treatment, and we aimed to genetically knockdown D5D to reserve more DGLA, thereby promoting the formation of 8-HOA to deliver its potential anti-cancer effect.

1.5. Summary of Research Aims in Present Study

DGLA is an exceptional ω-6 fatty acid associated with potential anti-inflammation and anti-cancer activities, thus it may represent a promising dietary source for cancer prevention and therapy especially considering the abundance of ω-6 fatty acids in our daily food. However, the molecular mechanisms of DGLA's anti-cancer activities have not been clarified until our present study. DGLA's availability and activity is greatly restricted due to the rapid conversion of DGLA to arachidonic acid in human body by D5D. We hypothesized that the anti-cancer activity of DGLA may be derived from its distinct byproduct 8-HOA formed during the COX-2 catalyzed peroxidation, and inhibition of cellular D5D activity/expression could promote formation of 8-HOA which consequently exert anti-cancer effect. More importantly, instead of inhibiting COX-2 expression in cancer cells, we plan to take advantage of the high COX-2 expression levels in colon cancer cells and tumors to promote DGLA peroxidation and therefore its associated anti-cancer activity, which may challenge the current paradigm of COX biology in cancer treatment.

To test these hypotheses, in this study, we aimed to (1) investigate the potential anti-cancer effect of DGLA's byproducts in colon cancer as well as the underlying molecular mechanisms; and (2) genetically knockdown cellular D5D expression to limit the conversion of DGLA and promote the formation of DGLA's beneficial byproducts for delivering anti-cancer effect (**Scheme 5**). We believe our novel strategy will result in a dual mechanism for inhibiting cancer growth, *i.e.* promoting the anti-cancer effects from DGLA while limiting the pro-cancer effect from AA, which will lead to a better and safer therapeutic effect in colon cancer treatment compared to the traditional COX-2 inhibition strategy.

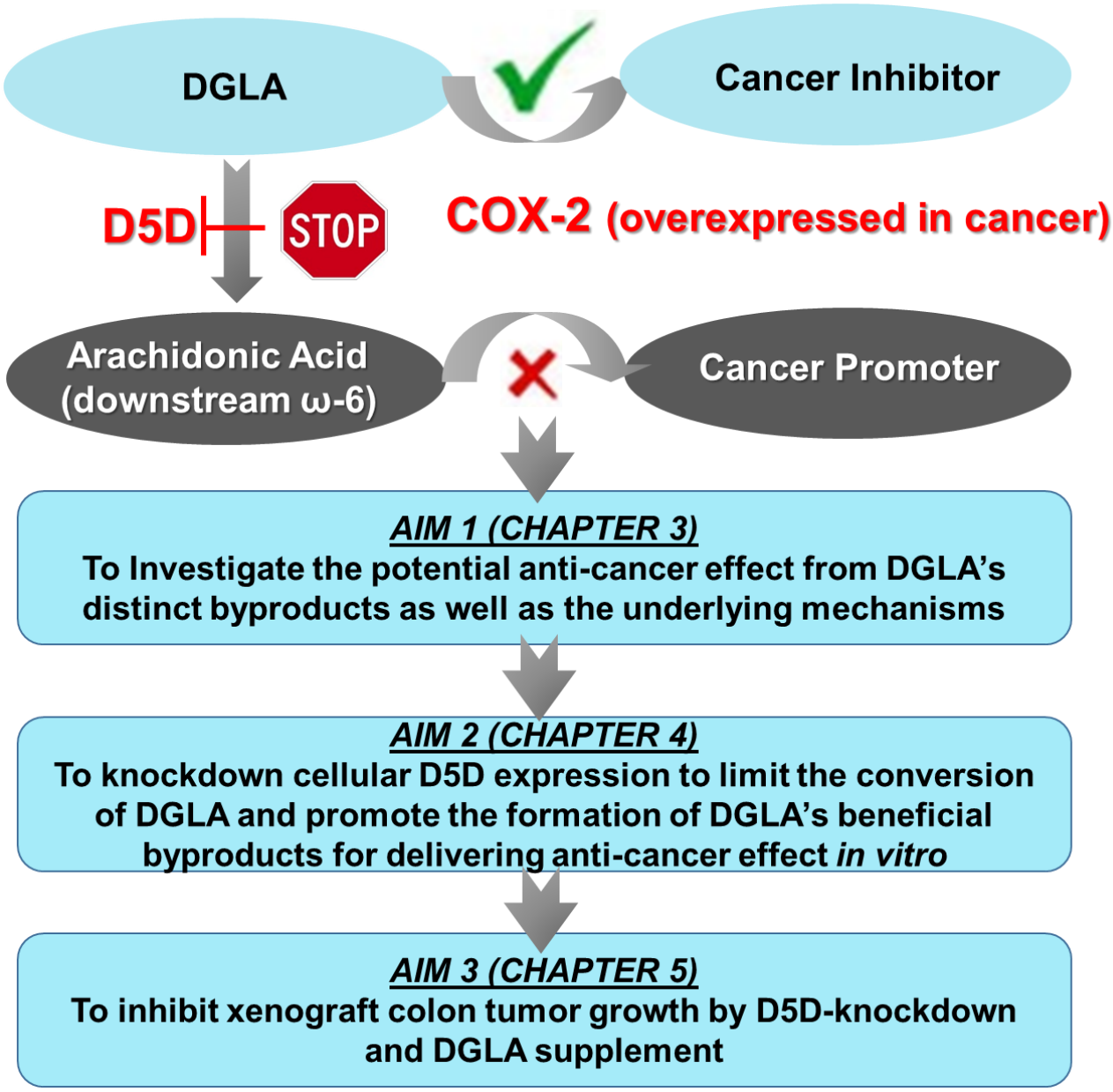

Scheme 5. Research outline in present study.

We hypothesized that the anti-cancer activity of DGLA may be derived from its COX-2 catalyzed peroxidation, therefore, in this study we aimed to investigate the potential anti-cancer effects of DGLA's distinct byproducts in colon cancer as well as the underlying molecular mechanisms. We also planned to genetically knockdown D5D expression and take advantage of the high COX-2 expression levels in colon cancer to promote the formation of DGLA's beneficial byproducts for delivering anti-cancer effects *in vitro* and *in vivo*.

2. METHODS AND MATERIALS

2.1. Chemicals and Reagents

Chemicals and materials: Pure DGLA for *in vitro* cell treatment was obtained from Nu-Chek-Prep (MN, USA). Analytical standard solution of AA, DGLA, PGE1, PGE2, AA-d_8, DGLA-d_6, PGE1-d_4 and PGE2-d_9 as well as DGLA ethyl ester for animal treatment were purchased from Cayman Chemical (MI, USA). 8-HOA and 5-FU were acquired from Sigma-Aldrich (MO, USA). Crystal violet, pentafluorobenzyl bromide, diisopropylethylamine, sodium dodecyl sulfate (SDS), ammonium persulfate (APS), tetramethylethylenediamine (TEMED), tris base, acrylamide/bis-acrylamide, glycine, NaCl, HPLC-MS grade water, acetonitrile, acetic acid and methanol were obtained from VWR (PA, USA). SampliQ Silica C18 ODS reverse phase SPE cartridge was obtained from Agilent Technology (CA, USA). X-ray film was purchased from Phoenix Research Products (NC, USA). CelLytic™ lysis reagent and Ribonuclease A were acquired from Sigma-Aldrich (MO, USA). Pierce ECL western blot substrates, Pure Link™ HQ Mini Plasmid DNA Purification Kit, T-Per tissue protein extraction reagent, NE-PER™ nuclear and cytoplasmic extraction reagents were bought from Thermo Fisher Scientific (MA, USA).

Biological reagents: D5D primary antibody produced from rabbit and X-tremeGENE HP DNA transfection reagent were acquired from Sigma-Aldrich (MO, USA). Negative control siRNA, D5D-targeting siRNA (catalog # 4390825), COX-2 targeted siRNA (catalog #4392422), Lipofectamine™ RNAiMAX transfection reagent and 24-well transwell chamber were purchased from Life Technologies (NY, USA). GlutaMAX™ Opti-MEM reduced serum medium and bovine serum albumin standard solution were bought from Thermo Fisher Scientific (MA, USA). BCA protein assay was obtained from Bio-Rad (CA, USA). CellTiter 96® AQueous One Solution Cell Proliferation Assay kit, mRNA reverse transcription system and qPCR master mix were purchased from Promega (WI, USA). HDAC activity colorimetric assay kit was obtained from Biovision (CA, USA). Fetal bovine serum (FBS), Dulbecco's Modified Eagle's Medium and McCoy's 5A Medium were obtained from VWR (PA, USA). Annexin V Apoptosis Detection Kit I were

acquired from BD Pharmingen™ (NJ, USA). RNeasy Mini Kit was purchased from Qiagen (Hilden, Germany). Primary antibodies for COX-2, matrix metalloproteinase-2, E-cadherin, cleaved PARP, Ki-67, and Alexa fluor-conjugated secondary antibodies were acquired from Abcam (MA, USA). γH_2AX primary antibody was purchased from Bethyl Laboratories (TX, USA). Primary antibodies for p53, matrix metalloproteinase -9, acetyl histone H3, histone H3, procaspase 9, procaspase 7, p21, vimentin, snail, β-actin and horseradish peroxidase-conjugated secondary antibodies were bought from Cell Signaling (MA, USA). D5D forward/reverse primers and DNA oligos encoding D5D-targeted pre-shRNA were obtained from Integrated DNA Technologies (IA, USA). BLOCK-iT Pol II miR RNAi Expression Vector Kit was purchased from Invitrogen (NY, USA).

2.2. Cell Culture

The human colon cancer cell lines HCA-7 colony 29 (from European Collection of Cell Cultures) were grown in Dulbecco's Modified Eagle's Medium supplemented with 10% FBS. HT-29 and HCT 116 cells (from American Type Culture Collection) were grown in McCoy's 5A Medium supplemented with 10% FBS. Cells were cultured in an incubator containing a 95% humidified atmosphere with 5% CO_2 at 37°C.

2.3. MTS Assay

Colon cancer cell *in vitro* proliferation was assessed *via* MTS assay using CellTiter 96® AQueous One Solution Cell Proliferation Assay, which is a colorimetric method for determining the number of viable cells. The CellTiter 96® AQueous One Solution Reagent contains a tetrazolium compound [3-(4,5-dimethylthiazol-2-yl)-5-(3-carboxymethoxyphenyl)-2-(4-sulfophenyl)-2H-tetrazolium inner salt, MTS] and an electron coupling reagent (phenazine ethosulfate, PES) [154]. PES has enhanced chemical stability that allows it to be combined with MTS to form a stable solution. In metabolically active cells, the MTS tetrazolium compound can

be bioreduced by NADPH or NADH (produced by dehydrogenase enzymes) into a soluble colored formazan product. The quantity of formazan product as measured by the absorbance at 490 nm therefore is directly proportional to the number of living cells in culture.

The MTS cell proliferation assay was performed according to the manufacturer's instructions. Briefly, cells were seeded at 8,000 cells (in 100 μL medium) per well into 96-well plates, incubated overnight and exposed to various treatment, including siRNA transfection, fatty acids, DGLA metabolites and/or chemotherapy drugs. At the end of treatment, 20 μL of CellTiter® 96 Aqueous One Solution Reagent was added into each well. After 4 h incubation at 37°C, the quantity of formazan product was measured by recording the absorbance at 490 nm with a 96-well plate reader (SpectraMax M5; Molecular Devices). Cells treated with vehicle (ethanol for DGLA, DMSO for all the other reagents, less than 0.1% in total volume) served as controls. Cell viabilities in treatment groups were calculated as percentages of the control group (normalized to 100%).

2.4. Colony Formation Assay

Cancer cell survival upon various treatment was assessed *in vitro* by a colony formation assay, which is a method based on the ability of a single cell to grow into a colony [155]. Briefly, cells were seeded at 1,000-2,000 cells per well into 6-well plates, incubated overnight and exposed to various treatments including siRNA transfection, fatty acids, DGLA metabolites and/or chemotherapy drugs. Then the cells were washed with phosphate buffered saline (PBS) and incubated with fresh complete medium for 10-14 days. At the end of incubation, the cells in each well were washed with 1.0 mL PBS, fixed with 2.0 mL of 10% neutral buffered formalin for 15 min, and stained with 2.0 mL of 0.05% (w/v) crystal violet solution for 30 min. Cell colonies with at least 50 cells/colony in each well were then counted using an inverted microscope. Plating

efficiency and survival fraction were calculated as bellows (the survival fractions of all the control groups were normalized to 100%):

$$Plating\ Efficiency = \frac{number\ of\ colonies\ counted}{number\ of\ cells\ plated}$$

$$Survival\ Fraction = \frac{plating\ efficiency\ in\ treatment\ group}{plating\ efficiency\ in\ control\ group}$$

2.5. *In Vitro* Cell Cycle Distribution Analysis

Cell cycle distribution upon treatments was analyzed using the propidium iodide (PI) staining method. PI is a fluorescent molecule that can bind to nucleic acids, thus it is commonly used as a DNA staining molecule to evaluate DNA content in cell cycle analysis [156]. Briefly, 3.0×10^5 cells were seeded overnight in each well of 6-well plates and exposed to different treatments including siRNA transfection, fatty acids, DGLA metabolites and/or chemotherapy drugs. At the end of treatment, the cells were harvested by trypsinization, washed with PBS and fixed with 70% ice cold ethanol at 1.0×10^6 cells/mL at 4°C for 30 min. After centrifugation for 5 min at 1,000 rpm, the supernatant was discarded, and the cells were washed with PBS which was removed by centrifugation again for 5 min at 1,000 rpm. Then the cell pellet was treated with 10 μL ribonuclase A (10 mg/mL) at room temperature for 5 min, followed by addition of 400 μL of PI (50 μg/mL) into each sample. The cell cycle distribution was measured after 30 min incubation using an Accuri C6 flow cytometer (Becton–Dickinson, NJ, USA), 10,000 cells were counted for each sample. Data were analyzed by FlowJo (TreeStar, Ashland, OR, USA).

2.6. *In Vitro* Cell Apoptosis Analysis

Cell apoptosis upon different treatments was analyzed *in vitro* using Annexin V Apoptosis Detection Kit I. Annexin V is a Ca^{2+} dependent phospholipid-binding protein that has a high affinity for phosphatidylserine. During early stage of apoptosis, the membrane phosphatidylserine

is translocated from the inner to the outer leaflet of the plasma membrane, thereby can be bound with Annexin V [157]. Staining with FITC-conjugated Annexin V is typically used in conjunction with propidium iodide to allow the investigator to distinguish between early apoptotic cells vs. dead or damaged cells. This is because viable cells with intact membranes exclude PI, whereas the membranes of dead and damaged cells are permeable to PI. Therefore, cells that are both FITC Annexin V and PI negative are considered viable; cells that are FITC Annexin V positive and PI negative are considered in early apoptosis; and cells that are both FITC Annexin V and PI positive are considered in late apoptosis or already dead.

Cell apoptosis analysis was performed according to the manufacturer's instruction. Briefly, 3.0×10^5 cells were seeded overnight in each well of 6-well plates followed by different treatment including siRNA transfection, fatty acids, DGLA metabolites and/or chemotherapy drugs. After exposure to treatment for certain time, the cells were harvested by trypsinization, washed with PBS and re-suspended in 1×binding buffer (supplied in the kit) at a concentration of 1.0×10^6 cells/ml. Then 100 μl/sample of such cell suspension was treated with 5.0 μL of FITC Annexin V and 5.0 μL of PI solution (supplied in the kit), and incubated for 15 min at 25°C in the dark. After mixed with 400 μL of 1×binding buffer, the samples was subject to apoptosis analysis using a Accuri C6 flow cytometer, 10,000 cells were counted for each sample. Unstained cells, cells stained with FITC Annexin V only and PI only was used to set up compensation and quadrants. Data were analyzed by FlowJo.

2.7. Wound Healing Assay

Wound healing assay was performed to assess cancer cell migration upon various treatments. Briefly, cells were seeded at 1.0×10^6 cells per well in 6-well plates to reach 90% confluence and incubated overnight. A sterile 200 μL pipette tip was used to scratch on the bottom

of cell culture plate to create a vertical wound down through the cell monolayer. Excessive force against the plate should be avoided as it may damage the cell culture surface. After washing with PBS to eliminate dislodged cells, the cells were incubated with cell culture medium supplemented with 1.0% FBS and subject to different treatments, *e.g.* fatty acids, DGLA metabolites and/or chemotherapy drugs. Images of cells in each well were captured by a bright field microscopy immediately after wound creation as well as at different experimental time points. The wound area in each image was analyzed using Image-J software (NIH, Bethesda, MD, USA). For different treatments, the percentage of wound area at 48 h *vs.* wound area at 0 h was calculated to evaluate cell migration ability.

2.8. HDAC Activity Assay

HDAC activity in colon cancer cells after different treatment was assessed using an HDAC Activity Colorimetric Assay Kit. Briefly, the cells were seeded at 3.0×10^5 per well in 6 well plates and exposed to various treatment for 48 h, then the nuclear protein was extracted using NE-PER™ nuclear and cytoplasmic extraction reagents. 100 µg of nuclear extract (diluted in 85 µL water) was added into each well of a 96-well plate, and mixed with 10 µL assay buffer and 5 µL of HDAC colorimetric substrate (supplied in kit) followed by 1 h incubation h at 37 °C. The HDAC substrate comprises an acetylated lysine side chain which can be deacetylated by HDAC and become sensitive to the Lysine Developer. Therefore, after 1 h incubation, 10 µL of the Lysine Developer (supplied in kit) was added into each well and the plate was incubated for another 30 min at 37 °C. The chromophore produced from the reaction of Lysine Developer and deacetylated substrate was analyzed using a plate reader and used as an index for HDAC activity.

2.9. Western Blot for *In Vitro* Experiment

2.9.1. Preparation of buffers and reagents

Protein standard solutions: for protein concentration assay, bovine serum albumin solution (2 mg/mL) was diluted with deionized water to prepare a series of concentration at 0.25, 0.5, 0.75, 1.0 and 1.5 mg/mL. 1.0 ml aliquots of the standard solutions were stored at -20 °C.

Protein assay reagent A': 1.0 mL of protein assay reagent A and 20 μL of protein assay reagent S supplied in DC^{TM} BCA protein assay were mixed immediately before use.

SDS (10%) solution was prepared by dissolving 1.0 g of SDS in 10 mL deionized water. APS (10%) solution was freshly prepared by dissolving 0.1 g of APS in 1 mL deionized water.

Tris buffer (1.5 M, pH 8.8) was prepared by transferring 18.2 g of Tris base into a 100 mL reagent bottle. 90 mL of deionized water was added and stirred to completely dissolve. The pH was adjusted to 8.8 ± 0.05 with HCl (10 N). The volume was made up to 100 mL with deionized water.

Tris buffer (1.0 M, pH 6.8) was prepared by transferring 12.1 g of Tris base into a 100 mL reagent bottle. 90 mL of deionized water was added and stirred to dissolve completely. The pH was adjusted to 6.8 ± 0.05 with concentrated HCl (10 N). The volume was made up to 100 mL with deionized water.

Running buffer 10× stock solution was prepared by transferring 30.3 g of Tris base, 144.0 g glycine and 10.0 g SDS into a 1000 mL reagent bottle. Then 900 mL of deionized water were added and stirred to dissolve completely. The volume was made up to 1000 mL with deionized water and stored at 4 °C. Running buffer 1× working solution was prepared by transferring 100 mL of 10× running buffer into a 1000 mL reagent bottle. The volume was made up to 1000 mL with deionized water and stored at 4 °C.

Transfer buffer 10× stock solution was prepared by transferring 22.1 g of CAPS into a 1000 mL reagent bottle. 900 mL of deionized water was added and stirred to dissolve completely. The pH was adjusted to 11.0 ± 0.05 with NaOH (10 N). The volume was made up to 1000 mL with deionized water and stored at 4°C. Transfer buffer 1×working solution was prepared by transferring 100 ml of 10×transfer buffer to a 1000 mL reagent bottle. 200 mL methanol was added. The volume was made up to 1000 ml with deionized water and stored at 4°C.

Tris buffered saline (TBS) 10×stock solution was prepared by transferring approximately 12.1 g of Tris base to a 1000 mL reagent bottle. 87.7 g of NaCl and 900 mL of deionized water was added and stirred to dissolve, and the pH adjusted with HCl (10 N) to 7.6.±.0.05. The volume was made up to 1000 mL with deionized water and stored at 4°C. TBS-T 1×working solution was prepared by transferring 100 mL of 10×TBS in a 1000 mL reagent bottle. Then 1.0 mL Tween-20 was added and the volume was made up 1000 mL with deionized water and stored at 4°C.

Blocking Solution (5% non-fat dry milk) was prepared by transferring approximately 5.0 g of non-fat dry milk in a 100 mL reagent bottle. 90 mL of 1×TBS-T was added and stirred to dissolve, the volume was made up to 100 mL with 1×TBS-T.

SDS-PAGE gel: The resolving gel (10%) and stacking gel (4%) were prepared using 1.5 mm plates according to **Table 1**.

Table 1. Components for casting SDS-PAGE gel

	Resolving Gel (10%)	Stacking Gel (4%)
H_2O	7.8 mL	7.25 mL
Tris buffer	2 mL (1.5 M, pH 8.8)	1.25 mL (1.0 M, pH 6.8)
acrylamide/bis-acrylamide (30% solution)	5 mL	1.3 mL
10% SDS	150 µL	100 µL
10 % APS	150 µL	100 µL
TEMED	15 µL	10 µL
Total	~15 mL	~10 mL

2.9.2. Western blot procedure

Protein Extraction: The cells were seeded in 6-well plates and exposed to different treatment including siRNA transfection, fatty acids, DGLA metabolites and/or chemotherapy drugs, *etc*. At experimental point, the culture medium was discarded and the cells were washed with PBS. Then ~100 µL of CelLytic™ lysis reagent was added into each well, the plates were allowed to sit on ice for 10-15 min. The cell lysates were then collected by scratching them off from the plates. After centrifugation at 12,000 rpm for 10 min, the supernatant was collected.

Protein Quantification: The protein concentrations in the cell lysates were measured using DC™ protein assay kit according to the manufacturer's instructions. Briefly, 5.0 µL of diluted cell lysate samples, 25 µL of reagent A' and 200 µl reagent B were added in each well of a 96-well plate and mixed well. After 15 minutes incubation at room temperature in the dark, the absorbances were read at 750 nm using a microplate reader. For every measurement, a series of protein standards was also included to construct a standard curve for quantification.

Sample Loading: Each protein sample was normalized to the same concentration by diluting with a certain amount of lysis buffer. The samples were mixed with 4×loading buffer

(sample: loading buffer = 3:1) and denatured at 95°C for 5 min. Then 40-60 μg protein in each sample was loaded onto a well of 10% SDS-PAGE gel, a protein weight marker (5.0 μL) was included for each gel.

Gel Electrophoresis: the gel was run at constant voltage of 90 V, and switched to 120 V after samples passed the stacking gel. The power was switched off just before the bromophenol blue line reached the bottom of gel.

Membrane Transferring: membranes, sponges and filter paper were soaked in transferring buffer for 15 min prior to transferring. Then the proteins on the gel were transferred electrophoretically to the membrane at constant voltage of 80 V for 2 h on ice.

Blotting: After transferring, the membranes were incubated in 6.0 mL of blocking solution with continuous rock for 15 min to prevent non-specific binding, then incubated with primary antibody (diluted in blocking solution) for overnight at 4°C in dark with continuous rocking. The next day, membranes were washed 3 times for 5 min each in 1×TBS-T, and incubated with secondary antibody (also diluted in blocking solution) for 2 h at room temperature with continuous rocking. Then the membranes were washed 3 times for 5 min each in 1×TBS-T again, incubated in ECL western blot substrates for 2 min, and exposed to X-ray film. Luminescent signals were captured on a Mini-Medical Automatic Film Processor (Imageworks). Image of the film was captured and analyzed using NIH ImageJ software.

2.10. SiRNA Transfection

2.10.1. Preparation of siRNA transfection mixture

D5D-targeting siRNA (catalog # 4390825) was purchased from Life Technologies (NY, USA). It contains a sense strand of ACAUCAUCCACUCACUAAAtt and an antisense strand of UUUAGUGAGUGGAUGAUGUcg.

For transfection in each well of 96-well plates, 0.15 μL D5D targeted siRNA (100 μM stock) and 0.6 μL of Lipofectamine™ RNAiMAX transfection reagent were diluted into 100 μL GlutaMAX™ Opti-MEM reduced serum medium, respectively. For transfection in each well of 6 well plates, 1.5 μL D5D targeted siRNA (100 μM stock) and 6.0 μL of Lipofectamine™ RNAiMAX transfection reagent were diluted into 1.0 mL GlutaMAX™ Opti-MEM reduced serum medium, respectively. Then the two dilutions were mixed together and incubated for 5 min prior to adding into each well.

2.10.2. Transfection of siRNA into cells

Human colon cells were seeded at 3.0×10^5 cells per well in a 6-well plate or 8,000 cells per well in a 96-well plate for different experiments. After overnight incubation, cell culture medium was removed and the cells were washed by PBS. Then 1.0 mL (for 6-well plate) or 100 μL (for 96-well plate) of abovementioned siRNA transfection mixture was prepared and added into each well of the plates. After 6 h transfection, the reduced serum medium was replaced by fresh complete cell culture medium supplemented with 10% FBS. After 48 hours, the transfected cells were ready for further treatments and other experiments, *e.g.* western blot, MTS assay, colony formation assay, LC/MS analysis, GC/MS analysis, cell cycle distribution and apoptosis analysis, *etc*. Cells transfected with a non-target siRNA were used as negative control (Nc-si).

2.11. Stable D5D Knockdown *via* ShRNA Transfection

In order to investigate the effect of D5D knockdown (D5D-*KD*) in tumor xenograft, we created a stable D5D-*KD* HCA-7 cell line *via* shRNA transfection to be injected into nude mice. Briefly, we designed and purchased D5D-targeted pre-shRNA, which was then cloned into pcDNAtm 6.2-GW/miR vector and transformed into *E.coli* (protocol available at https://tools.thermofisher.com/content/sfs/manuals/blockit_miRNAexpressionvector_man.pdf).

The plasmid DNA from expression clone was transfected into wild type (wt) HCA-7 cells followed by antibiotic selection to create stable D5D knockdown cell colonies (**Scheme 6**). The stable D5D-*KD* cells were then injected into nude mice to establish D5D-*KD* xenograft tumors.

Design of D5D-targeted DNA oligonucleotides: Using BLOCK-iT™ RNAi Designer (www.invitrogen.com/rnai), two strands of DNA oligonucleotides encoding D5D-targeted shRNA were designed and purchased. The sequences are as follows: target strand, TGCTGTAATCATCCAGGCCAAGTCCAGTTTTGGCCACTGACTGACTGGACTTGCTGG ATGATTA; complementary strand, CCTGTAATCATCCAGCAAGTCCAGTCAGTCAGTGG CCAAAACTGGACTTGGCCTGGATGATTAC.

Annealing Reaction: the reaction system was set up as shown in **Table 2** in a 0.5 ml sterile centrifuge tube at room temperature. The mixture was incubated at 95°C for 4 min and allowed to cool down to room temperature for 5-10 min during which time the single-stranded oligos would anneal to form a double-stranded oligo (at final concentration of 50 μM). Then the tube was centrifuged briefly (~5 seconds), gently mixed and stored at -20°C (stable for at least a year).

Ligation Reaction: prior to clone the double-stranded oligo into vector, the 50 μM stock solution was diluted to a final concentration of 10 nM working solution (i.e. 5,000-fold dilution) by two steps: firstly, 1.0 μL of 50 μM ds oligo stock was mixed with 99 μL of DNase/RNase-free water to obtain a final concentration of 500 nM; secondly, 1.0 μL of 500 nM ds oligo was mixed with 5.0 μL of 10×oligo annealing buffer and 44 μL of DNase/RNase-free water to obtain a final concentration of 10 nM. Then the ligation reaction was set up at room temperature according to **Table 3**. The reaction system was mixed well by pipetting (do not vortex) and incubated for 5 minutes at room temperature. The mixture was put on ice for transforming into *E. coli* immediately or stored at -20°C overnight.

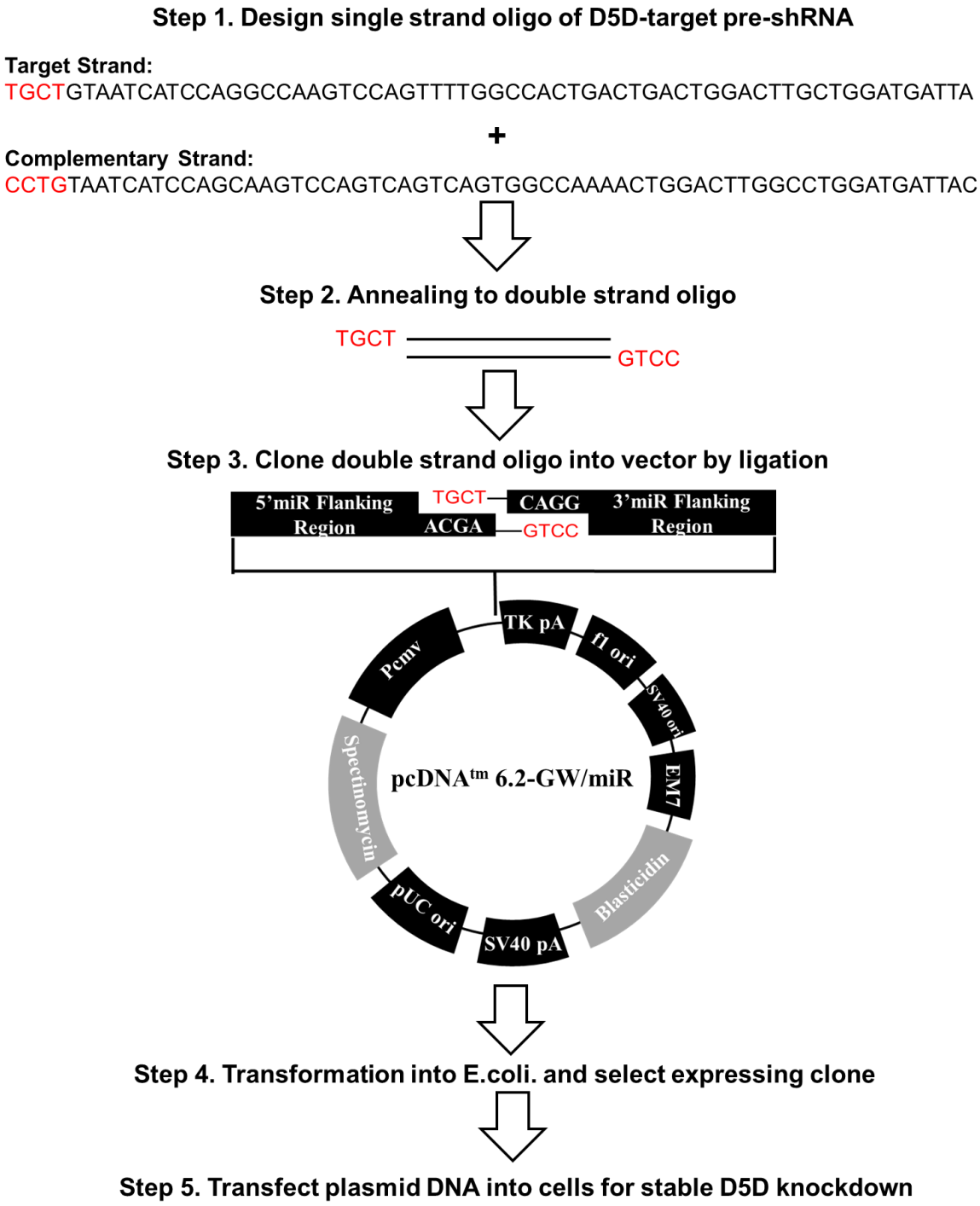

Scheme 6. Flow chart for creating the stable D5D-*KD* HCA-7 cell line.

Table 2. Preparation for annealing reaction

Reagent	Amount
Target strand DNA oligo (200 μM)	5.0 μL
Complementary strand DNA oligo (200 μM)	5.0 μL
10× Oligo Annealing Buffer	2.0 μL
DNase/RNase-Free Water	8.0 μL
Total	20 μL

Table 3. Preparation for ligation reaction

Reagent	Amount
5×Ligation Buffer	4.0 μL
pcDNA™6.2-GW/miR, linearized (5 ng/μl)	2.0 μL
ds oligo (10 nM)	4.0 μL
DNase/RNase-Free Water	9.0 μL
T4 DNA Ligase (1 U/μl)	1.0 μL
Total	20 μL

Transformation: 2.0 μl of the ligation reaction was added into a vial of One Shot® TOP10 chemically competent *E. coli* and mixed gently (do not mix by pipetting). The mixture was incubated on ice 30 minutes. The cells were then heat-shocked for 30 seconds at 42°C without shaking. The tube was immediately transferred to ice and added with 250 μl of room temperature low salt LB medium. The tube was then shaken horizontally at 200 rpm, 37°C for 1 hour. Then 50-200 μl from each transformation was spread on a pre-warmed low salt LB agar plate containing 100 μg/ml Blasticidin, followed by overnight incubation at 37°C.

Extraction of plasmid DNA: 5-10 Blasticidin-resistant colonies were collected and incubated overnight in LB medium containing 100 μg/ml Blasticidin. Then the plasmid DNA was isolated using PureLink™ HQ Mini Plasmid Purification Kit according to manufacturer's

instruction. The concentration of plasmid DNA in each sample was determined using Nanodrop Spectrophotometer.

Transfecting cells: in 6-well plates, cells were seeded at 3×10^5 cells/well and incubated overnight. The cell culture medium was removed and cells were washed with PBS. For transfection in one well, 1.0 µg of plasmid DNA and 6.0 µl X-tremeGENE HP DNA transfection reagent was diluted into 500 µl of reduced serum medium, respectively, then mixed together for 30 min at room temperature and added into each well. pcDNA™6.2-GW/± EmGFP-miR-neg control plasmid was also transfected into cells as a negative control. After six hours transfection, the reduced serum medium was replaced with fresh complete medium with 10% FBS and the cells were incubated overnight. Then the cells in each well of 6-well plates were trypsinized and re-plated into a 10 cm tissue culture plate in fresh complete medium containing 10 µg/ml of Blasticidin. The Blasticidin-containing medium was refreshed every 3-4 days until Blasticidin-resistant colonies were identified (~10-14 days). About 20 Blasticidin-resistant colonies were collected and expanded, followed by western blot analysis to evaluate the knockdown effect.

2.12. qRT PCR Analysis

qRT PCR analysis was performed to evaluate D5D knockdown efficiency in human colon cancer cell lines after siRNA transfection. The procedures are described as follows:

Extraction of mRNA: colon cancer cells were seeded at 3.0×10^5 cells per well in a 6-well plate, incubated overnight, followed by 48 h siRNA transfection. Then cellular mRNA was extracted using RNeasy Mini Kit according to manufacturer's instruction. Briefly, the cells were harvest by trypisinization and washed with PBS. After centrifugation, the cell pellet was collected and mixed with 350 µL of buffer RLT (supplied in kit) and 350 µL of 70% ethanol. The mixture was transferred to an RNeasy Mini spin column and placed on a 2.0 mL collection tube, followed

by centrifugation for 15s at 12,000 rpm, the flow-through was discarded. 700 µL of buffer RW1 (supplied in kit) was then added to the column followed by centrifugation for 15s at 12,000 rpm, the flow-through was discarded. Afterwards, 500 µL of buffer RPE (supplied in kit) was added to the column followed by centrifugation for 15s at 12,000 rpm, the flow-through was discarded. Another 500 µL of buffer RPE (supplied in kit) was then added to the column followed by centrifugation for 2 min at 12,000 rpm. The column was placed in a new collection tube, and 30-50 µL RNase-free water was added, followed by centrifugation for 1 min at 12,000 rpm to elute the RNA. The concentration of RNA in each sample was determined using a Nanodrop Spectrophotometer (Thermo Fisher Scientific).

cDNA synthesis: for each sample, 0.5 µL of random primer, 40 ng of mRNA sample were mixed in a PCR tube, DNase/RNase-free water was added to make a total 10 µL solution. The tube was processed in a thermal cycler at 70°C for 5min and kept at 4°C. Then a reaction mixture was prepared according to **Table 4**, and 15 uL of such mixture was added into each sample and mixed well, bubbles were avoided. The PCR tubes were processed in a cycler for cDNA synthesis with the program as follows: 16°C, 30 min; 42°C, 15 min ×2 cycles; 85°C, 5 min; 4°C, ∞ min.

Table 4. Preparation for cDNA synthesis

Reagent	Amount
MMLV RT 5*B	5.0 µL
dNTPs	5.0 µL
RNAs	0.625 µL
MMLV RT	1.0 µL
DNase/RNase-Free Water	3.375 µL
Total	15 µL

qRT PCR analysis: the primers used for human D5D and 18s rRNA (internal standard) are as follows: Reverse primer for D5D: 5'-AGTCTTCCTCCTCTTCTTCCA-3', forward primer for D5D: 5'-CCGACATCATCCACTCACTAAA-3'. Reverse primer for 18s: 5'-GCCTCGA AAGAGTCCTGTATTG-3', forward primer for 18s: 5'-CTGAGAAACGGCTACCACATC-3'. The reaction mixture was prepared according to **Table 5**, and added to each well of PCR plates. The plate was sealed and centrifuged for 3 min at 1500 rpm, followed by qRT PCR analysis using a ABI 7500 Fast qPCR. The program was set as follows: stage 1 (1 cycle), 50°C, 2 min; stage 2 (1 cycle), 95°C, 10 min; stage 3 (40 cycles), 95°C, 15 sec; 60°C, 1 min.

Table 5. Preparation for qRT PCR analysis

Reagent	Amount
SYBR green 2×	10 μL
Primer (D5D or 18s)	1.0 μL
DNase/RNase-Free Water	4.0 μL
Dilution of cDNA	5.0 μL
Total	20 μL

2.13. Extraction of Fatty Acids and Prostaglandins from Cells

The free ω-6s and PGs from cells treated with DGLA were quantified *via* LC/MS analysis as described elsewhere [138]. Briefly, cells were seeded at 3.0×10^5 cells per well in 6-well plates and incubated overnight, followed by siRNA transfection and fatty acids treatment. At different time points, the cells (scratched off from well) with 1.0 mL of culture medium were collected and mixed with 0.45 mL of methanol and 1.55 mL of water to make a total of 3 mL of 15% methanol solution. After adding internal standards (AA-d_8, DGLA-d_6, PGE1-d_4 and PGE2-d_9, 5.0 μL each), the mixture was vortexed for 1 min and set on ice for 30 min. Then sample solution were centrifuged for 15 min at 3,000 rpm, the supernatant was collected and adjusted to pH 3.0 using

1.0 N HCl, followed by solid phase extraction (SPE) using a reverse phase SPE cartridge (SampliQ Silica C18 ODS, Agilent Technology). For SPE, the cartridge was pre-conditioned with 2.0 mL water and 2.0 mL methanol, then 3.0 mL sample solution was loaded into each cartridge. After washing with 1.0 mL of water, the free fatty acids and PGs were eluted with 2.0 mL ethyl acetate from cartridge, the elution containing analytes was vacuumed to dryness and reconstituted with 100 μL ethanol for LC/MS analysis.

2.14. HPLC/MS Analysis of Fatty Acids and Prostaglandins from Cells

The LC/MS system consisting of Agilent 1200 series HPLC system and Agilent 6300 LC/MSD SL ion trap mass was used to quantify the free ω-6s and PGs in reconstituted sample solution described before. LC separations were performed on a C18 column (Zorbax Eclipse-XDB, 4.6□× 75 mm, 3.5 μm) with 5.0 μL sample injection at a flow rate of 0.8 mL/min. The gradient of mobile phases (A: H_2O with 0.01% acetic acid and B: acetonitril with 0.01% acetic acid) was as follows: 0-12 min (isocratic), 68% A and 32% B; 12-14 min, 68 to 44% A and 32 to 56% B; 14-28 min (isocratic), 44% A and 56% B; 28-30 min, 44 to 14% A and 56 to 86% B; 30-38 min, 14 to 4% A and 86 to 95% B; and 38-44 min (isocratic), 5% A and 95% B. MS settings were as follows: electrospray ionization in negative mode; total ion current chromatograms in full mass scan mode (m/z 50 to m/z 600) were performed; nebulizer press, 15 psi; dry gas flow rate, 5.0 L/min; dry temperature, 325°C; compound stability, 20%; number of scans, 50.

For quantification, an internal standard curve was constructed from a series of mixtures consisting of DGLA, AA, PGE1, PGE2 standard solution at various concentrations, and internal standards DGLA-d_6, AA-d_8, PGE1-d_4, PGE2-d_9 at a constant concentration. Extracted ion current were used to monitor the peak area of PGE1 (m/z 353), PGE1-d_4 (m/z 357), PGE2 (m/z 351), PGE2-d_9 (m/z 360), DGLA (m/z 305), AA (m/z 303), AA-d_8 (m/z 311) and DGLA-d_6 (m/z 311),

respectively. The concentrations of fatty acids and PGs in the samples were calculated using the internal standard curve by comparing the ratios of the peak areas of the analytes to the peak areas of their corresponding internal standards.

2.15. GC/MS Analysis of 8-HOA from Cells

Due to the stability issue, endogenous generation of 8-HOA cannot be detected in HPLC/MS and GC/MS system in its original form. Therefore, 8-HOA produced from cells treated with/without DGLA was quantified *via* GC/MS analysis in its derivative of pentafluorobenzyl bromide (PFB-Br, **Scheme 7**) [158]. Briefly, 3.0×10^5 cells were seeded overnight in each well of 6-well plate followed by various treatments including siRNA transfection, fatty acids and/or chemotherapy drugs. At experimental time points, the cells (scratched off from plate) and ~1.0 mL medium were collected and mixed with 500 μL of methanol containing internal standard (hexanoic acid), 50 μL of 1.0 N HCl, as well as 3.0 mL of dichloromethane. The mixture was then vortexed for 30s, centrifuged at 3,000 rpm for 4 min and the organic layer was collected. The same extraction was repeated once, and the dichloromethane layers were combined and evaporated to dryness using a vacuum evaporator. The sample was then reconstituted in 50 μL of 1.0% diisopropylethylamine in acetonitrile (v/v) and derivatized with 50 μL of 1% PFB-bromide in acetonitrile (w/v) at 37°C for 30 min. After the acetonitrile was removed using a vacuum evaporator, the residue was reconstituted in 100 μL of dichloromethane.

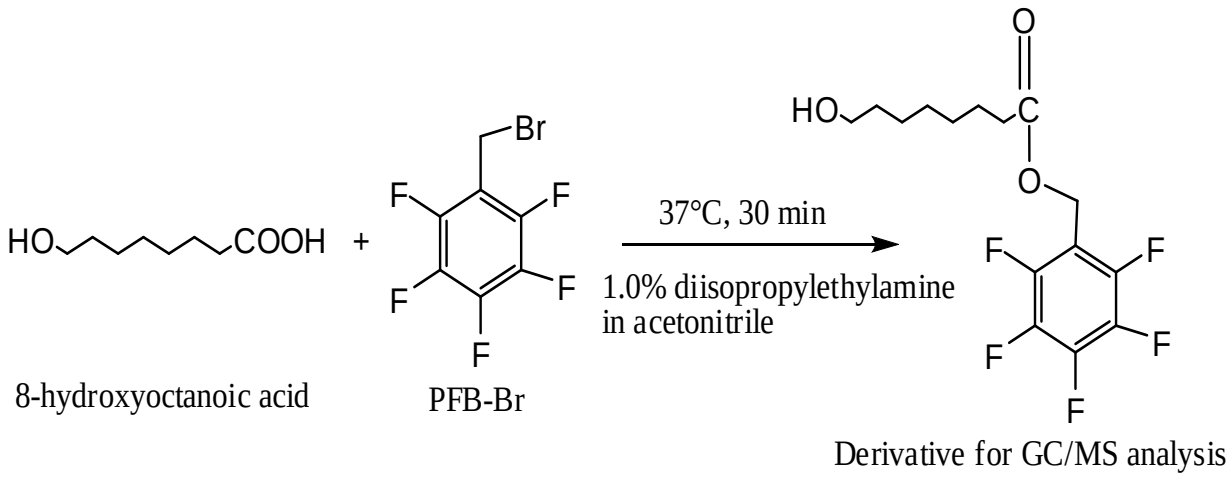

Scheme 7. Derivatization of 8-HOA with PFB-Br for GC/MS analysis.

Sample solution (2.0 μL) was injected into an Agilent 7890A gas chromatograph. The GC oven temperature was programmed from 60 to 300°C at 25°C/min. The injector and transfer line were kept at 280°C. Quantitative analysis was performed using a mass selective detector with a source temperature of 230°C. For quantification, an internal standard curve was constructed from a series of mixtures consisting of 8-HOA at various concentrations, and internal standard hexanoic at a constant concentration. Extracted ion current with m/z 181 (base peak for both 8-HOA-PFB and hexanoic acid-PFB derivatives) was used to monitor the peak area of 8-HOA and hexanoic acid derivatives. The concentrations of 8-HOA in the samples were calculated using the internal standard curve by comparing the ratios of the peak area of the 8-HOA to the peak area of internal standard.

2.16. Transwell Migration/Invasion Assay

Transwell migration assays were performed to assess cancer cell migration and invasion upon various treatment in a transwell chamber (24-well plates with insert, pore size: 8 mm, Corning, Life Sciences). For migration assay, 3.0×10^5 cells were seeded overnight in each well of 6-well plate followed by various treatments including siRNA transfection, fatty acids and/or chemotherapy drugs. Then 5×10^4 cells were collected by trypsinization and seeded in the top

chamber of transwell inserts with the non-coated membrane and incubated overnight. Then cell culture medium containing no serum or 10% serum was added to the top chamber and lower chamber, respectively. After another 48 h incubation, the cells were washed with PBS, fixed in 10% neutral buffered formalin for 30 min and stained with 0.05% crystal violet solution for 30 min. After removing the cells stayed at the top surface of the insert, cells that migrated through the pores to the lower surface of the inserts were counted under an inverted microscope. For each inserts, at least five view fields were counted.

For invasion assays, 3.0×10^5 cells were seeded overnight in each well of 6-well plate followed by various treatments including siRNA transfection, fatty acids and/or chemotherapy drugs. Then 5×10^4 cells were collected by trypsinization and seeded in the top chamber of transwell inserts coated with Matrigel. The following procedures were performed same as described in migration assay.

2.17. Mouse Xenograft Tumor Model

All the animal experiments were approved by Institutional Animal Care and Use Committees at North Dakota State University (protocol A16039). A total of 48 four-week old female nude mice (J:Nu, stock number 007850) were purchased from The Jackson Laboratory (Bar Harbor, ME). The mice were housed five per cage in the pathogen-free innovive IVC system with water and food *ad libitum*. After allowing the mice to acclimate for one week, tumor xenografts were established by subcutaneously injecting 2×10^6 wild type or D5D knockdown HCA-7 cells (suspended in 100 μL PBS) into both of the hind flank of mice. The mice were fed a standard diet for another two weeks to allow tumors to grow, then divided into four different treatment groups which received four-week treatment of vehicle control, DGLA supplementation (oral gavage), 5-FU injection (*iv.*), or combination of DGLA and 5-FU, respectively. All the mice received the

treatment at the same time, *i.e.* two weeks after cancer cell injection. Tumor growth was monitored twice a week using a digital caliper during the treatment. Tumor volume was calculated as: $V = L \times W^2/2$. At the endpoint, the mice were euthanized with an overdose of pentobarbital (200 mg/kg, *i.p.*) and the tumor tissues were collected for further analysis.

2.18. *In Vivo* DGLA and 5-FU Treatment

Mice injected with wild type or D5D knockdown HCA-7 cells were further divided into four sub groups and received: (1) vehicle control; (2) DGLA ethyl ester at a dose of 8 mg/mice, oral gavage, twice a week; (3) 5-FU at 30 mg/kg by *i.v.* injection, twice a week; and (4) combination of DGLA ethyl ester and 5-FU.

2.19. Quantification of Fatty Acids and Prostaglandins from Tumor Tissues

After four weeks treatment, the mice were euthanized and the tumor tissues were collected. 0.05-0.2 g tumor tissues from each mice were weighted, frozen in liquid nitrogen, and smashed to powder, then mixed with 2.55 mL of water and 0.45 mL of methanol. After adding internal standards (AA-d_8, DGLA-d_6, PGE1-d_4 and PGE2-d_9, 5.0 μL each), the mixture was vortexed for 1 min and set on ice for 30 min. followed by centrifugation for 15 min at 3,000 rpm. The supernatant was collected and adjusted to pH 3.0 using 1.0 N HCl, followed by solid phase extraction using SampliQ Silica C18 ODS cartridge. The free fatty acids and PGs eluted with 2.0 mL ethyl acetate from cartridge were vacuumed to dryness and reconstituted with 100 μL ethanol for LC/MS analysis as described previously.

2.20. Quantification of 8-HOA from Tumor Tissues

0.05-0.2 g freshly collected tumor tissues from each mice were weighted, frozen in liquid nitrogen, smashed to powder and suspended in 1.0 mL water. The suspension was mixed with 500 μL of methanol containing internal standard (hexanoic acid), 50 μL of 1.0 N HCl, as well as 3.0

mL of dichloromethane. The mixture was then vortexed for 30s, centrifuged at 3,000 rpm for 4 min and the organic layer was collected. The same extraction was repeated once, and the dichloromethane layers were combined and evaporated to dryness using a vacuum evaporator. The sample was then reconstituted in 50 μL of 1.0% diisopropylethylamine in acetonitrile (v/v) and derivatized with 50 μL of 1% PFB-bromide in acetonitrile (w/v) at 37°C for 30 min. After the acetonitrile was removed using a vacuum evaporator, the residue was reconstituted in 100 μL of dichloromethane and ready for GC/MS analysis as described previously.

2.21. Western Blot for Tumor Tissue Samples

The protein in tumor tissue powder was extracted using T-Per tissue protein extraction reagent. Briefly, the tissue samples were weighted and mixed with T-PER Reagent (1:20, g/mL). A smaller volume of reagent can be used to obtain more concentrated protein extracts. The mixture was homogenized on ice and centrifuged at 12,000 rpm for 5 minutes. The supernatant was then collected, and the expression of p53, procaspase9, γH2AX and acetyl histone H3 in tumor tissues was assessed by western blot assay as described previously.

2.22. Immunofluorescence Analysis

Expressions of D5D, COX-2, cleaved PARP, Ki-67, matrix metalloproteinase-2 and E-cadherin in tumor tissues was analyzed by immunofluorescence at Advanced Imaging & Microscopy Laboratory, NDSU. Briefly, freshly collected tumor tissues were fixed with 10 % formaldehyde and embedded in paraffin blocks. Tissues sections (4 μm) were deparaffinized with xylene, rinsed and rehydrated through a graded series of alcohol. Then the tumor sections were incubated with primary antibodies and fluorochrome-conjugated secondary antibodies subsequently. Cell nuclei were counter stained with DAPI. The images were acquired by a Zeiss Axio Imager M2 microscope and analyzed by Image Pro software.

Six tumor samples from every treatment group were analyzed for each target protein. For quantification analysis of D5D, COX-2, matrix metalloproteinase-2 and E-cadherin, the mean fluorescence intensities for target proteins in each sample were acquired using Image Pro software as index for their expression levels in tumor tissues. For cleaved PARP, the result were presented as percentage of cleaved PARP positive cells to the total number of cells in each image. Note, the total number of cells in one image were calculated as total DAPI positive area divided by mean area of a single nucleus. Similarly, for quantification of Ki-67, the result were presented as percentage of Ki-67 positive events to the total number of events in each image.

2.23. Statistics

For the *in vitro* studies, data were presented as mean ± standard deviation (SD) from at least three separate experiments. For the *in vivo* study, data were presented as mean ± SD from six tumor samples. All the original data were used for statistic analysis. Statistic differences between the mean values for different groups were evaluated by analysis of variance (ANOVA) and post hoc t-test, significant differences were considered with a p-value < 0.05.

3. ANTI-CANCER EFFECT FROM DGLA-DERIVED DISTINCT BYPRODUCT 8-HOA

Arachidonic acid is well known to promote colon cancer development by producing 2-series of prostaglandins from COX-2 catalyzed peroxidation [12-13, 98-99]. On the other hand, DGLA, the immediate precursor of arachidonic acid, has been show to associate with potential anti-cancer activities [19-20, 22, 24]. Although the mechanism underlying DGLA's anti-cancer effect is still unclear, evidence suggested that the free radical metabolites from COX-2 catalyzed DGLA peroxidation may play an important role [19, 22, 24], while others reported that PGE1 is mainly responsible for DGLA's bioactivity [159-162].

By developing and employing a novel HPLC/ESR (spin-trapping)/MS combined technique, Dr. Qian's group has previously identified and characterized both common and exclusive free radical byproducts produced from COX-2-catalyzed DGLA and arachidonic acid peroxidation (Schemes 3-4) [136-138]. The studies demonstrated that the different structural moiety in DGLA vs. arachidonic acid leads to the formation of two distinct DGLA derived free radical species from a unique C-8 oxygenation. Further quantification analysis showed that there were 0.01-0.1 μM DGLA-derived free radical species that could be trapped by a spin trapping agent and measured from cells after 48 h DGLA supplementation [136-139]. These free radical species were predicted to be converted into their corresponding stable forms in a cellular environment, *e.g.*, 8-HOA and HTA, which can accumulate to micro molar range [136-139].

We thus proposed that these distinct byproducts from COX-2-catalyzed DGLA peroxidation may be responsible for the anti-cancer activity of DGLA. In this chapter, we tested the potential anti-cancer effect from DGLA's distinct byproducts in colon cancer as well as investigated the associated molecular mechanisms. Results from this chapter will lay down the foundation for us to develop a ω-6s diet care strategy in colon cancer treatment and prevention.

3.1. DGLA-Derived Distinct Byproduct Inhibited Colon Cancer Cell Growth

To test our hypothesis that the anti-cancer effect of DGLA is derived from its distinct byproduct, we firstly assessed the effect of these byproducts on the proliferation of human colon cancer cell lines including HCA-7 cells (high COX-2, wt-/mutant p53 heterozygous), HT-29 cells (low COX-2, mutant p53) and HCT 116 (COX-2 deficient, wt-p53) [163]. Three free radical-derived byproducts were tested here, including a common byproduct from both DGLA and AA, *i.e.* HEX, and two exclusive byproducts from DGLA, *i.e.* HTA and 8-HOA (Schemes 3-4). The tested concentrations range from 0.1 μM to 10 μM, which is physiological relevant according to our previous report [164].

Results from the MTS assay showed that among all of the treatment, 48 h supplementation of 8-HOA, starting at 1.0 μM, significantly inhibited the viabilities of HCA-7, HT-29 and HCT 116 cells with the reduced cell viability at 75.2 ± 6.7%, 79.2 ± 1.2% and 89.4 ± 4.2%, respectively, compared to their corresponding controls (normalized to 100%, **Fig. 1A-C**). However, the other two DGLA byproducts HEX and HTA did not significantly influence cell growth at the same concentration range.

Besides free radical-derived metabolites, we also tested the effect of PGE1 on the growth of human colon cancer cell lines. PGE1 is the one of the major metabolite from COX-catalyzed DGLA peroxidation. It has been reported to possess certain anti-inflammation and anti-cancer activities [159-162]. Therefore, there is a general belief that PGE1 is the major bioactive metabolite from DGLA and may be responsible for DGLA's anticancer activity. However, our results showed that treatment of PGE1 at 0.1-10 μM (physiologically relevant concentration [164]) did not affect the viabilities of all three tested cell lines, suggesting the bioactivities of DGLA in cancer is not derived from PGE1 (Fig. 1).

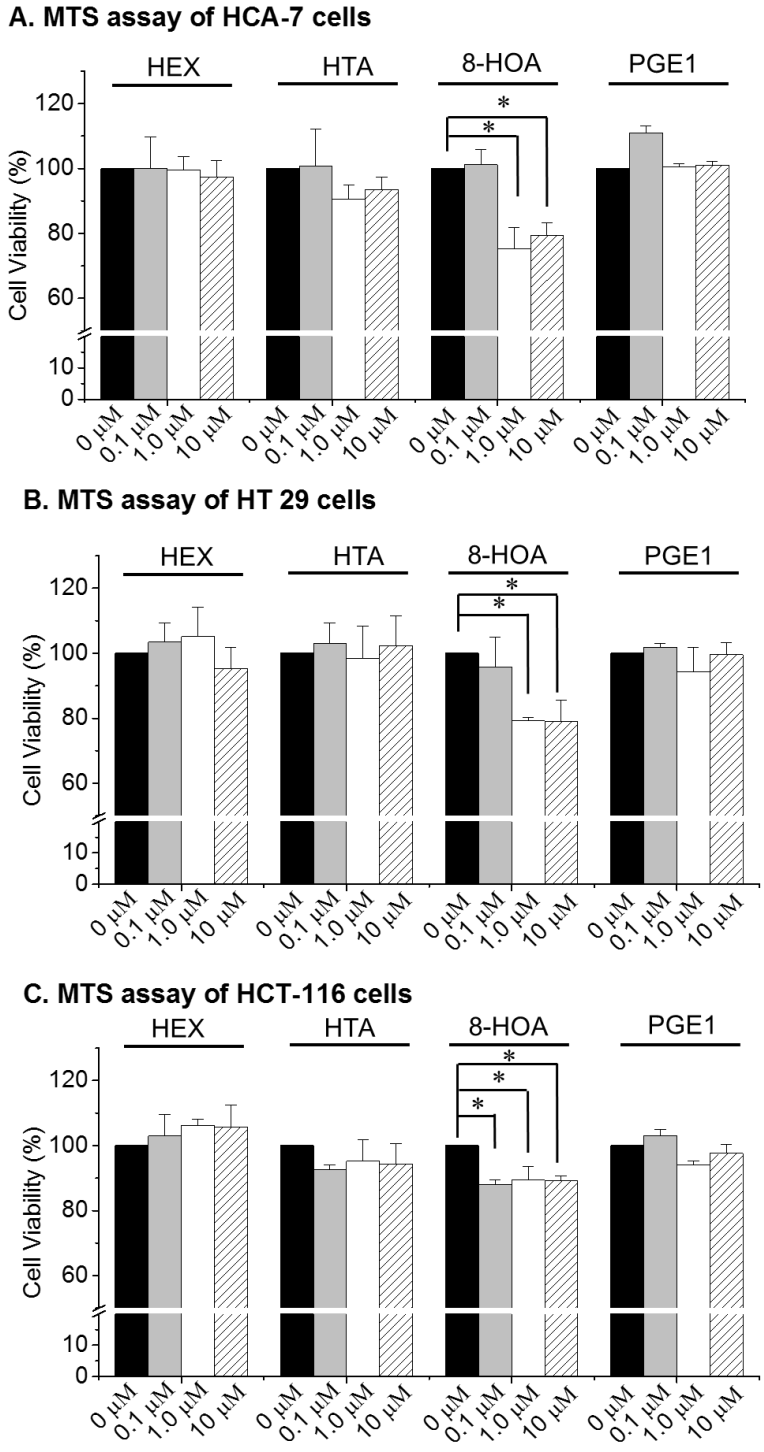

Figure 1. Effect of DGLA's byproducts on colon cancer cell viability at 48 h.
A. HCA-7 cells, **B.** HT-29 cells and **C.** HCT 116 cells were treated with HEX, HTA, 8-HOA and PGE1 at indicated concentrations for 48 h, followed by the MTS assay. Data represent mean ± SD with at least three separate experiments. The cell viabilities for control groups are normalized to 100% for every separate experiment to calculate the percentage of cell viabilities from treatment groups. (*: significant difference vs. control with $p < 0.05$) [163].

To further confirm the anti-cancer effect from 8-HOA, colony formation assays was also performed on the same three human colon cancer cell lines. Results showed that treatment of 8-HOA at 1.0 μM for 48h could significantly suppress colony formation of HCA-7, HT 29 and HCT 116 cells, with survival fraction of 75.9 ± 3.0%, 72.3 ± 2.5% and 72.9 ± 4.3%, respectively, compared to 100% in their corresponding controls (**Fig. 2A-C)** [164]. These data together with the MTS assay suggested that it might be the distinct free radical byproduct, *i.e.* 8-HOA, that is actually responsible for the DGLA's anti-cancer bioactivity.

3.2. 8-HOA Induced Cell Cycle Arrest in Colon Cancer Cell

The cell cycle is the series of events that leading to cell division and DNA replication. Modulation of cancer cell cycle progression is a complicated process that can lead to cell proliferation, senescence or apoptosis [165]. In order to investigate how 8-HOA could suppress colon cancer cell growth, we analyzed cell cycle distribution of HCA-7 colony 29 cells after 8-HOA treatment *via* PI staining followed by flow cytometry analysis.

Our data showed that supplementation of 8-HOA (1.0 μM, 48 h) resulted in a significantly higher population of HCA-7 cells (50.6 ± 2.5%) arresting at G1 phase during the cell cycle progress compared to vehicle control (only 39.9 ± 1.9%, **Fig. 3A**) [163]. In comparison, treatment of same amount of HEX and HTA did not have any significant effects compared to control.

We then tested the possible alteration of various key regulators involved in cell cycle progression, *e.g.* cyclin D, p21 and p27, *etc*, in HCA-7 cells upon 8-HOA treatment [163]. Among all the test proteins, it was found that 8-HOA could up-regulate the expression of p27, a cyclin-dependent kinase inhibitor commonly involved in G1 arrest[165], which may explain the observed G1 arrest from 8-HOA treatment in HCA-7 cells (**Fig. 3B)**. Again, other treatments including HEX and HTA did not have a significant effect on p27 expression.

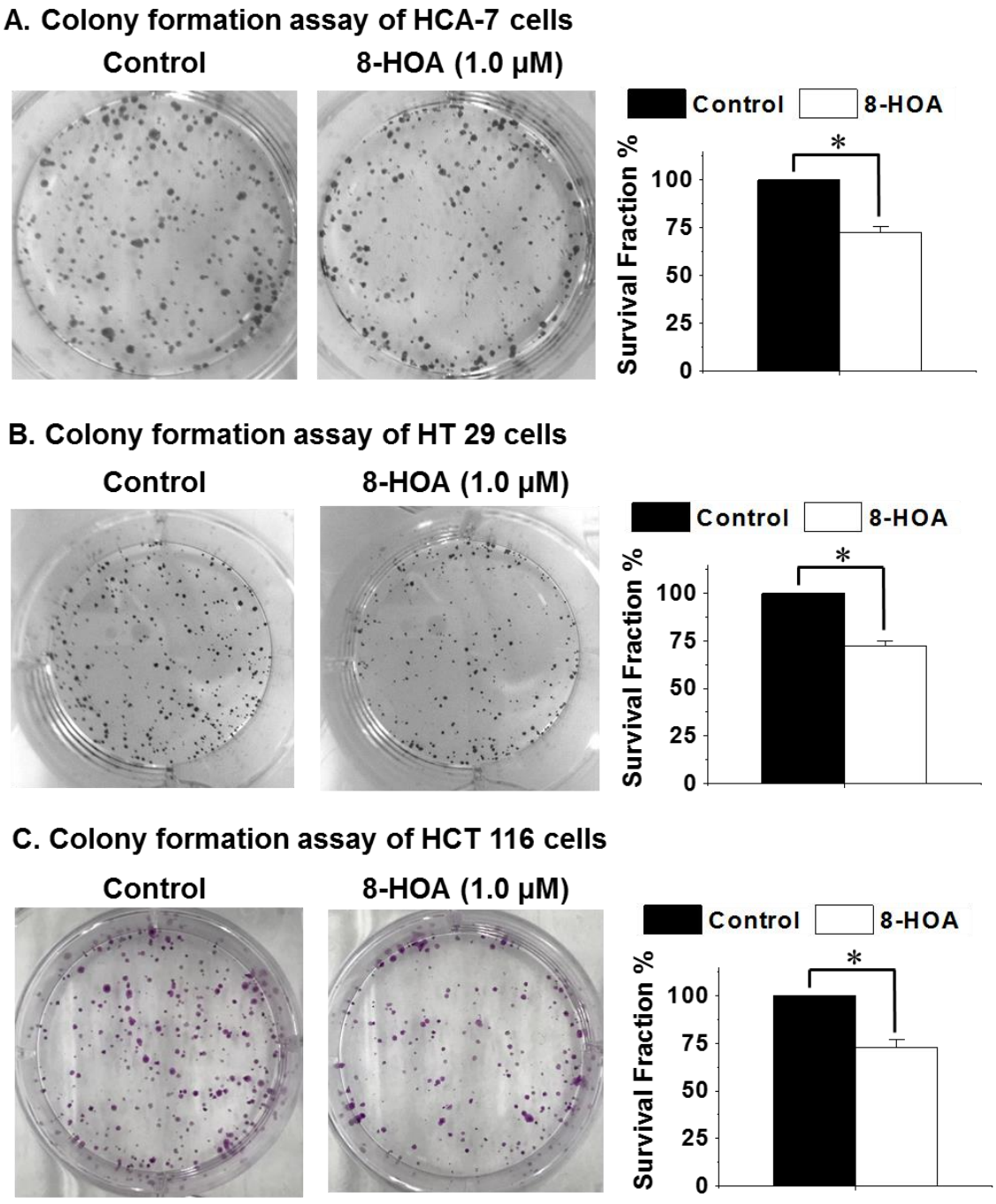

Figure 2. 8-HOA inhibited colony formation of human colon cancer cells.
Colony formation assay of **A.** HCA-7, **B.** HT-29 and **C.** HCT 116 cells treated with 8-HOA at 1.0 μM for 48 h. Data represent mean ± SD with at least three separate experiments. The survival fractions for control groups are normalized to 100% for every separate experiment. (*: significant difference vs. control with $p < 0.05$).

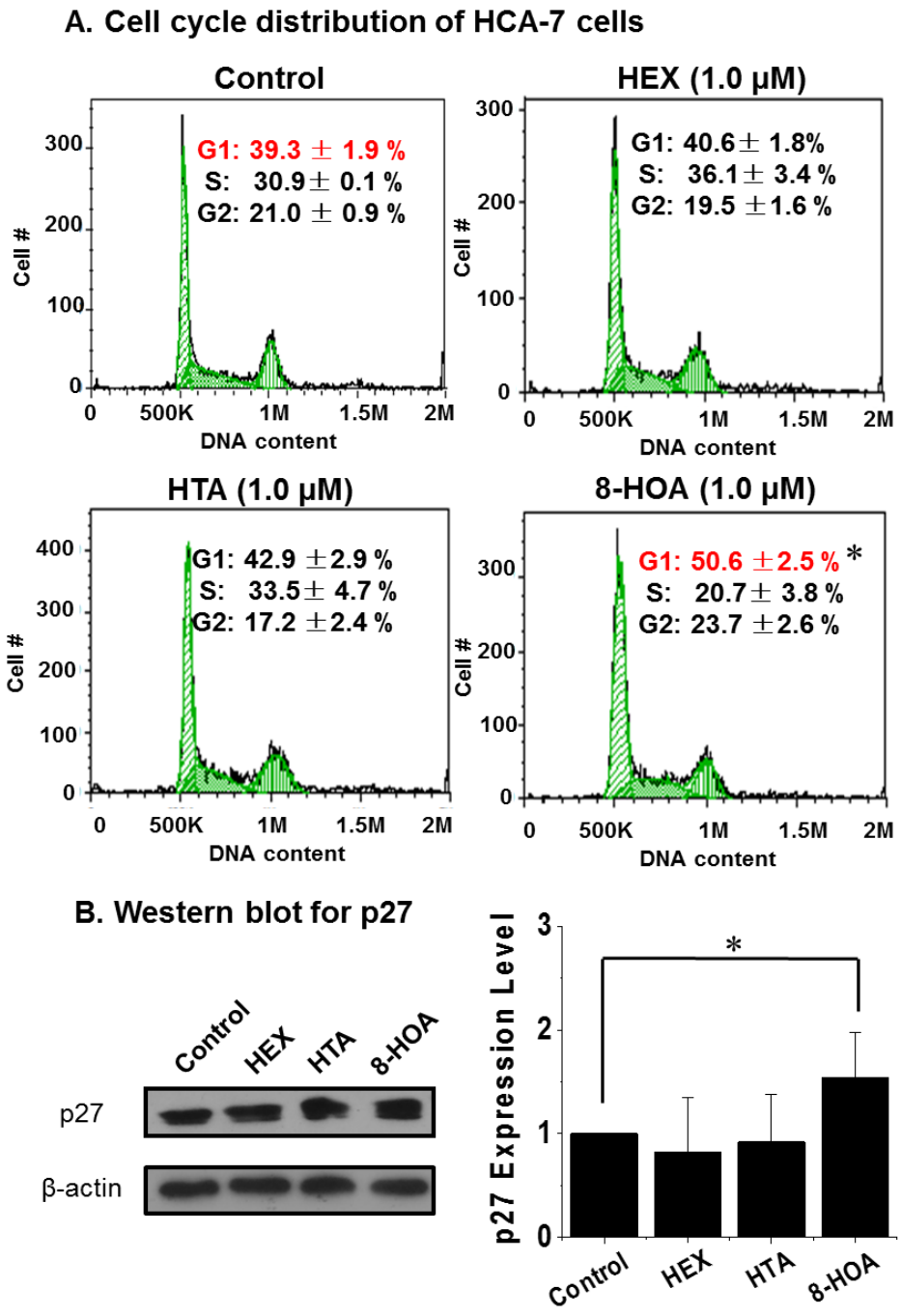

Figure 3. Effect of DGLA's byproducts on cell cycle distribution of HCA-7 cells.
A. Cell cycle distribution of HCA-7 colony 29 cells treated with HEX, HTA or 8-HOA at 1.0 μM for 48 h. **B.** Western blot for p27 expression in HCA-7 cells after 48 h treatment of DGLA's byproducts (1.0 μM). The p27 expression level in individual treatment was calculated as the ratio to beta-actin, and the level in the control group was normalized to 1. Data represent mean ± SD with at least three separate experiments. (*: significant difference vs. control with $p < 0.05$) [163]

3.3. Activation of p53-Dependent Apoptosis by 8-HOA

Apoptosis, a programmed cell death process, plays an important role in the treatment of cancer as it is a major target of many treatment strategies [166]. In our study, to determine whether 8-HOA could inhibit colon cancer cell growth by inducing cell apoptosis, HCA-7 cells were treated with 8-HOA at 1.0 μM for 48 h and subject to Annexin V-FITC/PI double staining followed by flow cytometry analysis for apoptosis.

The results showed that supplementation of 8-HOA led to a significantly increased early apoptotic cell population (10.5 ± 1.9%, stained with Annexin V-positive and PI-negative) compared to vehicle control (4.2 ± 0.8%, **Fig. 4A**) [163]. HTA, another distinct DGLA-derived byproduct, also promoted early cell apoptosis in HCA-7 cells, but with less effect (7.4 ± 0.2%) compared to 8-HOA. In comparison, no significant effect was observed from the treatment of HEX.

We also examined the possible alteration of cancer suppressor p53 (a key protein regulating the cell apoptotic pathway as well as cell cycle [166]) upon 8-HOA treatment. Consistent to the apoptosis data, it was observed that the exclusive DGLA's byproducts HTA and 8-HOA could significantly up-regulate the expression level of p53 in HCA-7 cells, which may be responsible for the observed cell apoptosis, while almost no change in p53 level was observed from the HEX treatment (**Fig. 4B)**.

3.4. Suppressed Colon Cancer Cell Migration by 8-HOA

Besides development of a primary tumor, cancer metastasis is also a severe issue for cancer patients and accounts for around 90% of cancer-associated death [167-169]. Here we tested whether direct treatment of 8-HOA could inhibit migration of colon cancer cells HCA-7.

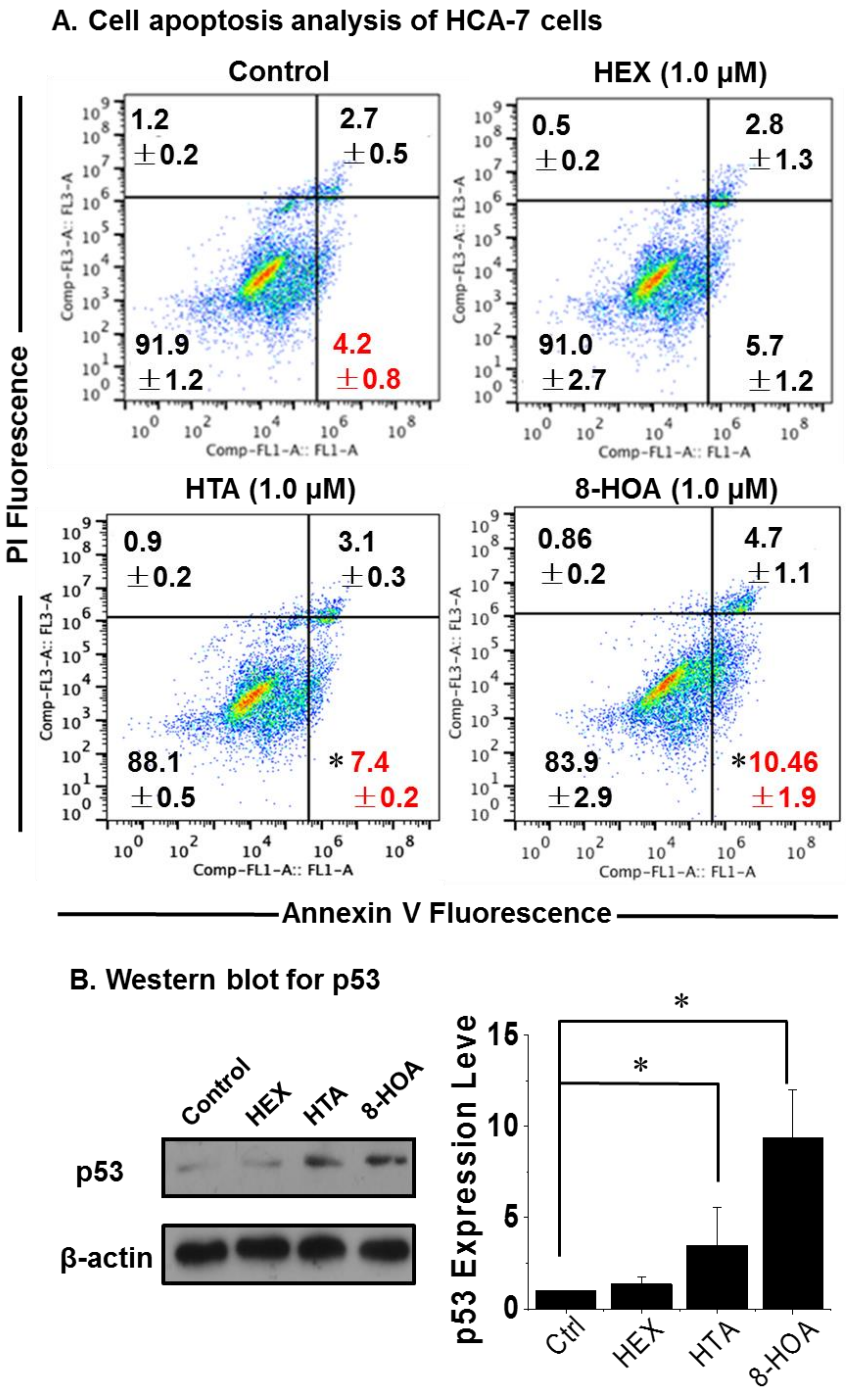

Figure 4. Effect of DGLA's byproducts on HCA-7 cell apoptosis.
A. Flow cytometry analysis (*via* FITC Annexin V/PI double staining) for cell apoptosis of HCA-7 colony 29 cells treated with HEX, HTA or 8-HOA at 1.0 μM for 48 h. **B.W** estern blot for p53 expression in HCA-7 cells after 48 h treatment of DGLA's byproducts (1.0 μM). The p53 expression level in individual treatment was calculated as the ratio to beta-actin, and the level in the control group was normalized to 1. Data represents mean ± SD with at least three separate experiments. (*: significant difference vs. control with $p < 0.05$) [163]

Results from a wound healing assay showed that 48 h of 8-HOA treatment at physiological concentration (1.0 μM) significantly slowed down the migration of HCA-7 cells, evident by a larger wound area (~ 73.0%) remaining at 48 h in the treatment group compared to only 47.4% wound area remaining in the control group (**Fig. 5A**) [170]. Further mechanistic studies showed that 8-HOA treatment led to decreased expressions of matrix metalloproteinase-2 (MMP-2) and matrix metalloproteinase-9 (MMP-9), two proteins involved in cancer cell migration/invasion by degrading extracellular matrix (**Fig. 5B**) [171-172].

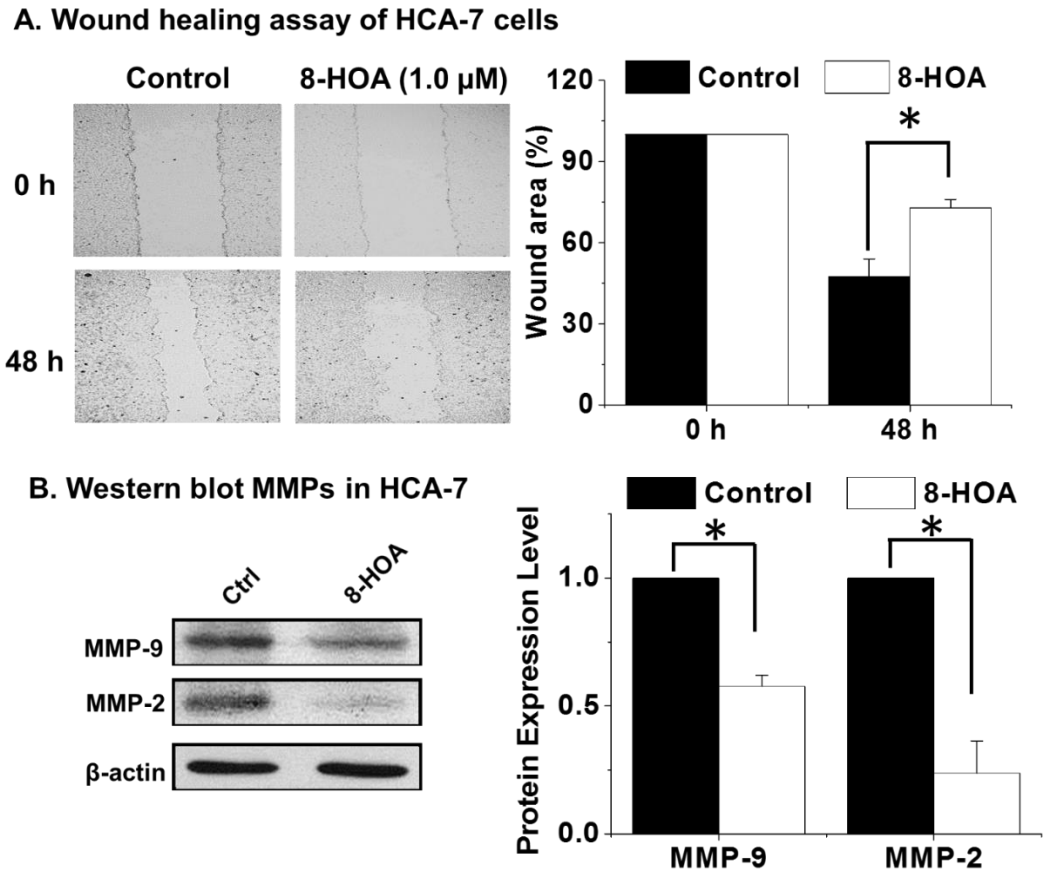

Figure 5. 8-HOA inhibited HCA-7 cell migration.
A. Wound healing assay of HCA-7 cells with 48 h of 8-HOA treatment (1.0 μM). The wound area at 0 h are normalized to 100% for every separate experiment. **B.** Western blot for MMP-2 and MMP-9 expression in HCA-7 cells after 48 h treatment of 8-HOA (1.0 μM). The MMPs expression level in the control group was normalized to 1. β-actin was used as a loading control. Data represents mean ± SD with at least three separate experiments. (*: significant difference vs. control with $p < 0.05$) [170]

3.5. 8-HOA Serves as an Histone Deacetylase Inhibitor and Induces DNA Damage

Histone deacetylases (HDACs) are a family of enzymes that remove acetyl groups from histone, which is an epigenetic modification widely involved in gene transcription, DNA replication, cell cycle progression, gene silencing, and genotoxic response [173-174]. It has been documented that HDACs may play important roles in regulating colon cell maturation and transformation, and their expression is upregulated in colon tumors. Consistently, downregulation of specific HDACs by HDAC inhibitors was shown to inhibit colon cancer growth and migration *in vitro* and *in vivo* [173-175].

Interestingly, research showed that various short chain fatty acids, such as butyrate and valproic acid, are potent inhibitors of HDACs and shown to inhibit cancer cell growth and migration, and induce cell cycle arrest and apoptosis in many types of cancer [175-180]. For example, it was reported that butyrate could inhibit Sp1/Sp3-associated HDAC activity, thereby leading to histone hyperacetylation and transcriptional activation of the p21 gene, which resulted in cancer cell cycle arrest [177]. Butyrate was also found to inhibit colon cancer cell invasion by regulating the expression of c-Src and focal adhesion kinase [175]. Valproic acid was shown to inhibit HDACs and consequently down-regulate amyloid precursor protein and inhibit colon cancer cell proliferation [180]. In addition, it was reported that concurrent application of HDAC inhibitors could improve chemotherapy and radiotherapy in colorectal cancer [179-182].

These observations led us to propose that 8-hydroxyloctanoic acid, as a short chain fatty acid, may also inhibit HDAC activity which is responsible for the observed growth and migration inhibitory effects (Fig. 1-5). In fact, a previous study from Gilbert *et al* was carried out to investigate the structure-activity relationship of short chain fatty acids as HDAC inhibitors [183].

It was found that heptanoic acid and octanoic acid could also inhibit HDAC activity in HeLa cell nuclear extracts, although only with ~50% potency compared to butyrate.

Consistently, in this study, results from the HDAC activity assay showed that 48 h of 8-HOA treatment led to significant inhibition of HDAC activity in HCA-7 cells, *e.g.* 63.9% remaining activity compared to 100% in the vehicle control (**Fig. 6A**). In association with that, western blot data showed that 8-HOA treatment led to a significant accumulation of acetyl histone H3 (AcH3, a substrate of HDAC) in HCA-7 cells, indicating suppressed HDAC activity (**Fig. 6B-C**) [164]. In addition, it has been reported that inhibition of HDAC could trigger DNA damage thereby inducing cell death in various cancer cells [184-185]. Consistent with that, here we also observed significant upregulation of γH2AX upon 8-HOA treatment, which is a sensitive marker for DNA double-strand breaks (Fig. 6B-C) [164, 184]. Together, these data together indicated that 8-HOA, by inhibiting deacetylation of histone, could regulate gene transcription and induce DNA damage, then subsequently induce cell cycle arrest and apoptosis, eventually resulting in the suppression of cancer cell growth and migration (**Scheme 8**).

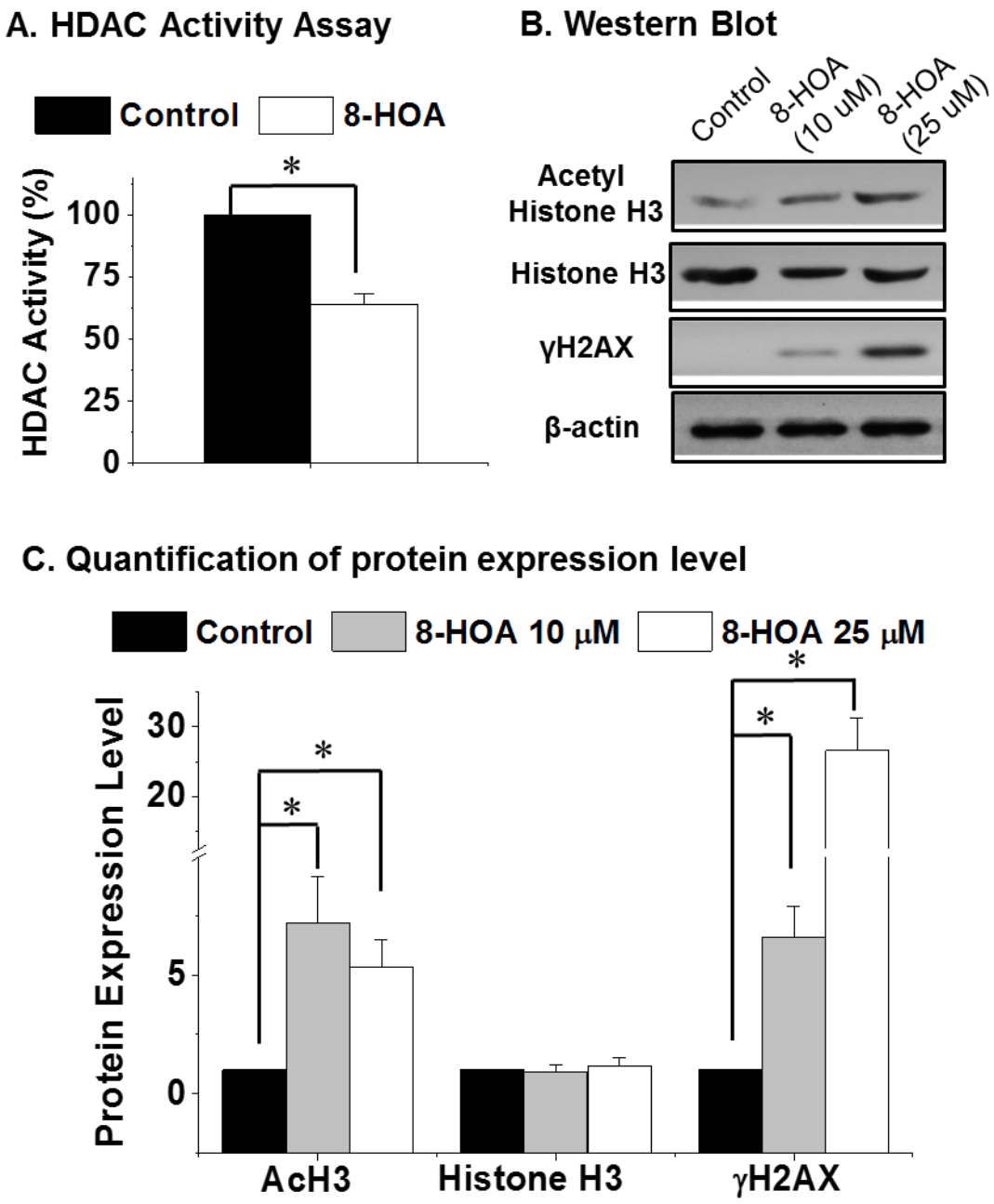

Figure 6. Inhibition of HDAC activity in HCA-7 cells by 8-HOA.
A. HDAC activity assay of HCA-7 cells treated with 10 μM 8-HOA for 48 h, and **B-C.** Western blots and quantification for acetyl-histone H3, histone H3 and γH2AX expression in HCA-7 cells treated with 8-HOA (10 and 25 μM) for 48 h. The proteins expression level in individual treatment was calculated as the ratio of target protein to β-actin, and the ratio in the control group was normalized to 1. Data represents mean ± SD with at least three separate experiments. (*: significant difference vs. control with $p < 0.05$) [164]

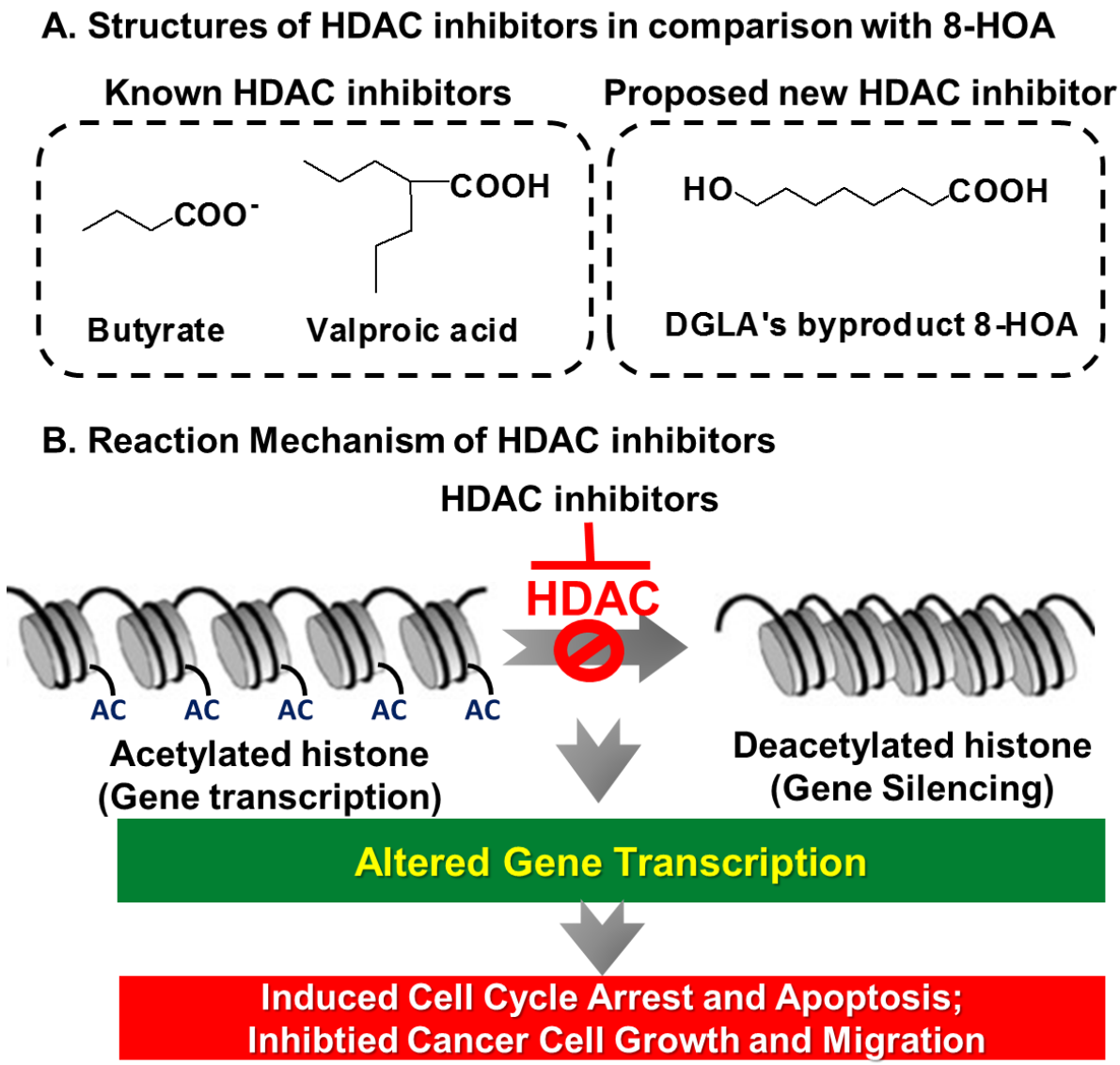

Scheme 8. 8-HOA serves as an HDAC inhibitor and inhibits colon cancer growth and migration. **A.** Structures of known HDAC inhibitors in comparison with 8-HOA. **B.** Action mechanism for HDAC inhibitors. Short chain fatty acids such as butyrate, valproic acid and 8-HOA could inhibit HDAC activity and regulate the expression of genes involved in cancer growth and migration, therefore, exerting anti-cancer effects.

3.6. Improved Anti-Cancer Effects from Combination of 8-HOA and Chemo-Drug

Chemo-resistance has been a major obstacle for cancer therapy [186]. For example, 5-fluorouracil (5-FU) is one of the most commonly used first-line chemo-drugs in colon cancer, it is a pyrimidine analog and acts as a thymidylate synthase inhibitor to interfere with DNA synthesis and inhibit cancer cell growth. However, many cancer cell lines are resistant to 5-FU's cytotoxicity [187]. Therefore, combinations of 5-FU with various other cancer therapeutic agents as well as fatty acid supplementation have been extensively studied to enhance the efficacy of 5-FU against cancer [188-194]. Here we tested whether 8-HOA could improve the efficacy of 5-FU on a resistant colon cancer cell line HCA-7 colony 29.

Consistent with the study from other research [190], our data from MTS assay showed that the HCA-7 colony 29 cells are insensitive to 5-FU with an observed IC50 around 1.0 mM (**Fig. 7A**), while concurrent treatment of 8-HOA (1.0 μM) led to a better growth inhibitory effect compared to 5-FU treatment alone at various concentrations [163]. For example, 5-FU treatment alone at 0.25 mM reduced HCA-7 cell viability to 78.3 ± 7.3% compared to 100% in control, while combination of 5-FU and 1.0 μM 8-HOA further reduced the cell viability to 61.1 ± 11.3%; concurrent application of 0.5 mM 5-FU and 1.0 μM 8-HOA reduced cell viability to 50.6 ± 4.4% compared to 64.3 ± 3.3% in 5-FU treatment alone; and the combination of 1.0 mM 5-FU and 1.0 μM 8-HOA reduced the cell viability to 44.8 ± 2.4% compared to 51.7 ± 2.3% in 5-FU treatment alone (Fig. 7A). Noteworthy, a decreased IC 50 at ~ 0.5 mM of 5-FU was achieved when the cells were concurrently treated with 5-FU and 8-HOA. Consistently, concurrent supplementation of 8-HOA in HT-29 and HCT 116 cells led to better growth inhibitory effects compared to 5-FU alone at a range of concentrations (**Fig. 7B-C**). In fact, an improved IC50 for 5-FU was achieved in both of HT-29 (from original 10 μM to 5.0 μM) and HCT 116 cells (from original 2.5 μM to 1.0 μM).

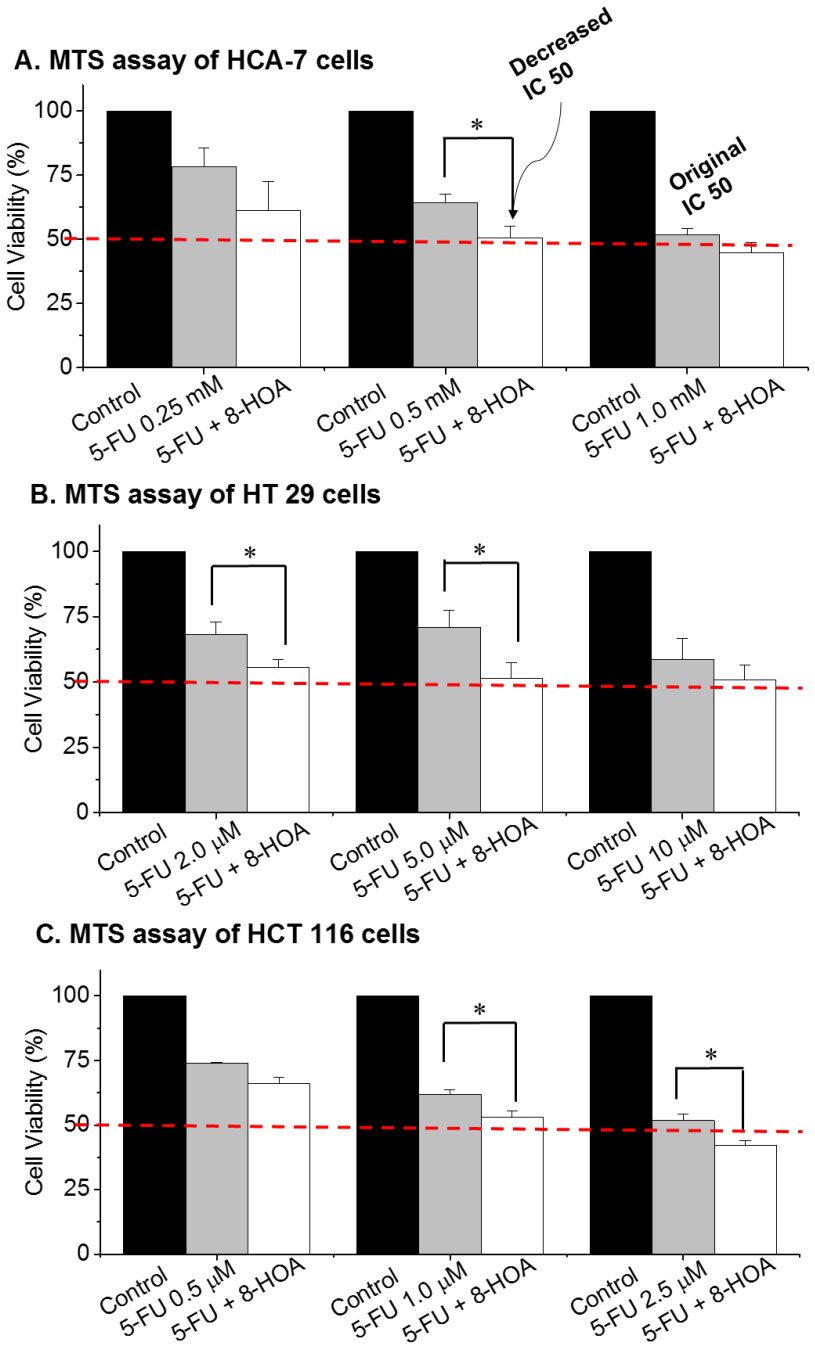

Figure 7. Cell viabilities after 48 h combined treatment of 5-FU and 8-HOA.
A. MTS assay of HCA-7 colony 29 cells treated with 5-FU (0.25, 0.5 and 1.0 mM) alone or in combination with 8-HOA (1.0 μM) for 48 h. **B.** MTS assay of HT-29 cells treated with 5-FU (2.0, 5.0 and 10 μM) alone or in combination with 8-HOA (1.0 μM) for 48 h. **C.** MTS assay of HCT 116 cells treated with 5-FU (0.5, 1.0 and 2.5 μM) alone or in combination with 8-HOA (1.0 μM) for 48 h. Cell viability was presented as the percentage compared to control (treated with vehicle). Red dash line indicates 50% inhibitory effect. Data represents mean ± SD with at least three separate experiments. The cell viabilities for control groups are normalized to 100% for every separate experiment. (*: significant difference with $p < 0.05$)

3.7. Conclusion And Discussion

Previous results from our group first showed that DGLA could go through a unique C-8 oxygenation pathway during COX-catalyzed peroxidation to produce exclusive free radicals, *e.g.* 8-HOA [136-138, 163]. In this chapter, we demonstrated that 8-HOA could serve as an HDAC inhibitor and DNA damage reagent, which affect the expressions of key regulators (*e.g*. p27 and p53) in cancer cell growth and migration, thereby inducing cell cycle arrest and apoptosis [163-164, 170]. We also showed that concurrent supplementation of 8-HOA could enhance 5-FU's cytotoxicity towards resistant colon cancer cells [163].

Prostaglandin E1 is one of the major metabolites from DGLA peroxidation and has been reported to possess certain anti-inflammation and anti-cancer effect [159-162]. Therefore, people generally considered PGE1 the major beneficial bioactive metabolite from DGLA. Here we tested the potential effect of PGE1 on colon cancer cell growth at the concentration range from 0.1 μM to 10 μM. The tested concentration range was selected based on PGE1 production from cells treated with 100 μM of DGLA [164]. However, our data showed that the cell growth of all three tested cell lines was not affected by PGE1 treatment (Fig. 1), probably due to the low (but physiological relevant) concentration employed in our experiment compared to that in other research [159-162, 195]. On the other hand, the exclusive DGLA byproduct 8-HOA was found to significantly inhibit cancer cell growth at the same concentration range, suggesting that 8-HOA may be actually responsible for the anti-cancer effects of DGLA at physiological conditions (Figs. 1-2).

To investigate how 8-HOA could regulate colon cancer cell growth, we also examined the cell cycle distribution and apoptosis in HCA-7 cells upon 8-HOA treatment. Results showed that 8-HOA could arrest cell cycle progression at the G1 phase and induce apoptosis, and was

associated with a significant induction of a cell cycle inhibitor p27 and a cancer suppressor p53 (Figs. 3-4). In fact, our results showed that 8-HOA could inhibit the growth of cell lines with different p53 status, *e.g.* HCA-7 cells (wt-/mutant p53 heterozygous), HT-29 cells (mutant p53) and HCT 116 (wt-p53) (Fig. 1), indicating that 8-HOA could cause cancer cell death *via* p53-dependent as well as p53-independent mechanisms. Considering the fact that many cancer cells bear a mutant p53 gene, in our future study we will further investigate the possible p53-independent mechanism by which 8-HOA could deliver anti-cancer effects.

Our results also showed that 8-HOA could act as an HDAC inhibitor and consequently lead to DNA damage, which may explain the observed cell cycle arrest, apoptosis and growth inhibition in colon cancer cells (Fig. 6). However, HDAC consists of a family of iso-forms which may interact with various target proteins, and HDAC inhibition may lead to various biological consequences through different mechanisms [173-179, 184-185]. Therefore, further mechanistic and kinetic studies are required to elaborate whether and how 8-HOA could interact with specific HDACs and trigger inhibitory effects on cancer cell growth and migration.

5-FU is a pyrimidine analog which induces cancer cell apoptosis by interfering with DNA replication. It has been widely used as a first line of standard chemotherapy for patients with advanced colorectal cancer. However, chemoresistance to 5-FU remains a major limitation of 5-FU-based cancer therapy [187]. We proposed and tested the ability of DGLA's byproduct 8-HOA to enhance the cytotoxicity of 5-FU in the human colon cancer cell line, HCA-7 colony 29, which is reported as 5-FU insensitive (IC50 = 1.1 mM) [190]. In fact, a significantly improved IC50 of 5-FU (to 0.5 mM) was observed when the cells were treated with 5-FU in combination with 8-HOA (Fig. 7) [163]. Similar effects were also achieved in HT-29 and HCT 116 cells, indicating

such combination may result in a better therapeutic outcome in colon cancer compared to 5-FUalone.

COX-2 is overexpressed in 85% of adenocarcinomas and can promote cancer development by catalyzing AA peroxidation to produce PGE2 [25-28]. Therefore, COX-2 inhibition has become a conventional strategy for the treatment of cancers [106-108]. However, COX-2 can be induced rapidly in the cancer environment even with the presence of COX-2 inhibitors, which raises the question about the therapeutic efficacy from COX-2 inhibitors in cancer patients [31]. In addition, COX-2 inhibitors can cause critical safety issues, including severe gastrointestinal tract injury and increased risk of cardiovascular diseases (*e.g.*, heart attacks and strokes) [30, 32-34]. The results from this chapter showed that, under the catalysis of COX-2, DGLA can produce the beneficial byproduct 8-HOA with anti-cancer activity. This new observation leads to a possibility that instead of inhibiting COX-2, one can take advantage of the high COX-2 expression in cancer cells to produce DGLA-derived beneficial metabolites to control cancer cell growth. This innovative idea of making use the hallmark of cancer cell (*i.e.* high levels of COX-2) to work against cancer cell itself may provide a novel insight into cancer therapy and may challenge the current paradigm of COX biology in cancer treatment.

In summary, results from this chapter provide the first evidence demonstrating that the exclusive DGLA free radical byproduct 8-HOA inhibited colon cancer cell growth and migration, induced cell cycle arrest and apoptosis, and these effects may be mediated by HDAC inhibition. This may explain the reported anti-cancer activities for DGLA.

4. D5D KNOCKDOWN PROMOTED 8-HOA FOMATION FROM COX-2 CATALYZED DGLA PEROXIDATION AND INHIBITED COLON CANCER CELL GROWTH/MIGRATION

Our results from Chapter 3 showed that the distinct byproduct 8-HOA produced from COX-2 catalyzed DGLA peroxidation can serve as an HDAC inhibitor and suppress colon cancer cell growth and migration. These observations indicated that DGLA may represent a promising dietary factor for cancer treatment. However, DGLA can be effectively converted to its downstream ω-6 fatty acid arachidonic acid by delta-5-desaturase, which greatly restricts DGLA's bioavailability and activity [139]. We proposed that knockdown of D5D could limit the conversion from DGLA to arachidonic acid, thus promote 8-HOA formation from COX-2 catalyzed DGLA peroxidation to a threshold level which could inhibit colon cancer growth and migration. To test this hypothesis, we knocked down D5D expression in HCA-7 cells (high COX-2 expression) *via* siRNA transfection, and assessed the cell growth response upon DGLA treatment *via* various biological analyses.

COX-2 is overexpressed in 85% of adenocarcinomas, and it can promote colon cancer progression by catalyzing arachidonic acid peroxidation to produce the deleterious metabolite PGE2 [106-109]. Therefore, COX-2 inhibition, which aims at limiting the COX-2/arachidonic acid pathway, has been extensively studied as a conventional strategy for the treatment of cancers. However, COX-2 can be induced rapidly in cancer environment even with the presence of COX-2 inhibitors, therefore COX-2 inhibitors failed in clinic treatment for cancer patient [31]. In addition, application of COX-2 inhibitors is associated with a high risk of GI injury and cardiovascular side effects in patients [30, 32-34].

In our research, instead of inhibiting COX-2, we aimed to take advantage of the high COX-2 expression in cancer cells to produce the DGLA-derived beneficial byproduct 8-HOA to control cancer cell growth. Therefore, three colon cancer cell lines with different COX-2 expression levels were tested in our study. In addition, a COX-2 knockdown analog of HCA-7 cells was also included to investigate the role of COX-2 in our proposed novel strategy. We anticipate that our novel strategy will result in a dual mechanism for inhibiting cancer growth, *i.e.* promoting anti-cancer effect with DGLA, at the meantime limiting the pro-cancer effect with AA. Therefore, it will lead to a better therapeutic effect in colon cancer treatment compared to the traditional COX-2 inhibition strategy.

4.1. D5D-Knockdown and DGLA Supplementation Inhibited Colon Cancer Cell Growth

SiRNA (small interfering RNA) is a synthetic RNA duplex which specifically binds to a target mRNA for degradation. It is commonly used for inducing transient silencing of protein coding genes. In our study, in order to limit the conversion of DGLA to AA and promote 8-HOA formation, we transfected HCA-7 colony 29 cells with D5D targeted siRNA, which contains a sense strand of ACAUCAUCCACUCACUAAAtt and an antisense strand of UUUAGUGAGUGGAUGAUGUcg. The D5D knockdown efficacy was then evaluated by western blot and qRT PCR analysis. Results showed that siRNA transfection in HCA-7 cells led to significantly less D5D mRNA and protein expression levels (~30% remaining) compared to those in cells transfected with negative control siRNA (**Figs. 8A-B**) [164].

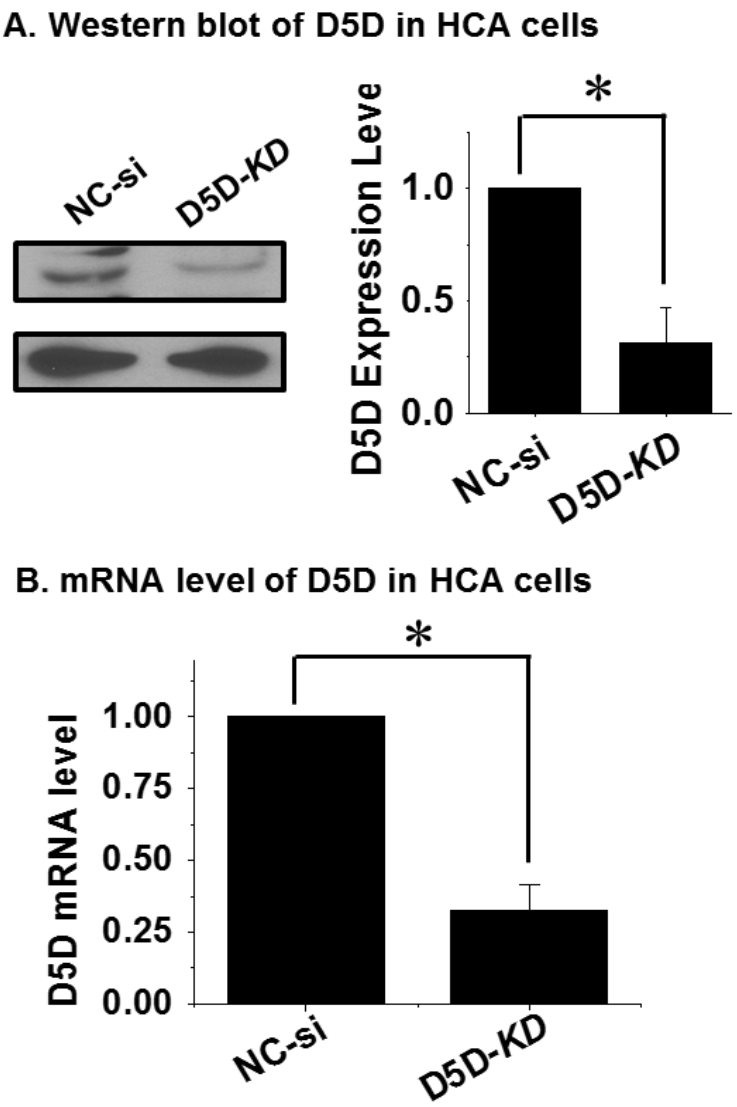

Figure 8. Knockdown of D5D expression in HCA-7 cells by siRNA transfection.
A. Western blot and relative expression level of D5D in negative siRNA transfected (Nc-si) and D5D-siRNA transfected (D5D-*KD*) HCA-7 colony 29 cells (loading control: β-actin). The ratio of D5D to β-actin in control was normalized to 1; **B.** mRNA level of D5D in HCA-7 cells after siRNA transfection. The mRNA level of D5D in control was normalized to 1. Data represents mean ± SD with at least three separate experiments. (*: significant difference with $p < 0.05$)

We proposed that D5D knockdown (D5D-*KD*) would preserve DGLA to promote endogenous 8-HOA formation, thereby eliciting anti-cancer effects. Hence, after confirming D5D-*KD* efficiency in HCA-7 cells, we performed colony formation assay to test whether D5D-*KD* along with DGLA treatment could inhibit colon cancer cell growth as observed from direct 8-HOA treatment. Results showed that 48 h treatment of 100 μM DGLA significantly inhibited the colony formation in D5D-*KD* HCA-7 cells with a surviving fraction of 66.8 ± 5.7% vs. 100% in vehicle control, while no growth inhibition effect was observed from DGLA treatment on the control siRNA transfected cells (surviving fraction: 98.4 ± 7.3%, **Fig. 9A-B**) [164].

4.2. Anti-Migration Effect from D5D-*KD* and DGLA Supplementation in Colon Cancer Cells

In Chapter 3, we demonstrated that direct 8-HOA treatment could inhibit colon cancer cell migration (Fig. 5) [170], therefore, here we tested whether D5D-*KD* along with DGLA supplementation could also inhibit HCA-7 cell migration by promoting the formation of 8-HOA from cells.

Results from the wound healing assay showed that DGLA treatment (100 μM, 48 h) in D5D-*KD* HCA-7 cells significantly inhibited cell migration evident by a larger wound area remaining (75.0%) at 48 h compared to 45.3% in the control group (**Fig. 10A**). Consistent with the wound healing assay, results from the transwell assays showed that 48 h DGLA treatment in D5D-*KD* HCA-7 cells resulted in a significant inhibitory effect on cancer cell migration and invasion, evidenced by less migrated and invaded cells compared to vehicle control groups (**Fig. 10B-C**) [170].

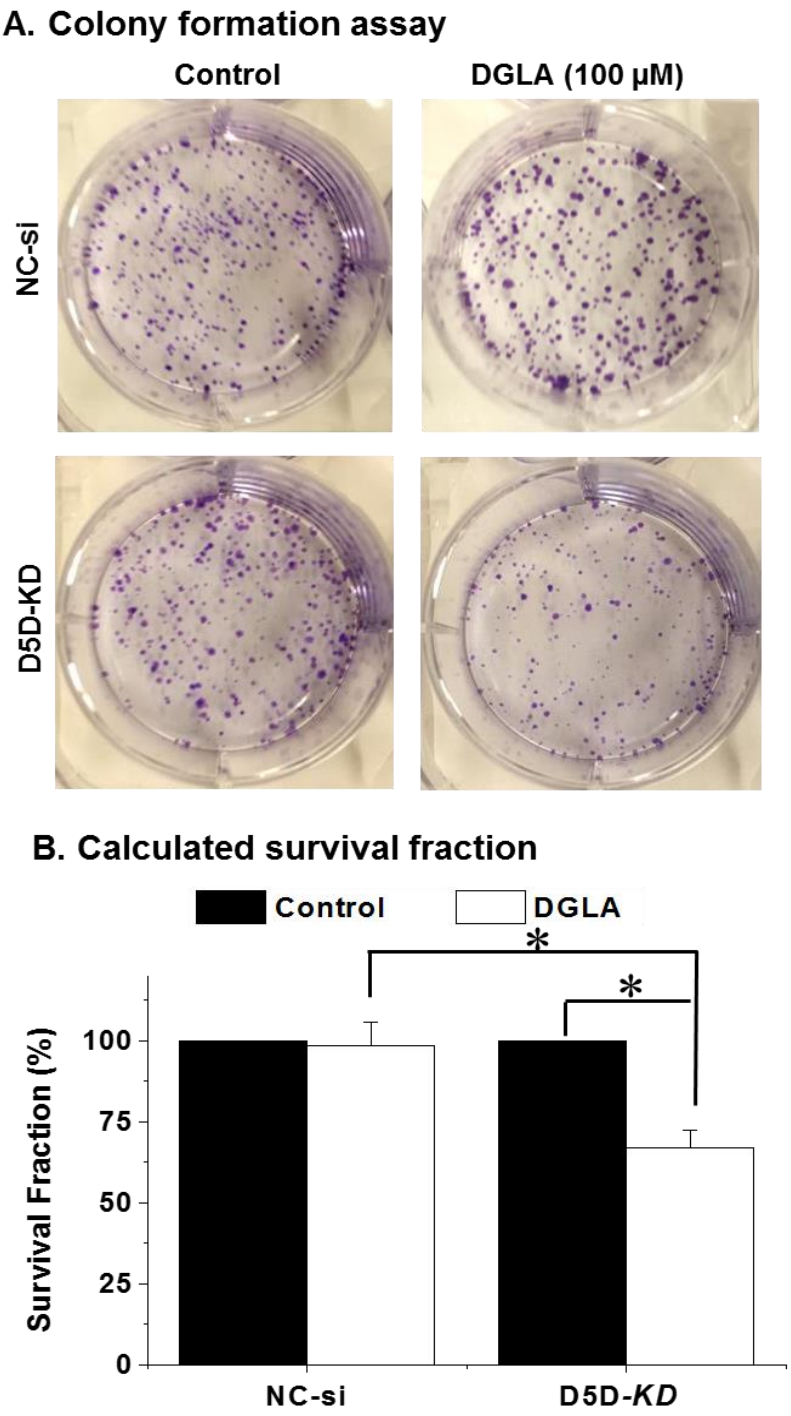

Figure 9. D5D knockdown and DGLA treatment inhibited HCA-7 cell growth.
A. Colony formation of Nc-si or D5D-*KD* HCA-7 cells 10 days after DGLA treatment (100 μM for 48h); **B.** Calculated survival fraction from colony formation assay. Data represent mean ± SD with at least three separate experiments. The survival fractions for control groups are normalized to 100% for every separate experiment. (*: significant difference with $p < 0.05$) [164]

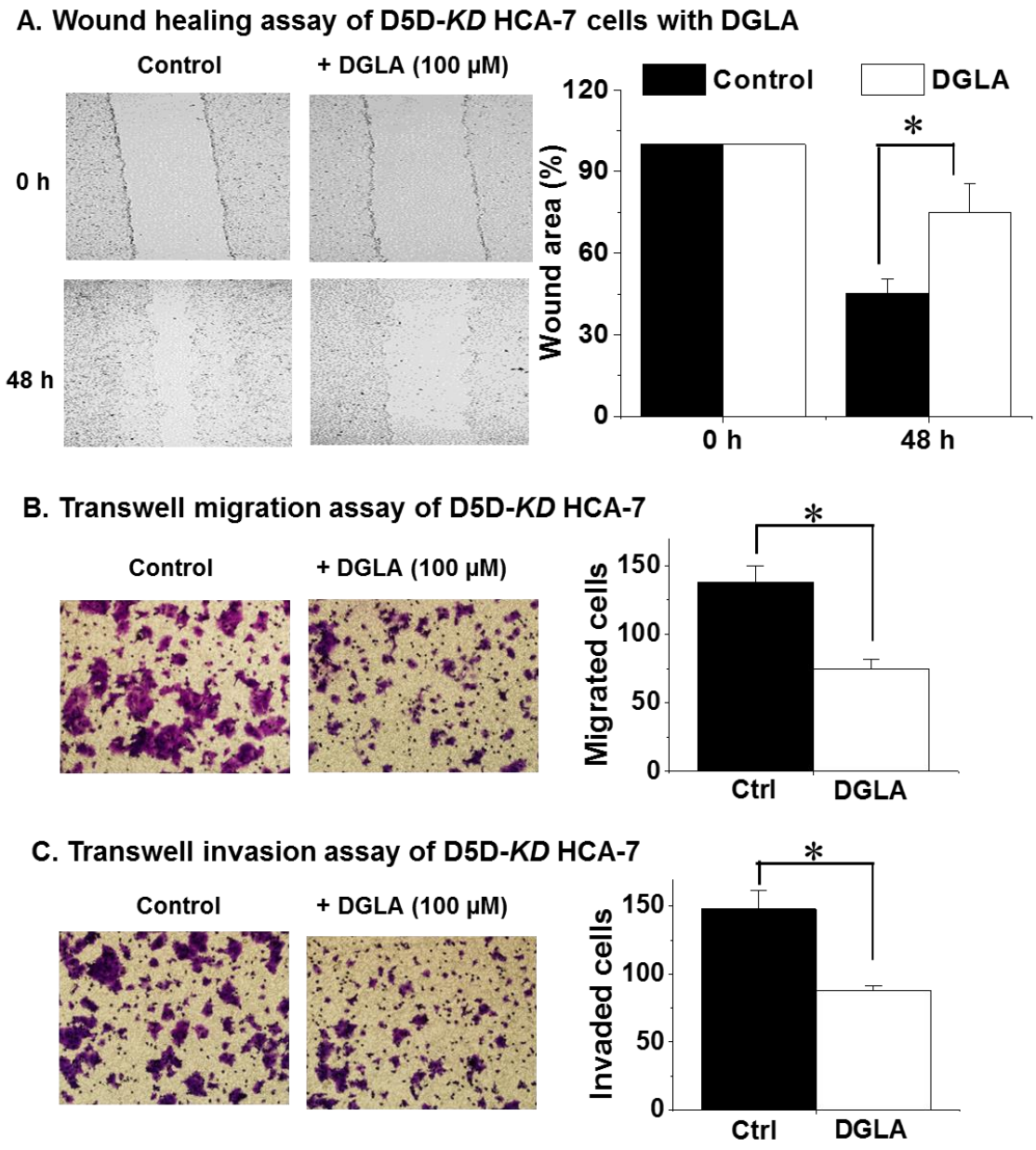

Figure 10. D5D-*KD* and DGLA supplementation inhibited migration/invasion in HCA-7 cells. **A.** Wound healing assays of D5D-*KD* HCA-7 cells upon DGLA (100 μM, 48 h) treatment vs. controls (without DGLA). The wound area at 0 h for both control and DGLA treatment groups are normalized to 100% in order to calculate the percentage of wound area at 48 h. **B.** Transwell migration assay of D5D-*KD* HCA-7 cells upon DGLA (100 μM, 48 h) treatment vs. controls; **C.** Transwell invasion assay of D5D-*KD* HCA-7 cells upon DGLA (100 μM, 48 h) treatment vs. controls; Data represent mean ± SD with at least three separate experiments. (*: significant difference with $p < 0.05$) [170]

4.3. D5D-*KD* Promoted 8-HOA Formation from COX-2 Catalyzed DGLA Peroxidation

We proposed that D5D knockdown in HCA-7 cells could limit the conversion of DGLA to AA, therefore reserving more DGLA to promote 8-HOA production from COX-2 catalyzed peroxidation. To test this hypothesis, we quantified the levels of free DGLA, AA and their corresponding COX-2-catalyzed metabolites (*e.g.* PGE1 and PGE2) in D5D-*KD* and Nc-si HCA-7 cells treated with 100 μM DGLA.

HPLC/MS data showed that, during 48 h incubation with DGLA, D5D-*KD* cells always have a higher level of free DGLA and less free AA compared to those in Nc-si cells, indicating that D5D-*KD* could effectively limit the conversion of DGLA to AA (**Fig. 11A-B**) [164]. Notably, although the free DGLA decreased overtime in both D5D-*KD* and NC-si cells (due to cellular consumption), there is still much higher DGLA available in D5D-*KD* cells at 48 h (4.3 ± 0.3 μM), while there is only 0.9 ± 0.3 μM remaining in Nc-si cells.

Consistently, we also observed a significant increase of PGE1, the most stable metabolite from DGLA peroxidation, in D5D-*KD* cells compared to those Nc-si cells (**Fig. 11C**). For example, in Nc-si cells, PGE1 retained a stable concentration range (0.35 μM to 0.39 μM) during the 48 h incubation, while PGE1 in D5D-*KD* cells was able to accumulate from ~0.5 μM (8 h-12 h) to 0.8 μM in 48 h. We previous observed that PGE1 did not inhibit cancer cell growth at a concentration range from 0.1 μM to 10 μM (Fig. 1), thus, these data together suggested that DGLA's anti-cancer activity is not from PGE1 at a physiologically relevant concentration. In addition, consistent with the decreased AA level in D5D-*KD* cells, we also observed a significant decrease of PGE2 level in D5D-*KD* cells compared to that in Nc-si cells during a 48 h incubation (**Fig. 11D**), suggesting that D5D-*KD* not only accumulated byproduct from DGLA, but can also limited the production of PGE2 from AA and achieve a similar outcome as a COX-2 inhibitor.

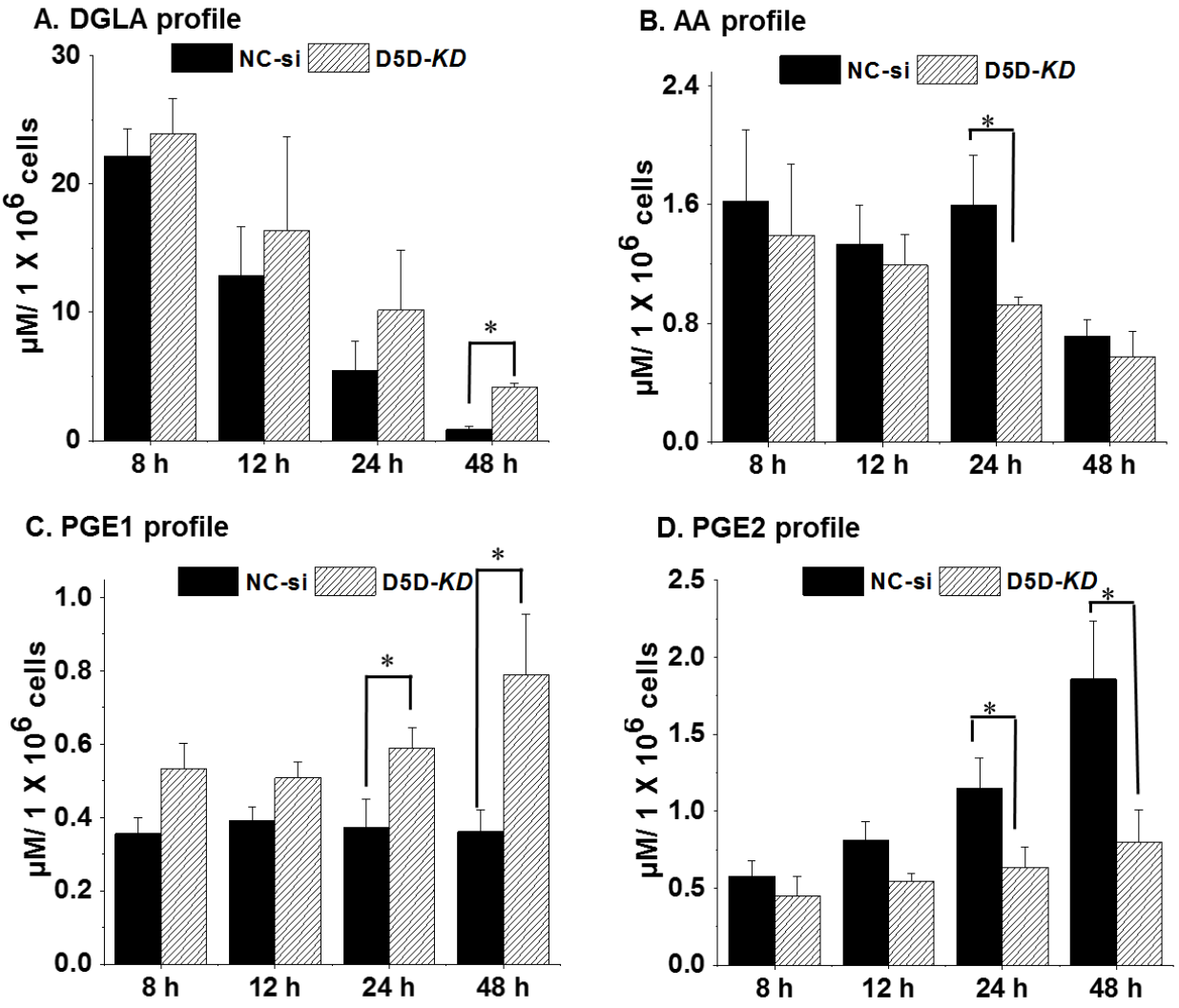

Figure 11. D5D-*KD* preserved DGLA while limiting arachidonic acid synthesis in HCA-7 cells. **A-B.** LC/MS quantification of DGLA and AA from cell medium containing 1.0×10^6 of Nc-si or D5D-*KD* HCA-7 cells after DGLA treatment (100 μM); **C-D.** LC/MS quantification of PGE1 and PGE2 from cell medium containing 1.0×10^6 of Nc-si transfected or D5D-*KD* HCA-7 cells after DGLA treatment Data represents mean ± SD with at least three separate experiments. (*: significant difference with $p < 0.05$) [164]

We proposed that the anti-proliferation and anti-migration effect observed after DGLA supplementation is actually derived from its distinct byproduct 8-HOA. Therefore, we also quantified the endogenous formation 8-HOA in HCA-7 cells after DGLA treatment. As expected, we observed a significant increase of 8-HOA in D5D-*KD* cells compared to that in Nc-si cells (**Fig. 12A**). GC/MS data showed that 8-HOA accumulated and reached a plateau at 24 h to 48 h (0.92 ± 0.09 μM at 48 h) in D5D-*KD* HCA-7 cells treated with DGLA. However, in Nc-si HCA-7 cells, 8-HOA only reached at maximal level of ~ 0.5 μM at the 24 h time point. Our previous observation in Chapter 3 showed that 8-HOA significantly inhibited HCA-7 cell growth at a dose of 1.0 μM (Fig. 1), thus, these data together suggested that 8-HOA is the bioactive metabolite responsible for the anti-cancer effects of DGLA, and to maintain a threshold range of endogenous 8-HOA, ~ 0.5 μM to 1.0 μM, is essential for eliciting DGLA's anti-cancer activity.

We have previous demonstrated that direct treatment of 8-HOA could inhibit HDAC activity and induce DNA damage in HCA-7 cells, which is responsible for its anti-cancer effects (Fig. 6) [164]. Consistently, results from western blot analysis showed that DGLA treatment in D5D-*KD* HCA-7 cells also resulted in a significant increase of acetyl histone H3 and γH2AX (**Fig. 12B**), which is similar to the observation from exogenous 8-HOA treatment, suggesting the observed anti-cancer effect of DGLA in D5D-*KD* cells is indeed derived from formation of 8-HOA.

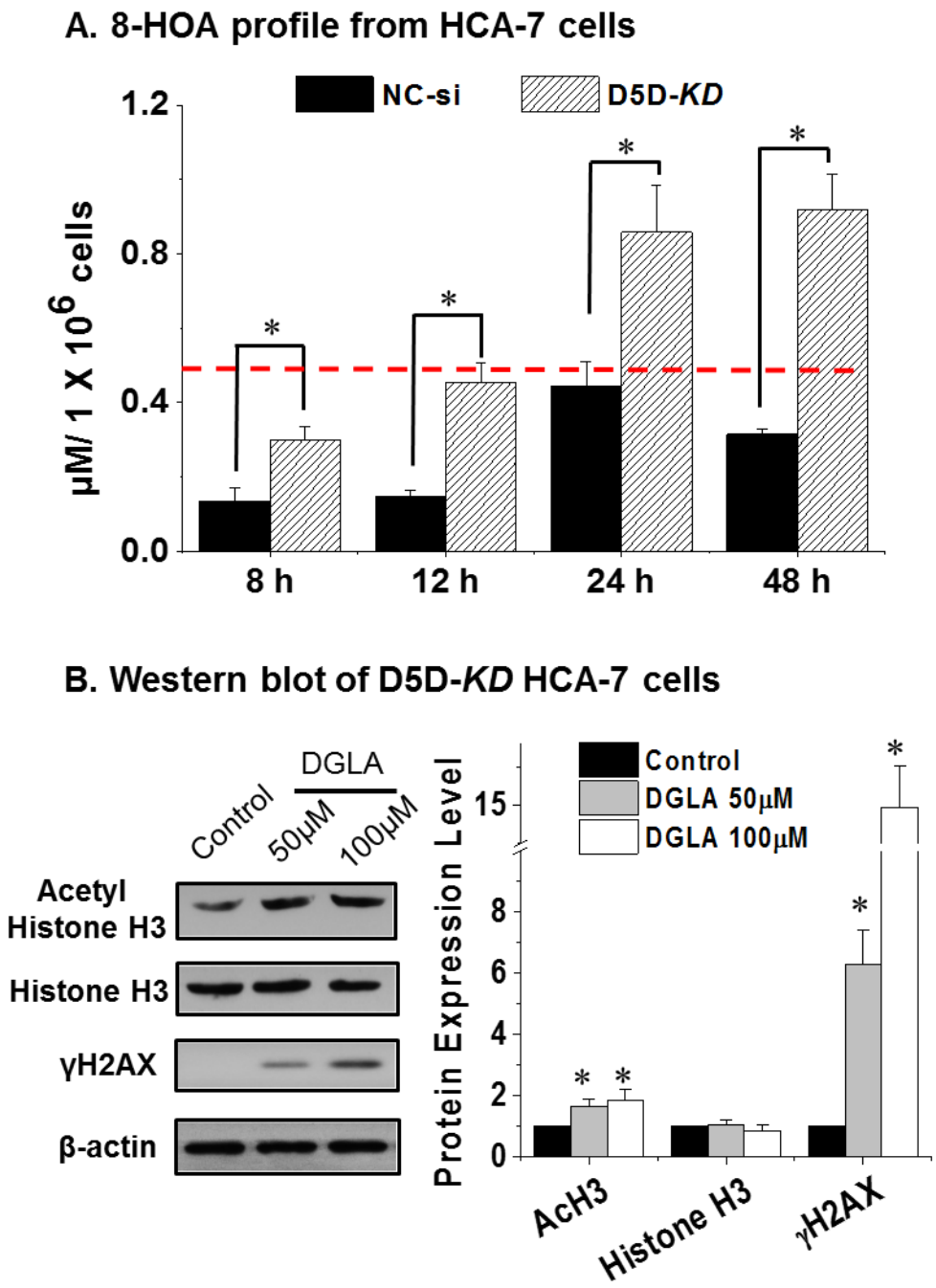

Figure 12. HDAC inhibition by promoted 8-HOA formation in D5D-*KD* HCA-7 cells.
A. GC/MS quantification of 8-HOA from cell medium containing 1.0×10^6 of Nc-si or D5D-*KD* HCA-7 cells after DGLA treatment. Red dash line indicates the propose threshold level of endogenous 8-HOA; **B.** Western blot of acetyl-histone H3, histone H3 and γH2AX in D5D-*KD* HCA-7 cells treated by DGLA (50 and 100 μM). The protein expression level in vehicle control were normalized to 1, β-actin serves as loading control. Data represents mean ± SD with at least three separate experiments. (*: significant difference vs. control with $p < 0.05$) [164]

4.4. DGLA's Anti-Cancer Activity Is Derived from Its COX-2 Catalyzed Peroxidation

To further confirm that DGLA's anti-cancer effects are derived from its COX-2 catalyzed peroxidation, we knocked down D5D and COX-2 individually or simultaneously in HCA-7 cells, then investigated the cell growth response after 48 h DGLA treatment (100 μM) by MTS assay (**Fig. 13A-B**). Results showed that DGLA supplementation significantly inhibited cell viabilities in D5D-*KD* cells; however, this inhibitory effect was abolished in D5D/COX-2 double-KD cells, suggesting that COX-2 is essential in DGLA's anti-cancer effects (Fig. 13A). This observation provides evidence to further support our hypothesis that 8-HOA formed from COX-2 catalyzed DGLA peroxidation is responsible for DGLA's anti-cancer activity.

In addition to DGLA, we also tested the potential anti-cancer effect of LA, the precursor and main dietary source of ω-6 fatty acids. We proposed that LA could be converted to DGLA in cells and then elicit certain anti-cancer activity. Results showed that treatment of 100 μM LA also led to decreased cell viability at 48 h (89.8 ± 2.4%) in D5D-*KD* cells compared to vehicle control (Fig. 13B), although it is not as effective as DGLA. Consistently, this growth inhibitory effect from LA was also abolished in D5D/COX-2 double-KD cells, suggesting that this effect is derived from a COX-2-catalyzed metabolism pathway as well.

We also tested our D5D-*KD* and DGLA supplementation strategy in other colon cancer cell lines with different COX expression levels. *e.g.* HT-29 (low COX-2) and HCT 116 (COX-2 deficient, **Fig. 14A-B**). Results showed that 48 h DGLA treatment (100 μM) only led to a minimal growth inhibition effect in D5D-*KD* HT-29 cells with cell viability reduced to 87.9 ± 4.4%, while no inhibitory effect from DGLA was observed in D5D-*KD* HCT 116 cells. This is because there is much less 8-HOA generated from DGLA in these two cell lines due to their low/deficient COX-2 levels (data not shown).

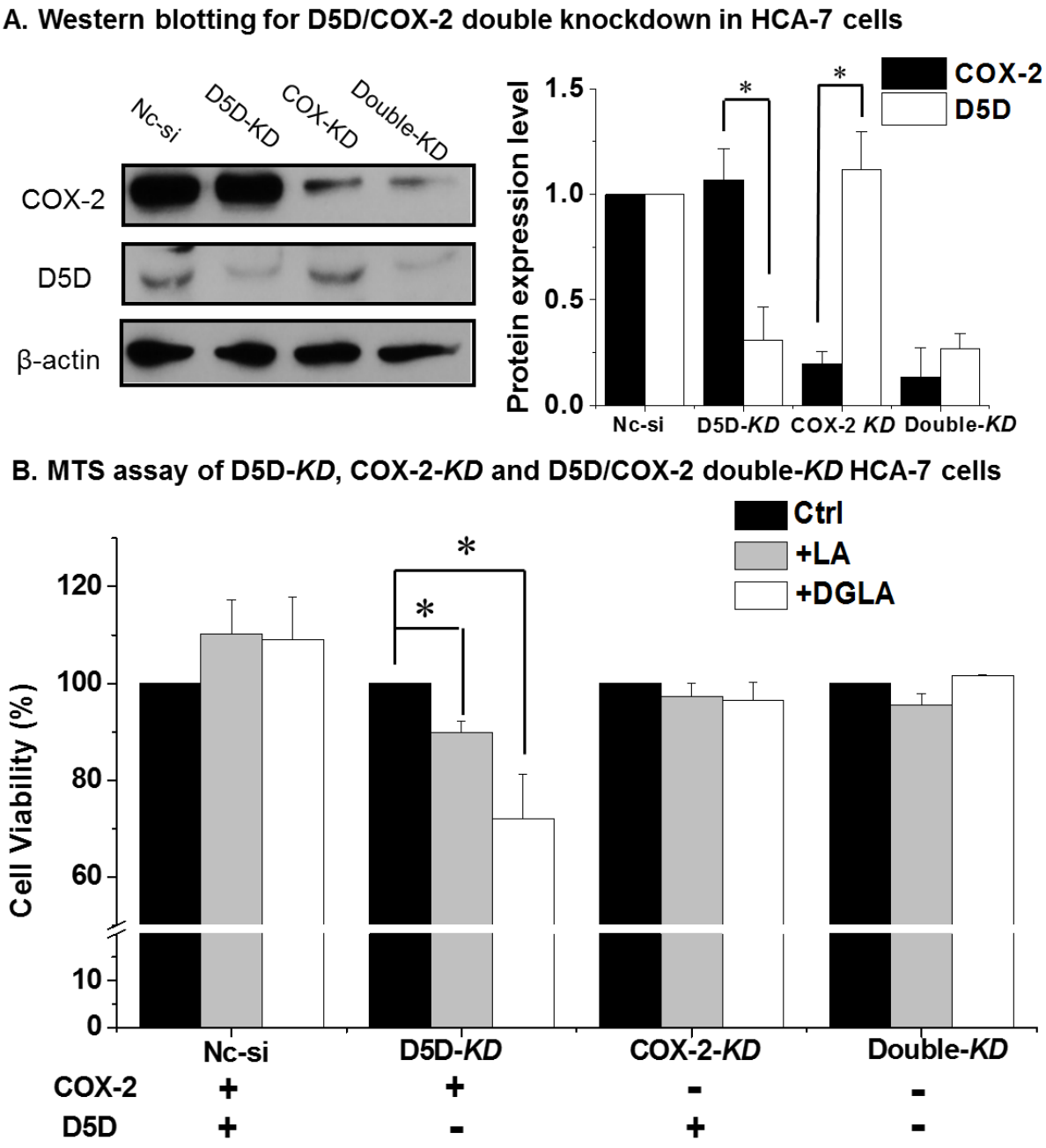

Figure 13. DGLA's anti-cancer activity is derived from its COX-2 catalyzed peroxidation. **A.** Western blot and expression rate of D5D and COX-2 in HCA-7 cells transfected with negative control siRNA, D5D targeted siRNA, COX-2 targeted siRNA and D5D/COX-2 combination siRNAs, respectively. The ratios of different proteins to β-actin in control were normalized to 1, respectively. **B.** MTS assay of siRNA transfected HCA-7 cells treated with LA or DGLA (100 μM for 48h). Data represent mean ± SD with at least three separate experiments. The cell viabilities for control groups are normalized to 100% for every separate experiment. (*: significant difference with $p < 0.05$)

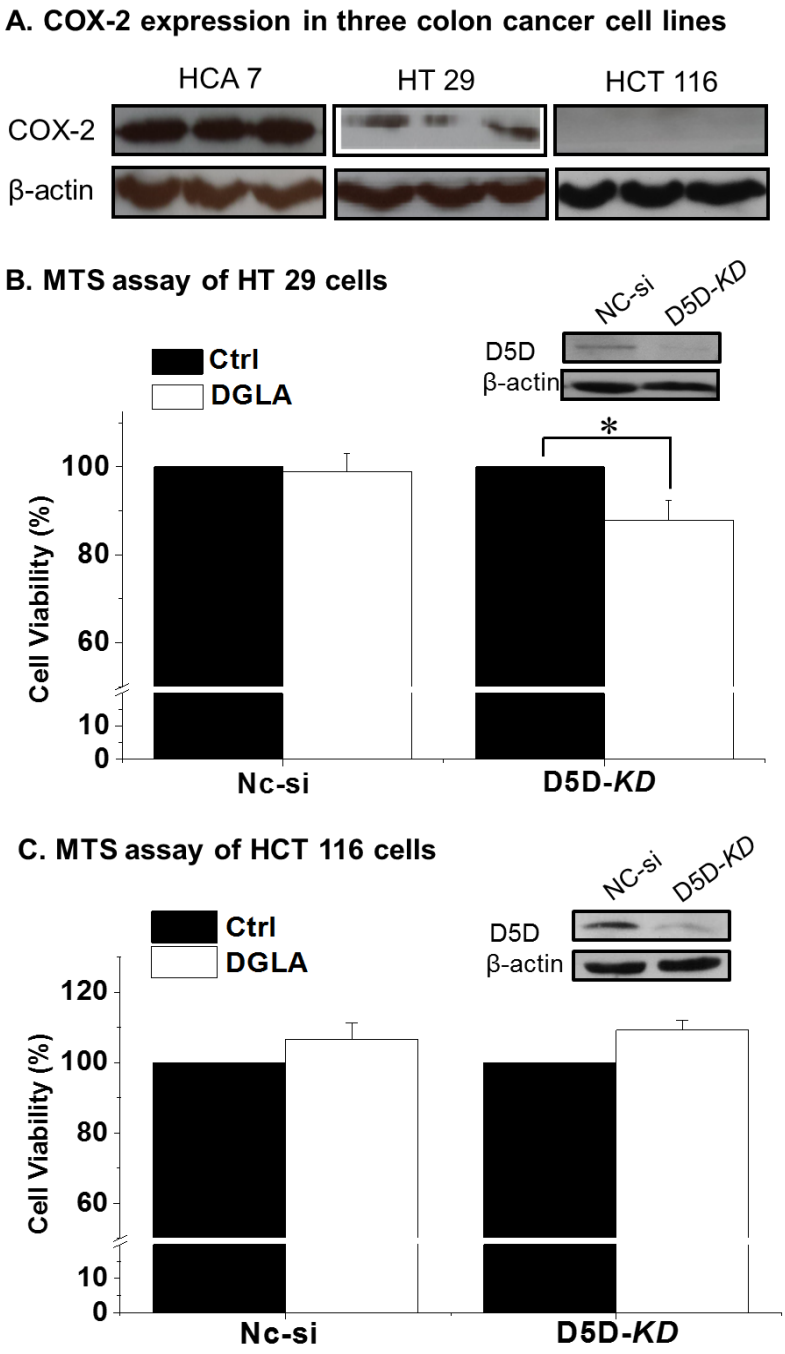

Figure 14. Growth response of HT29 and HCT116 cells from D5D-*KD* and DGLA supplement. **A.** Western blot of COX-2 in HCA-7, HT-29 and HCT 116 cells **B.** MTS assay of Nc-si or D5D-*KD* HT-29 cells treated with DGLA (100 μM for 48h). Insert: western blot of D5D expression in Nc-si or D5D-*KD* HT-29 cells; **C.** MTS assay of Nc-si or D5D-*KD* HCT 116 cells treated with DGLA (100 μM for 48h). Insert: western blot of D5D expression in Nc-si or D5D-*KD* HCT 116 cells. Data represent mean ± SD with at least three separate experiments. The cell viabilities for control groups are normalized to 100% for every separate experiment. (*: significant difference with $p < 0.05$).

4.5. Improved Anti-Proliferation Effect from D5D-*KD*, DGLA and 5-FU Treatment

Chemo-resistance has been a major obstacle for cancer therapy [186]. Combinations of 5-FU with various other cancer therapeutic agents as well as fatty acid supplementation have been extensively studied to enhance the efficacy of 5-FU against cancer [188-194]. In Chapter 3, we showed that combination of 8-HOA and 5-FU led to a better growth inhibitory effect on HCA-7 cells compared to 5-FU alone. Here we further tested whether DGLA supplementation along with D5D-*KD* could enhance the efficacy of 5-FU in HCA-7 cells. Results from colony formation assay showed that while 5-FU (50 μM) treatment alone could inhibit the D5D-*KD* cell growth with a survival fraction at 51.9 ± 2.9%, co-treatment of DGLA (100 μM) and 5-FU in D5D-*KD* HCA-7 cells led to more significant cell growth inhibition effect (survival fraction 20.1 ± 4.8%, **Fig. 15**) [164]. On the other hand, DGLA had no influence on 5-FU's effect on control siRNA transfected HCA-7 cells (surviving fraction of 62.3% ± 7.7% compared to 60.3% ± 6.5% with 5-FU treatment alone).

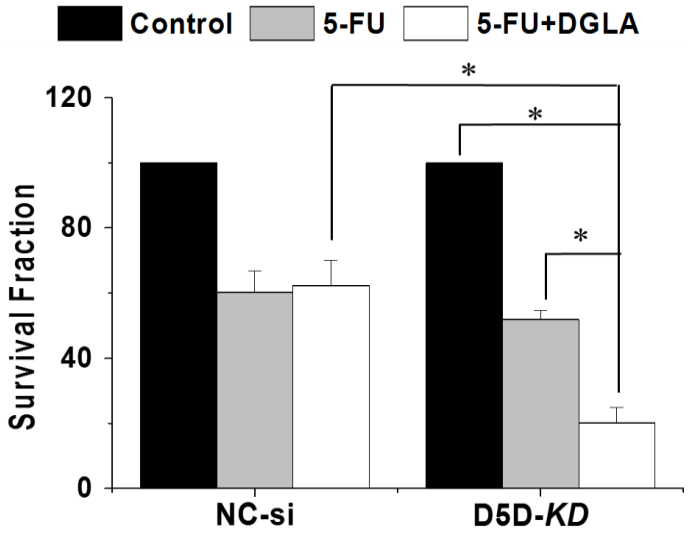

Figure 15. Improved anti-proliferation effect from D5D-*KD*, DGLA and 5-FU treatment in HCA-7 cells.
Nc-si and D5D-*KD* HCA-7 cells were treated with vehicle, 5-FU (50 μM) or 5-FU+DGLA (100 μM) for 48 h, followed by another 10 days incubation before examined for colony formation. (*: significant difference with $p < 0.05$ from $n \geq 3$). Data represent mean ± SD with at least three separate experiments. The survival fractions for control groups are normalized to 100% for every separate experiment. (*: significant difference with $p < 0.05$) [164].

5-FU can block DNA synthesis and induce cell cycle arrest at G1/S point in cancer cells [196]. Consistently, we observed that 5-FU treatment alone induced G1 arrest in both Nc-si HCA-7 cells (50.5% ± 4.5%) and D5D-*KD* HCA-7 cells (57.5% ± 1.2%) compared to their corresponding vehicle controls (37.9 % ± 5.8% and 40.4 % ± 2.1%, respectively, **Fig. 16**). Concurrent supplementation of DGLA further promoted 5-FU-induced G1 arrest in D5D-*KD* cells to 64.0% ± 3.6%. However, in Nc-si cells, the combination treatment did not lead to a significant difference compared to 5-FU treatment alone. This is because Nc-si cells cannot generate enough 8-HOA to elicit any growth inhibitory effect (Fig 12A).

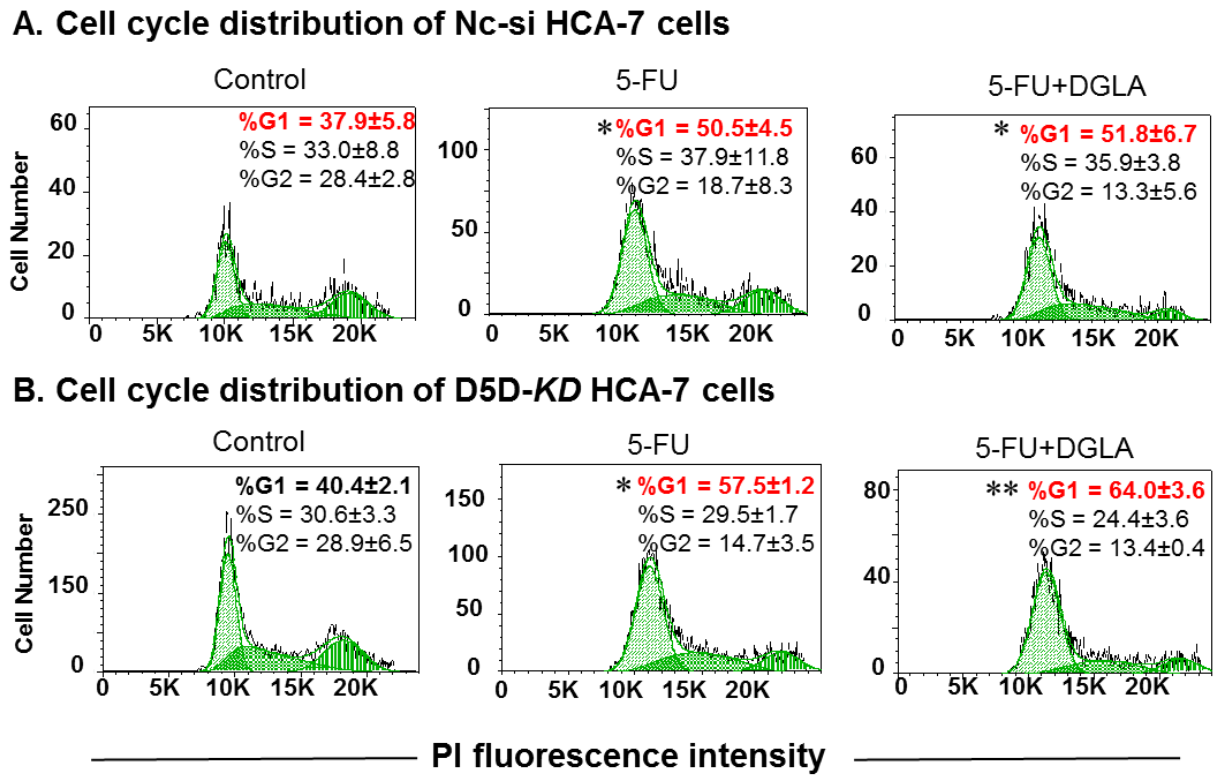

Figure 16. Cell cycle distribution of HCA-7 cells after DGLA and 5-FU treatment.
A. Cell cycle distribution of Nc-si HCA-7 cells and **B.** Cell cycle distribution of D5D-*KD* HCA-7 cells treated with vehicle, 5-FU (0.2 mM), or 5-FU+DGLA (100 μM)for 48 h. Cell cycle was examined *via* flow cytometer followed by PI staining. At least 10,000 cells were counted for each sample. Data represents mean ± SD with at least three separate experiments (*: significant difference vs. control with $p < 0.05$; **: significant difference vs. 5-FU group with $p < 0.05$) [164]

5-FU is also known to inhibit cancer cell growth by inducing apoptosis [197-198]. Our results showed that 5-FU alone induced apoptosis in both Nc-si and D5D-*KD* HCA-7 cells as demonstrated by the annexin V-positive/PI-negative staining (population of early apoptotic cells 10.0% ± 1.7% *vs.* 17.7% ± 2.1%, respectively, **Fig. 17**), whereas concurrent DGLA treatment (100 μM) further promoted 5-FU-induced apoptosis in D5D-*KD* cells (to 27.0% ± 3.4%). On the other hand, there is no enhanced effect could be observed from the combination treatment in Nc-si cells.

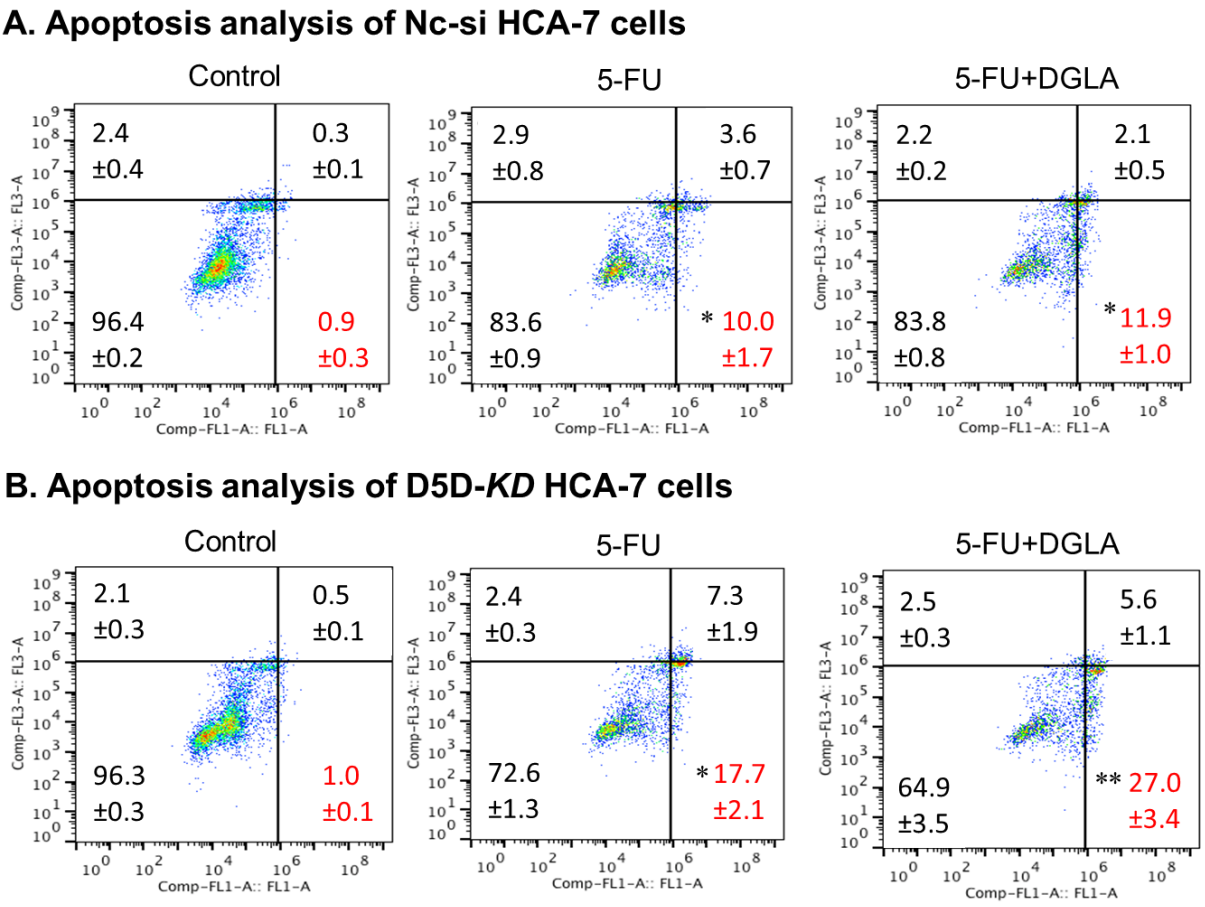

Figure 17. HCA-7 cell apoptosis from DGLA and 5-FU treatment.
A. Cell apoptosis of Nc-si HCA-7 cells and **B.** Cell apoptosis of D5D-*KD* HCA-7 cells treated with vehicle, 5-FU (0.2 mM), or 5-FU+DGLA (100 μM) for 48 h. Apoptosis was examined *via* flow cytometer followed by annexin V-FITC/PI double staining. At least 10,000 cells were counted for each sample. Data represent mean ± SD with at least three separate experiments (*: significant difference vs. control with $p < 0.05$; **: significant difference vs. 5-FU group with $p < 0.05$). [164]

Further mechanistic study showed that 5-FU treatment alone could up-regulate the tumor suppressor p53, activate procaspase 9 and cleave PARP in D5D-*KD* HCA-7 cells (**Fig. 18**). However, when the cells were co-treated with DGLA (100 μM) and 5-FU, an ~ 1.5 fold p53 upregulation, ~ 2 fold decreased procaspase 9, and ~2 fold increase of cleaved PARP were observed compared to 5-FU treatment alone [164]. These results suggested that DGLA and D5D-*KD* can improve the efficacy of 5-FU potentially through the activation of pro-apoptotic proteins, *e.g*., p53, caspase 9. In addition, linoleic acid was also found to further activate the pro-apoptotic proteins in D5D-*KD* cells treated with 5-FU (Fig. 18).

4.6. Improved Anti-Migration/Invasion Effects from D5D-*KD,* DGLA and 5-FU Treatment

In addition to inhibiting cancer cell growth, 5-FU has also been used to suppress colon cancer metastasis [199-202]. Therefore, we tested whether our strategy could enhance 5-FU's efficacy in inhibiting cancer cell migration and invasion.

Results from the transwell migration assay showed that while 5-FU alone inhibited cell migration compared to vehicle control (~63 migrated cells vs. 138 in control), co-treatment of DGLA and 5-FU led to even more significant inhibitory effect on cell migration (~36 migrated cells). Similarly, concurrent supplementation of DGLA also led to more significantly suppressed cell invasion compared to 5-FU treatment alone (~ 43 invaded cells for co-treatment vs. ~ 65 for 5-FU only, **Fig. 19A-B**) [170].

Further mechanistic study showed that 5-FU alone could downregulate the expressions of MMP-9, vimentin (a mesenchymal marker) and snail (EMT-inducing transcription factor), while upregulating the expression of E-cadherin (essential for epithelial cell adhesion) [203-205]. Concurrent supplementation of DGLA in D5D-*KD* HCA-7 cells further decreased expression of MMP-9, vimentin and snail, while increasing expression of E-cadherin compared to treatment 5-FU alone (**Fig. 20**) [170].

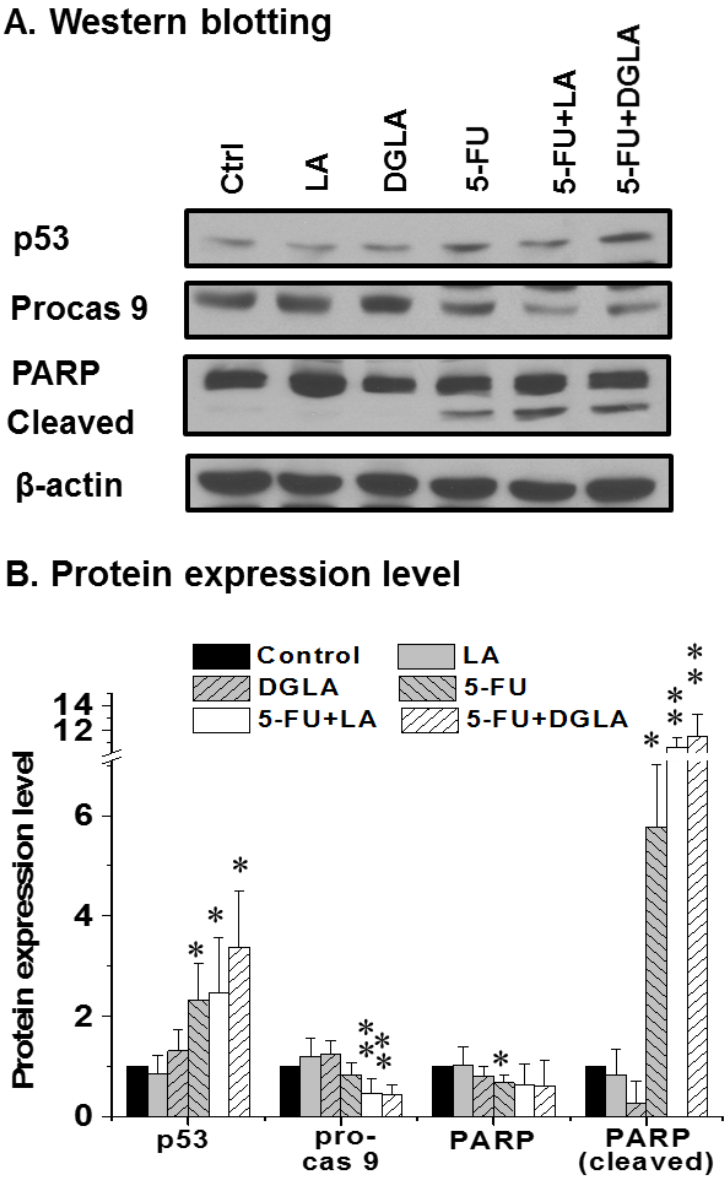

Figure 18. Altered expression level of apoptotic proteins in D5D-*KD* HCA-7 cells.
A. Western blot and **B.** Expression rate of p53, procaspase 9, procaspase 7, PARP, cleaved PARP and p21 from D5D-*KD* HCA-7 cells treated with 5-FU (0.2 mM), DGLA (100 μM), LA (100 μM) 5-FU+DGLA, and 5-FU+LA for 48 h. Protein expression levels were calculated as the ratio of target proteins to β-actin. The ratios in controls were normalized to 1. Data represent mean ± SD with at least three separate experiments. (*: significant difference vs. control with $p < 0.05$; **: significant difference vs. 5-FU group with $p < 0.05$) [164]

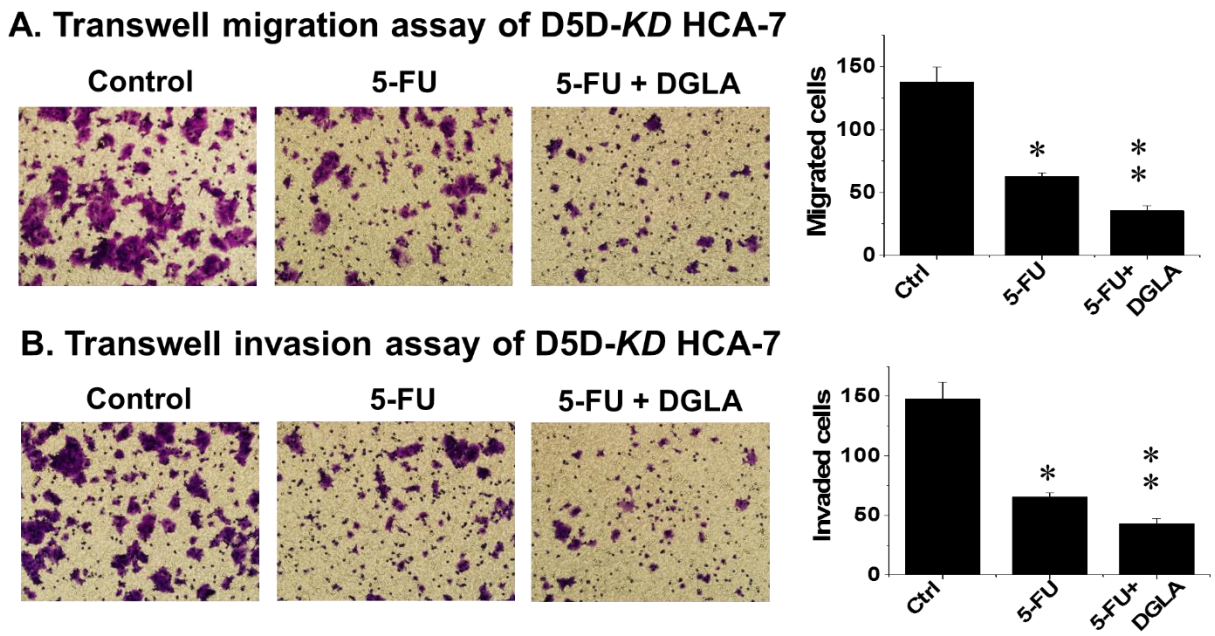

Figure 19. Improved inhibitory effects on HCA-7 cell migration and invasion from D5D-*KD,* DGLA and 5-FU treatment.

A. Transwell migration assay of D5D-*KD* HCA-7 cells with treatment of vehicle control, 5-FU (0.2 mM) alone or 5-FU + DGLA (100 μM); **B.** Transwell invasion assay of D5D-*KD* HCA-7 cells with treatment of vehicle control, DGLA (100 μM), 5-FU (0.2 mM) alone or 5-FU + DGLA; Data represent mean ± SD with at least three separate experiments. (*: significant difference vs. control with $p < 0.05$; **: significant difference vs. 5-FU group with $p < 0.05$) [170]

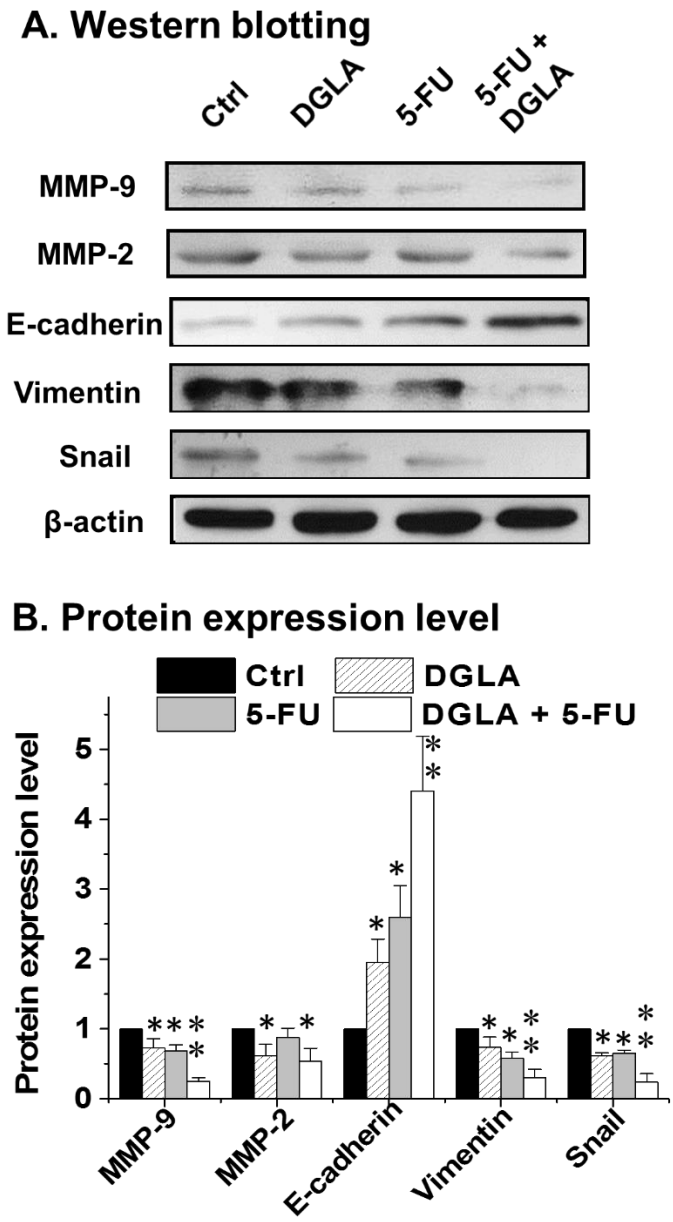

Figure 20. Altered protein level involved in cell migration/invasion in D5D-*KD* HCA-7 cells. **A.** Western blot and **B.** Protein expression rate of acetyl histone H3, MMP-2, MMP-9, E-cadherin, vimentin and snail from D5D-*KD* HCA-7 cells treated with vehicle control, DGLA (100 μM), 5-FU (0.2 mM) or 5-FU + DGLA. Protein expression levels were calculated as the ratio of target proteins to β-actin. The ratios in controls were normalized to 1. Data represent mean ± SD with at least three separate experiments. (*: significant difference vs. control with $p < 0.05$; **: significant difference vs. 5-FU group with $p < 0.05$) [170]

4.7. Anti-Cancer Effects of D5D-*KD* and DGLA in Combination with Other Cancer Drugs

In addition to 5-FU, we also tested whether the strategy of DGLA supplementation along with D5D-*KD* could enhance the cytotoxicity of other commonly used chemo/targeted therapeutic drugs, such as irinotecan, doxorubicin and a recently FDA-approved targeted therapy drug, regorafenib. These three drugs are all commonly used in treating colon cancers with different mechanisms. For example, after activated by hydrolysis, irinotecan inhibits topoisomerase I which leads to inhibition of both DNA replication and transcription [206]. Doxorubicin stabilizes the topoisomerase II complex during DNA replication process, thereby preventing the DNA double helix from being resealed and eventually blocking the process of replication [207]. Regorafenib is targeted therapy drug approved by the US FDA in 2012 for treating metastatic colorectal cancer. It acts as an oral multi-kinase inhibitor which inhibits multiple membrane-bound and intracellular kinases that are involved in normal cellular functions and pathologic processes [208]. We proposed that our D5D-*KD* and DGLA supplementation strategy could enhance the anti-cancer effects from these drugs due to their distinct mechanisms.

MTS assays showed that concurrent DGLA supplementation (100 μM, 48 h) resulted in better growth inhibitory effects compared to drug treatment alone on D5D-*KD* cells, but not of Nc-si cells (**Fig. 21A-C)**. For example, combination of DGLA and regorafenib (10 μM) in D5D-*KD* HCA-7 cells led to more significantly reduced cell viability at 46.9% ± 1.3% compared to 65.9% ± 7.5% in regorafenib treatment alone. Similarly, co-treatment of DGLA and irinotican (40 μM) in D5D-*KD* cells further reduced cell viability to 46.2% ± 7.5% compared to 66.2% ± 5.7% in irinotican treatment alone, while combination of DGLA and doxorubicin (1.5 μM) also resulted in more decreased cell viability at 25.7% ± 3.5% compared to 41.4% ± 7.9% in doxorubicin treatment alone.

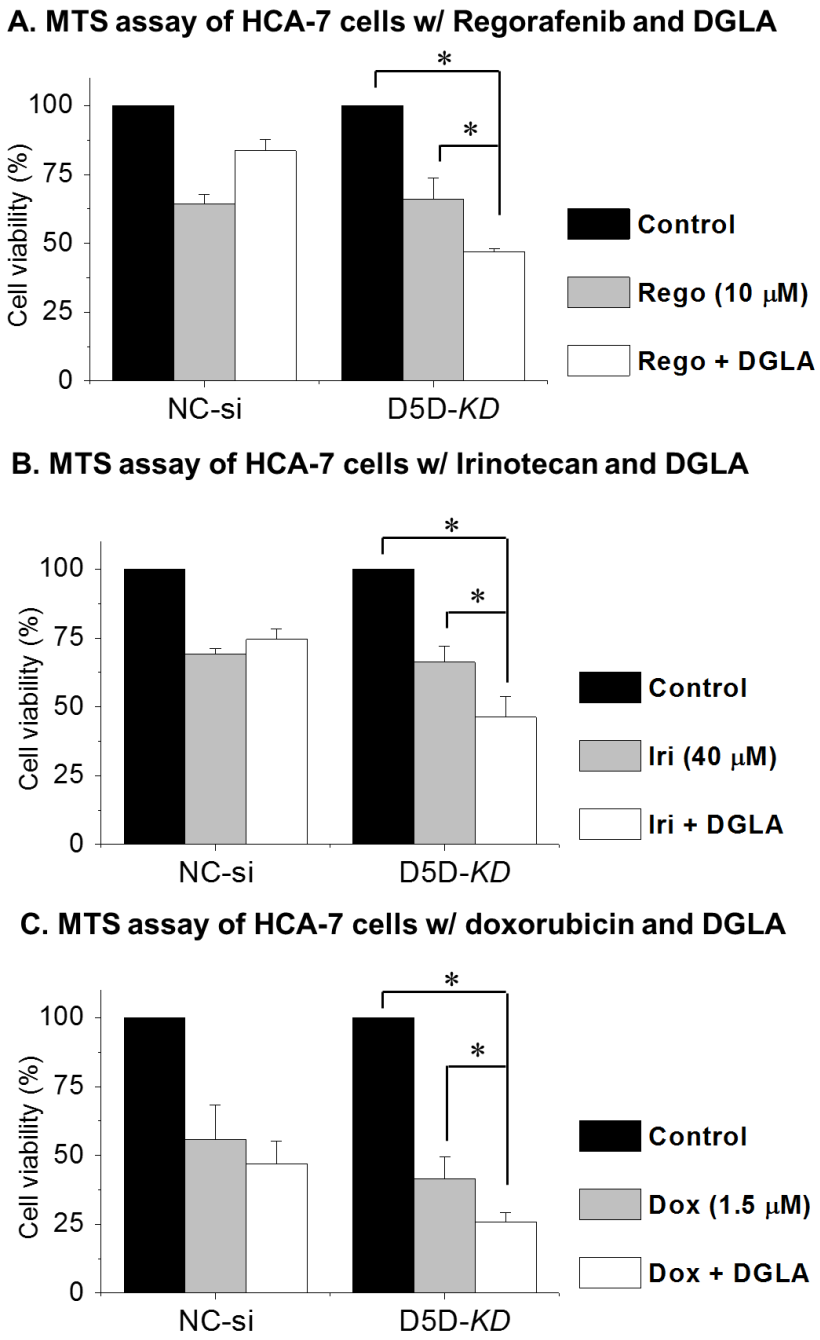

Figure 21. Anti-cancer effects from D5D-*KD* and DGLA in combination with other chemo-drugs in HCA-7 cells.

A. MTS assay of Nc-si or D5D-*KD* HCA-7 cells treated with vehicle, regorafenib (10 μM), or regorafenib+ DGLA (100 μM) for 48 h; **B.** MTS assay of Nc-si or D5D-*KD* HCA-7 cells treated with vehicle, irinotecan (40 μM), or irinotecan + DGLA (100 μM) for 48 h; **C.** MTS assay of Nc-si or D5D-*KD* HCA-7 cells treated with vehicle, doxorubicin (1.5 μM), or doxorubicin + DGLA (100 μM) for 48 h. Data represent mean ± SD with at least three separate experiments The cell viabilities for control groups are normalized to 100% for every separate experiment. (*: significant difference vs. control with $p < 0.05$)

4.8. Conclusion and Discussion

In this chapter, we demonstrated that D5D-*KD* is an effective strategy to limit the conversion from DGLA to AA, thus promote 8-HOA formation from COX-2 catalyzed DGLA peroxidation to a threshold level which could inhibit colon cancer growth and migration/invasion. More importantly, the commonly highly expressed COX-2 in cancer cells was exploited to kill cancer cells, which is a paradigm shifting concept in contrast to the classic COX inhibition strategy. Furthermore, combined treatments of D5D knockdown, DGLA supplementation and chemo-drugs were found to result in better growth inhibitory effects in colon cancer cells compared to drug treatment alone.

In Chapter 3, we have shown that exogenous treatment of 8-HOA at 1.0 μM could significantly inhibit colon cancer cell growth (Fig. 1) [163]. Therefore, we made the first effort to quantify endogenous 8-HOA from COX-2 catalyzed DGLA peroxidation in cancer cells. Our results showed D5D-*KD* in HCA-7 cells could lead to the accumulation of 8-HOA to the threshold level that is required for delivering DGLA's anti-cancer effect. In comparison, although a similar level of PGE1 was detected in D5D-*KD* cells after DGLA supplementation, we have previously demonstrated that PGE1 was unable to affect colon cancer cell growth at this concentration range (Fig. 1). Taken together, our data suggest that the anti-cancer effects of DGLA are derived from 8-HOA, rather than PGE1. In addition, western blot data also showed that DGLA treatment in D5D-*KD* cells can inhibit histone deacetylase and lead to DNA damage (Fig. 12), which is consistent with the results from direct 8-HOA treatment (Fig. 6), further confirming that 8-HOA is responsible for DGLA's anti-cancer activity.

To confirm the role of COX-2 in DGLA's anti-cancer activity, we further knocked down COX-2 expression in D5D-*KD* HCA-7 cells, which was found to abolish DGLA's anti-cancer

effects (Fig. 13). We also tested the effect of DGLA in cancer cells with different COX-2 expression levels (Fig. 14**)**. Results showed that DGLA and D5D-*KD* could lead to the most significant growth inhibitory effects in HCA-7 cells (high COX-2), while only moderate effects were observed in HT-29 (low COX-2) cells and no effects were observed in HCT 116 cells (COX-2 deficient). These results together suggested that DGLA's anti-cancer activity is dependent on COX-2 catalyzed peroxidation (by generating 8-HOA), and the overexpression of COX-2 in cancer cells can be exploited to promote the formation of 8-HOA from DGLA to kill colon cancer cells.

Although COX-2 is essential for eliciting DGLA's anti-cancer effect, we have demonstrated that regardless of the COX-2 expression levels, the growth of HCA-7, HT-29 and HCT 116 cells could all be significantly suppressed by direct treatment of 8-HOA (Fig. 1). This observation suggested that even in the cancer cells with limited level of COX-2, our strategy will also be effective as the stromal cells in tumor environment with elevated level of COX-2 could also produce 8-HOA, which may act in a local hormone-like manner to trigger anti-cancer effects [209]. In addition, a recent study from Mustafi *et al* established a xenograft colon tumor model using HCT 116 cells, in which they observed an interaction between tumor cells and stromal cells that led to an upregulation of COX-2 levels in both types of cells [210]. This indicates that the COX-2 level in both cancer cells and stromal cells will be upregulated in the tumor environment, which makes the tumor more vulnerable to our strategy.

In this Chapter, we observed that promoted 8-HOA formation from D5D-*KD* and DGLA could induce p53-dependent apoptosis in HCA-7 cells. However, p53 is frequently mutated in many cancer types including colon cancer, which may result in resistance to p53-dependent anti-cancer therapy. In fact, our results showed that our strategy could also inhibit the growth of HT-

29 cells with mutated p53 (Fig. 14B), indicating that 8-HOA can also cause cancer cell death *via* p53-independent mechanisms. Therefore, in our future work we also plan to investigate the potential p53-independent mechanisms of 8-HOA's anti-cancer effect.

Our results showed that treatment with LA, the precursor and main dietary source of ω-6, also suppressed the growth of D5D-*KD* cancer cells (Fig. 13). Although the effect was moderate due to the limited conversion rate from LA to DGLA and the short incubation time (48 h), we expect more significant anti-cancer effects in our future animal study in which we will modulate fatty acids consumption on a daily basis. Further investigation of LA may provide information to develop a more practical ω-6-based diet care strategy in cancer treatment since LA is prevalent in the human diet.

Chemo-resistance is the major obstacle for current cancer chemotherapy. To overcome drug resistance to 5-FU, various drug combination strategies have been studied in which 5-FU was concurrently administered with other therapeutic agents. Among the various combinations, the co-treatment of indomethacin (a nonselective COX inhibitor) and NS-398 (a selective COX-2 inhibitor), could significantly sensitize colon cancer cell to 5-FU, suggesting the regulation of COX-mediated ω-6 metabolism may be an effective strategy to reverse chemoresistance to 5-FU [188-190]. As our strategy shares a common objective as a COX inhibitor (*i.e.* limiting COX/AA peroxidation), we believe our strategy could also sensitize colon cancer cells to 5-FU and may even reach a better therapeutic outcome considering the dual anti-cancer mechanism from our strategy. In fact, we observed that concurrent DGLA supplementation in combination 5-FU led to significantly improved inhibitory effects on D5D-*KD* HCA-7 cell growth and migration, compared to 5-FU alone (Figs. 15-20) [164, 170]. In addition, we also demonstrated that our strategy resulted in better anti-cancer outcomes when combined with many other chemotherapy drugs including,

irinotecan and doxorubicin, as well as a targeted therapy regorafenib (Fig. 21). These observations suggested that our strategy can be applied as a novel adjuvant treatment for colon cancer in combination with various anti-cancer agents with distinct mechanisms.

5. D5D KNOCKDOWN AND DGLA SUPPLEMENTATION PROMOTED 8-HOA FORMATION AND SUPPRESSED COLON TUMOR GROWTH IN A MOUSE XENOGRAFT MODEL

Studies from chapter 4 demonstrated that D5D-*KD* in human colon cancer cells with high COX-2 expression could promote 8-HOA formation from DGLA peroxidation to a threshold level, which in turn inhibited cancer cell growth and migration. However, the *in vitro* experimental system cannot completely represent the complex tumor environment in patients. Therefore, we further tested the anti-cancer effects of our novel strategy in a xenograft tumor model using immune-deficient mice, which is a commonly used model for cancer research that are more related to human patients. The immune-deficient mice (J:Nu, 007850, The Jackson Lab) are homozygous for the $Foxn1^{nu}$ mutation, which makes the mice hairless and athymic. The lack of thymus in these mice blocks the differentiation and maturation of T cells, resulting in an immunodeficiency that permits transplantation of tumor cell xenografts [211]. In addition, the hairless phenotype of nude mice is also ideal for evaluation of subcutaneous tumor growth and whole body imaging.

In this chapter, a stable D5D-*KD* HCA-7 colony 29 cell line was created and transplanted subcutaneously into the hind flank of immuno-deficient mice to establish a D5D-*KD* xenograft tumor model. As a parallel experiment, wild type HCA-7 cells were implanted into nude mice and subjected to same follow up treatment. After two weeks of tumor growth, the mice were further divided into four sub-groups and received different treatment for 4 weeks, including 1) vehicle control, 2) DGLA supplementation, 3) 5-FU injection, and 4) combination of DGLA and 5-FU (**Scheme 9**). The tumor size was measured twice a week to test whether D5D-*KD* along with DGLA supplementation could inhibit xenograft tumor growth. At the end of the treatment, the mice were euthanized and the tumor tissues were collected. HPLC/MS and GC/MS analysis was

performed to detect fatty acids and 8-HOA profiles in tumor tissues. Immunofluorescence and western blotting were conducted to determine the potential inhibitory effects and mechanisms on tumor growth and migration from our treatment strategy.

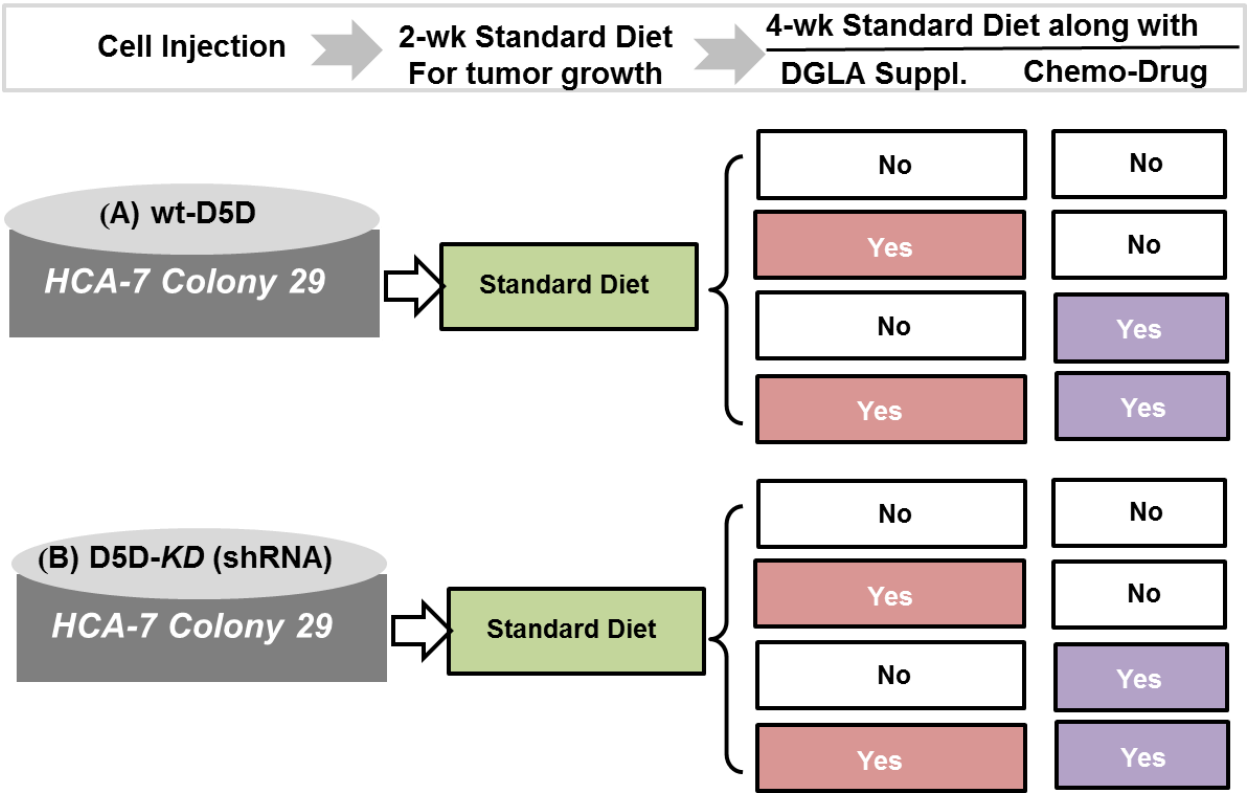

Scheme 9. Animal experiment design.
A total of 48 mice were used for the *in vivo* experiment as described below (6 mice/group × 8 groups). Wt-D5D and D5D-*KD* HCA-7 colony 29 cells were transplanted subcutaneously into the hind flank of two different groups of immuno-deficient mice to establish a xenograft tumor model. After two weeks for tumor growth, the mice bearing wt-D5D or D5D-*KD* tumor were further divided into four sub-groups and received different treatment for 4 weeks, including 1) vehicle control, 2) DGLA supplementation, 3) 5-FU injection, and 4) combination of DGLA and 5-FU. The tumor size was measured twice a week to test whether D5D-*KD* along with DGLA supplementation could inhibit xenograft tumor growth. At the end of the treatment, the mice were euthanized and the tumor tissues were collected for further analysis.

5.1. Establishment of a Stable D5D Knockdown Cell Line

In Chapter 4, we used siRNA to transiently knockdown cellular D5D expression. However, the siRNA cannot incorporate into host cells' DNA, thus only leads to a short-term knockdown effect. Hence, in order to investigate the effect of D5D knockdown in tumor xenograft, we created a stable D5D-*KD* HCA-7 cell line *via* shRNA transfection.

Briefly, D5D-targeted pre-shRNA was designed using BLOCK-iT™ RNAi Designer (www.invitrogen.com/rnai) and purchased from Integrated DNA Technology. The oligo was cloned into pcDNA^{tm} 6.2-GW/miR vector, which was then transformed into *E.coli*. The plasmid DNA from expression clone was transfected into wild type HCA-7 cells followed by antibiotic selection to create stable D5D knockdown cell colonies. The D5D-*KD* efficiency (~70%) was evaluated by western blot (**Fig. 22**). The stable D5D-*KD* cells were then transplanted into nude mice to establish D5D-*KD* xenograft tumors.

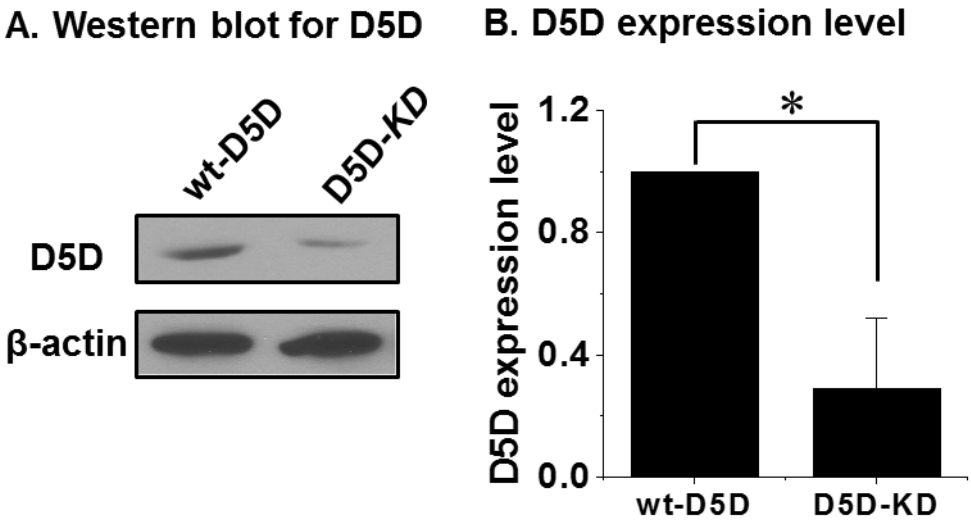

Figure 22. D5D knockdown efficiency in HCA-7 cells *via* sh RNA transfection.
A. Western blot and **B.** Relative expression level of D5D in wt-D5D and stable D5D-*KD* HCA-7 cells. The ratio of D5D to β-actin in control was normalized to 1. Data represent mean ± SD with at least three separate experiments. (*: significant difference with $p < 0.05$)

5.2. DGLA Treatment Inhibited the Growth of D5D-*KD* Xenograft Tumor in Mice

Wild type or D5D-*KD* HCA-7 cells were transplanted subcutaneously into the hind flank of immuno-deficient mice to establish a xenograft tumor model. After two weeks of tumor growth, the mice were further divided into four sub-groups and received different treatments for 4 weeks, including: 1) vehicle control (No DGLA and 5-FU), 2) DGLA supplementation (8 mg/mice, twice a week), 3) 5-FU injection (30 mg/kg, twice a week), and 4) combination of DGLA and 5-FU (Scheme 9). The tumor size was measured twice a week to test whether D5D-*KD* along with DGLA supplementation could inhibit xenograft tumor growth.

Results showed that, for the mice bearing wt-D5D tumors, 4-week DGLA treatment did not decrease, but even increased tumor size (313.7 ± 54.3 mm^3, **Fig. 23**) compared to that in the control group (306.6 ± 65.4 mm^3). This is because wt-D5D rapidly converted DGLA to AA, leading to limited production of 8-HOA which was unable to trigger any anti-cancer effect, while the elevated level of AA resulted in increased production of PGE2 which could promote tumor growth (data in section 5.3).

5-FU was also administered to mice bearing wt-D5D tumors in order to compare the effect from our strategy with the first line chemo-drug, as well as to test whether our strategy could improve the efficacy of 5-FU in xenograft tumor. Data showed that, 4-week of 5-FU injection significantly limited the tumor growth (205.3 ± 55.3 mm^3) compared to the control group. The combination of 5-FU and DGLA also significant decreased the tumor size (231.3 ± 42.3 mm^3) *vs.* control, however, the tumor size was larger when compared to 5-FU alone. Again, this is because DGLA was converted to AA, thereby led to increased production of PGE2 which promote tumor growth.

On other hand, for mice bearing D5D-*KD* tumors, 4 weeks of DGLA supplementation resulted in significantly reduced tumor size (178.2 ± 31.9 mm^3, **Fig. 24**) compared to that in the control group (257.6 ± 60.8 mm^3), by promoting 8-HOA formation to a threshold level (data in 5.3). This is consistent with previous observation in Chapter 4 that promoted 8-HOA formation from COX-2 catalyzed DGLA peroxidation could inhibit colon cancer cell growth.

4-week of 5-FU injection also significantly limited the D5D-*KD* tumor growth (133.7 ± 32.4 mm^3, Fig 24) *vs.* the control group. Noteworthy, the anti-tumor activity from DGLA supplementation was comparable with the effect from 5-FU treatment alone. In addition, mice received the combination of DGLA and 5-FU have even smaller tumor size (100.1 ± 24.3 mm^3) compared to 5-FU alone, suggesting that promoted 8-HOA formation from DGLA peroxidation could improve the chemotherapy *in vivo*, which is consistent with the observation in Chapter 4.

When comparing D5D-*KD* control *vs.* wt-D5D control group (Fig. 23-24), the size of D5D-*KD* tumors (257.6 ± 60.8 mm^3) was less than that of wt-D5D tumors (306.6 ± 65.4 mm^3) even without any additional treatment. This is probably because the upstream ω-6 fatty acids (*e.g.* LA) in the standard diet could also be converted to DGLA and produce certain level of 8-HOA that exerted anti-cancer activity in D5D-*KD* tumors.

The body weight of the mice was also monitored throughout the experiment, no significant change was observed in any control or treatment groups during the four-week period (Fig. 23-24**)**, suggesting that there is no severe toxicity observed from our treatments.

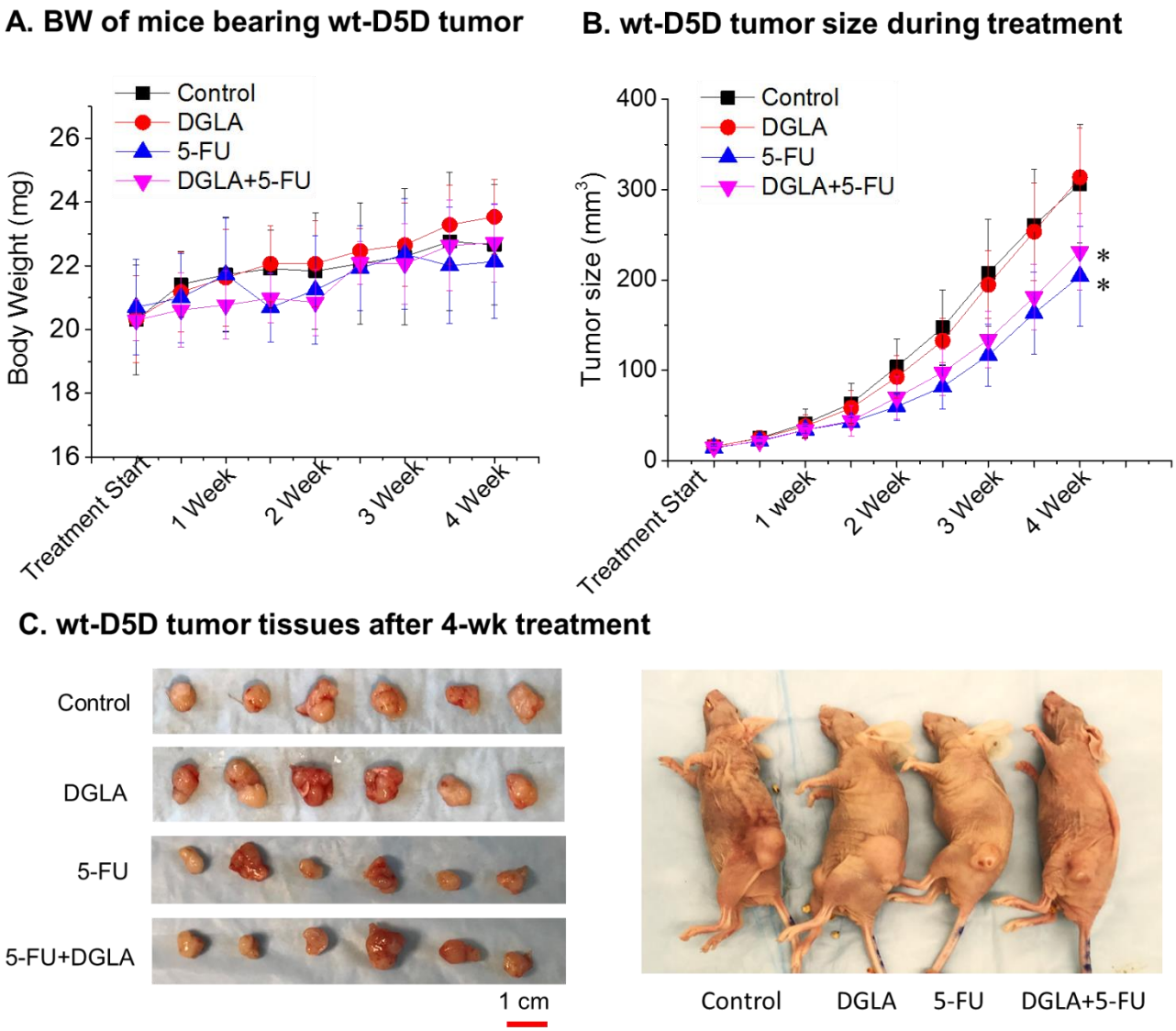

Figure 23. Effect of DGLA supplementation on wt-D5D HCA-7 xenograft tumor growth.
A. Body weight (BW) of mice bearing wt-D5D tumor during 4-week treatment; **B.** wt-D5D tumor size during 4-week treatment; **C.** Photos of tumor tissues and mice at the end of the treatment (*: significant difference vs. control with $p < 0.05$).

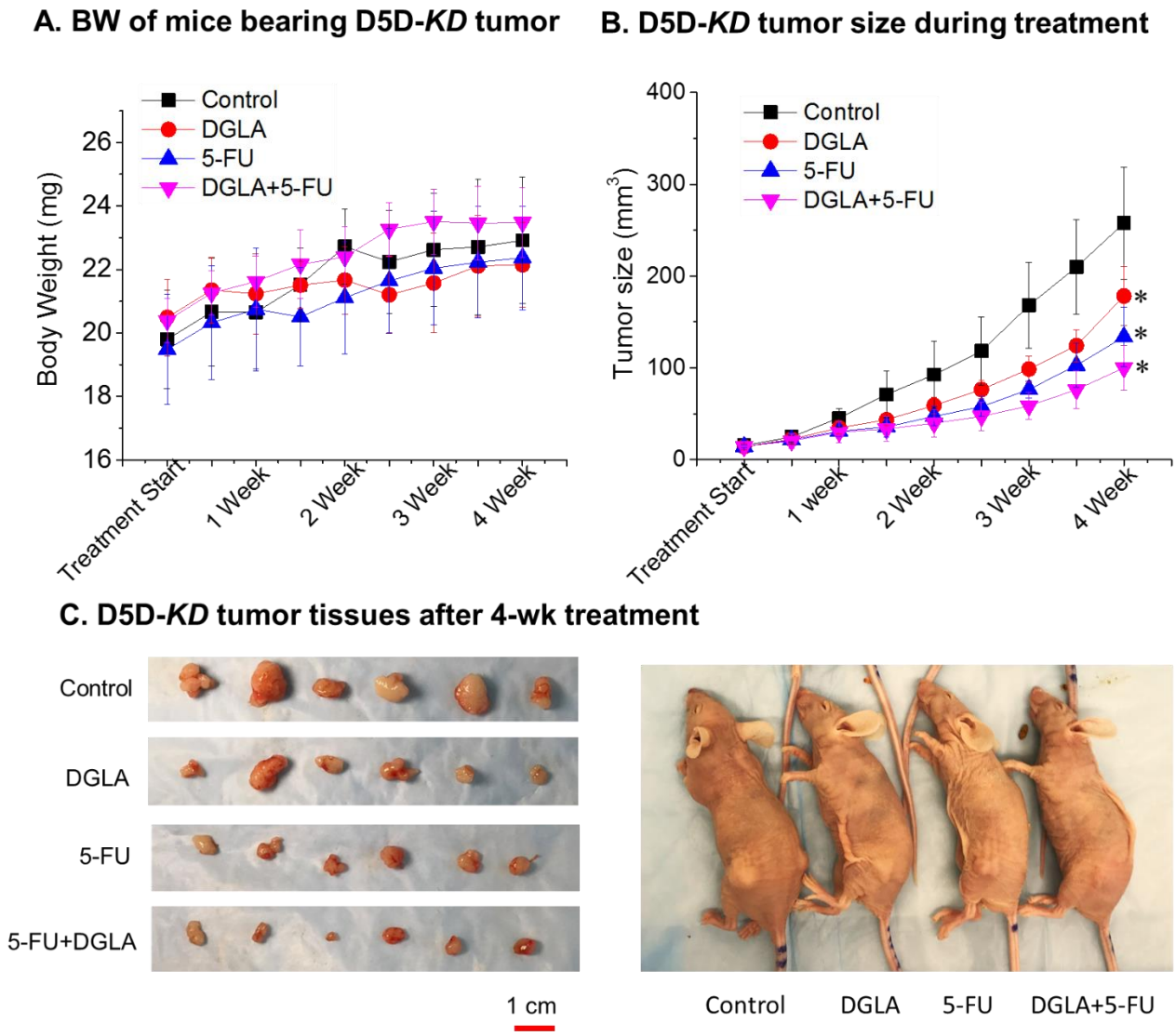

Figure 24. Effect of DGLA supplementation on D5D-*KD* HCA-7 xenograft tumor growth. **A.** Body weight of mice bearing D5D-*KD* tumor during 4-week treatment; **B.** D5D-*KD* tumor size during 4-week treatment; **C.** Photos of tumor tissues and mice at the end of the treatment (*: significant difference vs. control with $p < 0.05$).

5.3. Promoted 8-HOA Production in D5D-*KD* Tumors from DGLA Treatment

We proposed that the observed tumor growth inhibitory effects are due to the promoted formation of 8-HOA by D5D-*KD* and COX-2 catalyzed DGLA peroxidation. D5D and COX-2 are two key components in out hypothesis and their expression levels are crucial in our strategy. Therefore, we first assessed D5D and COX-2 expression in tumor tissues by immunofluorescence. Results showed that, despite different treatments, the tumor tissues from mice injected with D5D-*KD* HCA-7 cells have significantly less D5D expression compared to those from mice injected with wt-D5D cells (**Fig. 25**). On the other hand, no significant differences in COX-2 expression levels were observed in all groups of mice (**Fig. 26**).

We then quantified the levels of DGLA, AA, 8-HOA, PGE1 and PGE2 in tumor tissues to investigate whether the tumor growth inhibitory effects in D5D-*KD* tumors is associated with promoted formation of 8-HOA from DGLA treatment as well as decreased PGE2 formation from AA peroxidation. Results showed that, for the both wt-D5D and D5D-*KD* mice without any DGLA supplementation (*e.g.* treated with control or 5-FU only), we only detected basal levels of DGLA (**Fig. 27**). However, after 4 weeks of DGLA supplementation (including combination of DGLA and 5-FU), we observed a dramatic increase in the level of DGLA in both wt-D5D group and D5D-*KD* groups of mice compared to mice without DGLA treatment. More importantly, in D5D-*KD* tumors with DGLA supplementation, we detected significantly higher levels of DGLA compared to those in wt-D5D tumors with DGLA supplementation (Fig. 27).

Consistent with DGLA profile, for the mice without any DGLA supplementation (*e.g.* treated with control or 5-FU only), 8-HOA and PGE1 were under the detection limit (**Fig. 28**). After 4 weeks of DGLA supplementation (including combination of DGLA and 5-FU), we observed a dramatic increase in the levels of 8-HOA and PGE1 in both wt-D5D group and D5D-

KD group of mice compared to mice without DGLA treatment. More importantly, in D5D-*KD* tumors with DGLA supplementation, we detected significantly higher levels of 8-HOA (*e.g.* ~0.5 μg/g) compared to those in wt-D5D tumors with DGLA supplementation (*e.g.* ~0.15 μg/g, Fig. 28). These data indicated that D5D-*KD* in tumor tissues effectively limited the conversion of DGLA to AA and promoted the formation of 8-HOA, which led to the observed growth inhibitory effect.

In addition to altered levels of DGLA and 8-HOA, we observed that D5D-*KD* in tumor cells led to significant decreased level of AA and PGE2 compared to those in wt-D5D tumors (Figs 27-28). For example, in D5D-*KD* tumors with DGLA supplementation, we detected significantly lower levels of PGE2 (*e.g.* ~2.5 μg/g) compared to those in wt-D5D tumors with DGLA supplementation (*e.g.* ~4.3 μg/g, Fig. 28). These data suggested that decreased PGE2 level may also account for the inhibitory effect on tumor growth.

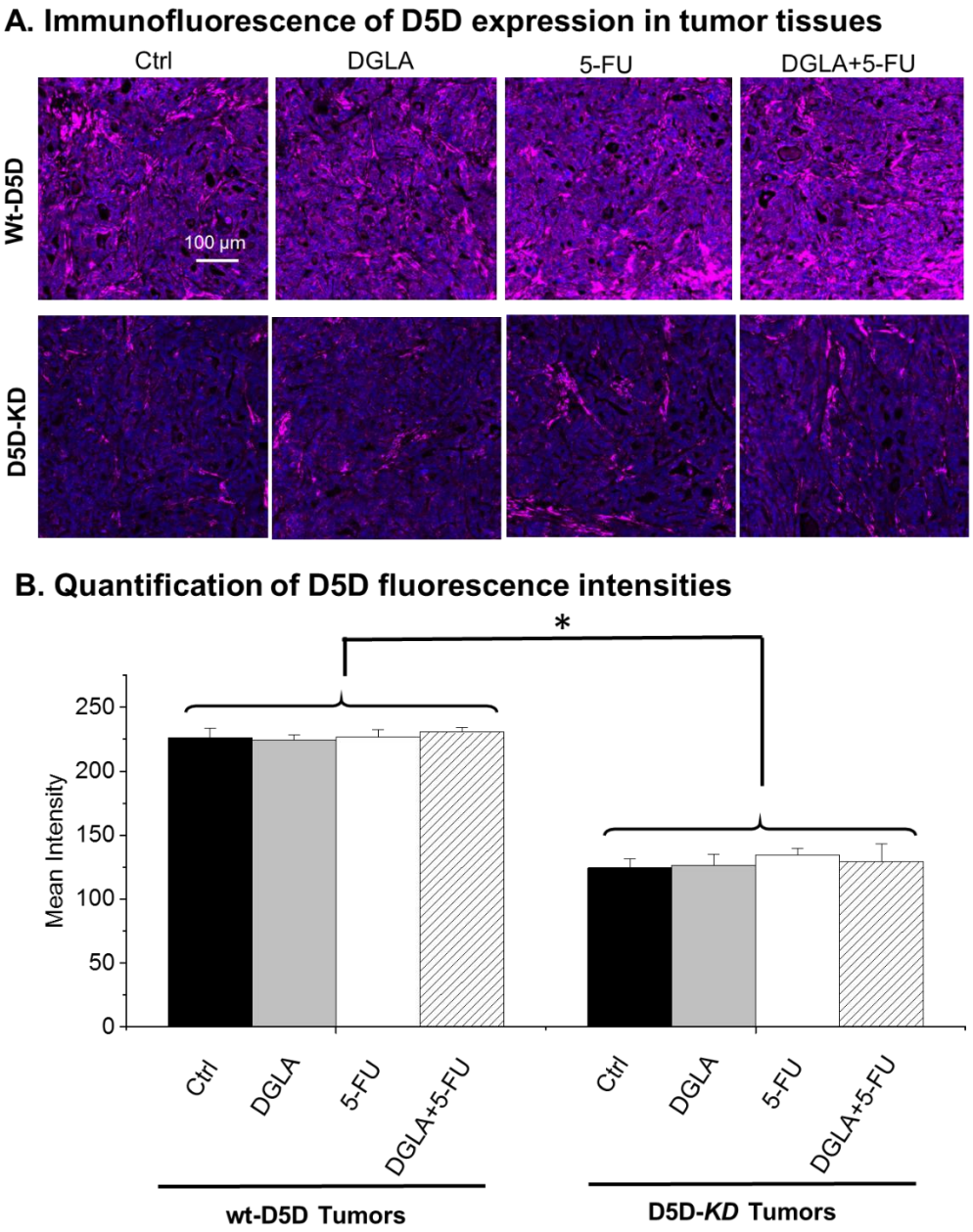

Figure 25. Immunofluorescence analysis of D5D expression in tumor tissues.
A. Representative images for D5D expression in tumor tissues, D5D was stained in pink, cell nuclei were counter stained with DAPI ; **B.** Mean intensity of D5D in each sample was quantified as an index of its expression level in tumor tissue (*: significant difference with $p < 0.05$).

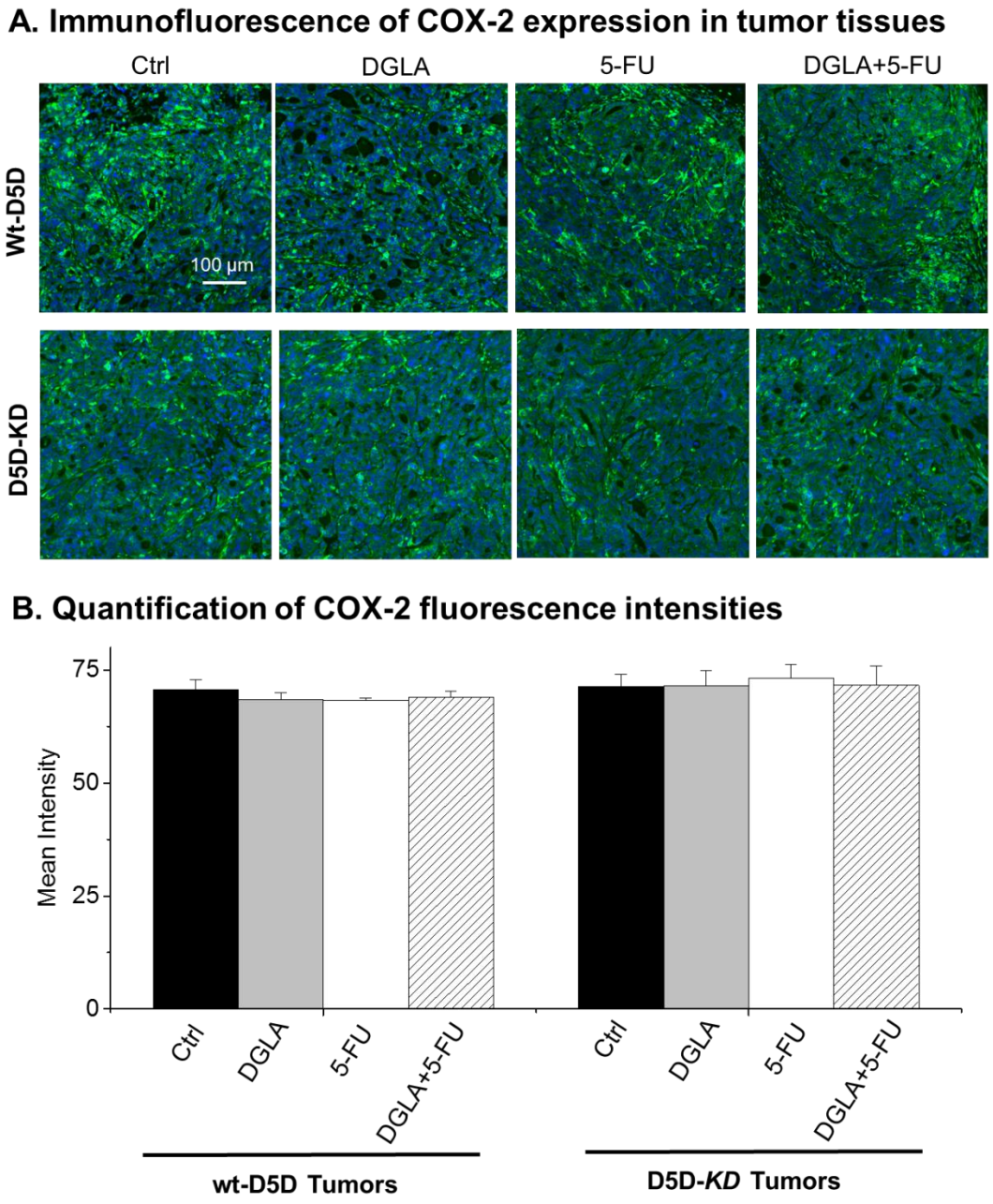

Figure 26. Immunofluorescence analysis of COX-2 expression in tumor tissues.
A. Representative images for COX-2 expression in tumor tissues, COX-2 was stained in green, cell nuclei were counter stained with DAPI; **B.** Mean intensity of COX-2 in each sample was quantified as an index of its expression level in tumor tissue.

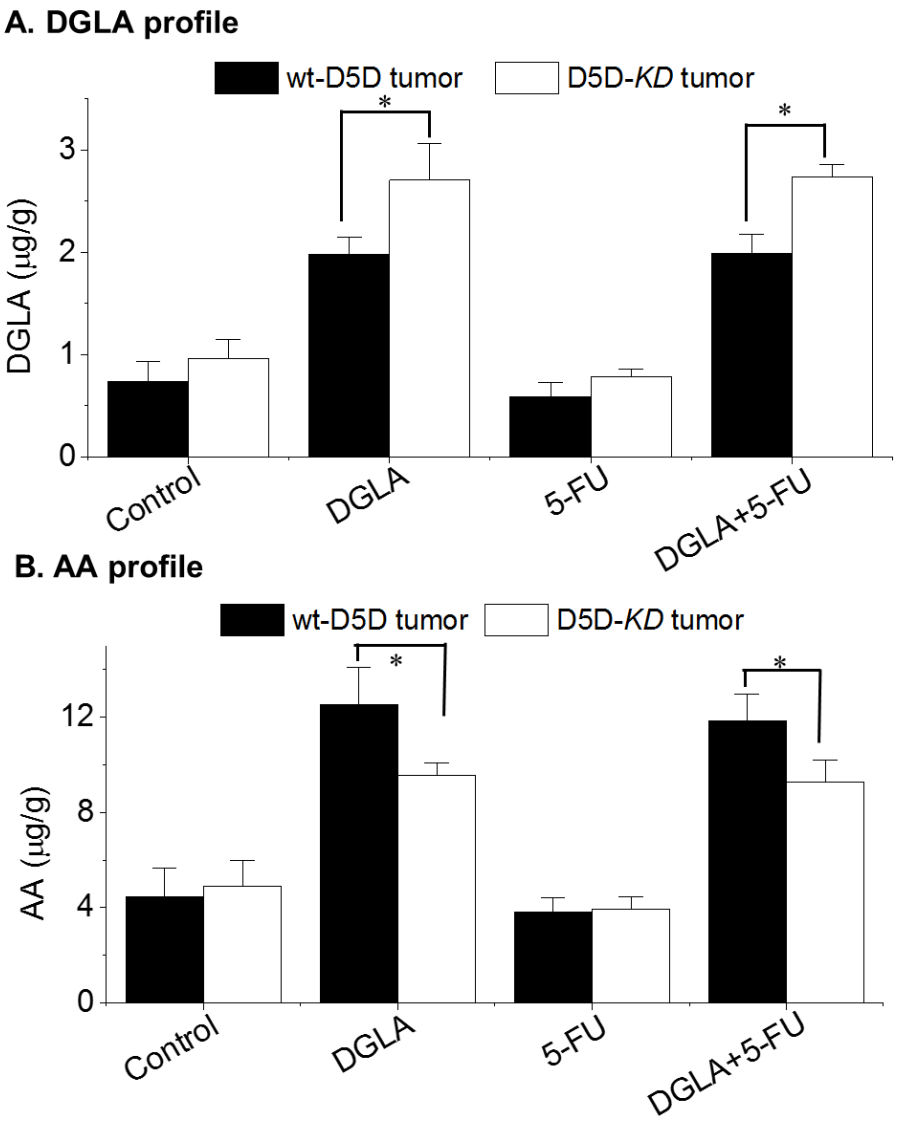

Figure 27. D5D-*KD* suppressed DGLA conversion in tumors.
A. HPLC/MS analysis of DGLA in wt-D5D and D5D-*KD* tumors; **B.** HPLC/MS analysis of AA in wt-D5D and D5D-*KD* tumors. Data represent mean ± SD (*: significant difference between wt-D5D tumor vs. D5D-*KD* tumor, with $p < 0.05$).

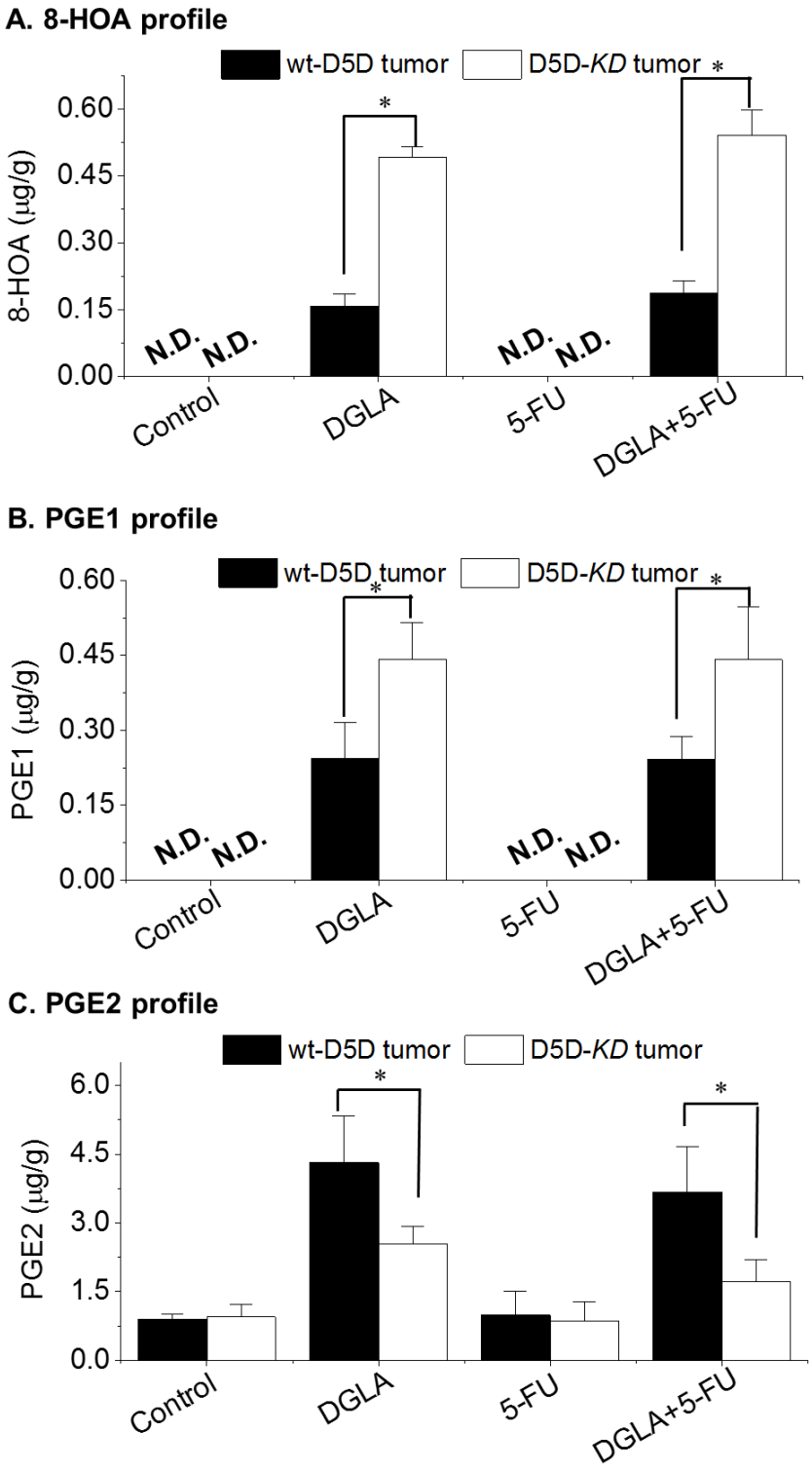

Figure 28. D5D-*KD* and DGLA supplementation promoted formation of 8-HOA in tumors. **A.** GC/MS analysis of 8-HOA in tumor tissues. **B-C.** HPLC/MS analysis of PGE1 and PGE2 in wt-D5D and D5D-*KD* tumors. Data represents mean ± SD (*: significant difference between wt-D5D tumor vs. D5D-*KD* tumor, with $p < 0.05$).

5.4. DGLA Supplementation Induced Apoptosis in D5D-*KD* Tumors

Data from Chapter 4 suggested that D5D-*KD* and DGLA supplementation could inhibit colon cancer cell growth and induce apoptosis *in vitro* from promoted 8-HOA formation *via* COX-2 peroxidation. We, thus, performed immunofluorescence studies to test whether our strategy could also inhibit tumor proliferation and induce apoptosis *in vivo*.

Results showed that, for the mice bearing wt-D5D tumors, DGLA supplementation did not have any influence the expression of Ki-67 (a cell proliferation marker [212]) compared to the control group, whereas treatment of 5-FU as well as the combination of 5-FU and DGLA significantly decreased Ki-67 expression (**Fig. 29**). On the other hand, for mice bearing D5D-*KD* tumors, 4-week of DGLA supplementation significantly reduced Ki-67 expression (*e.g*. percentage of Ki-67 positive cells 19.9 ± 1.4%) compared to vehicle control (percentage of Ki-67 positive cells 30.0 ± 0.5%). These data suggested that the promoted 8-HOA formation (above a threshold level) from D5D-*KD* and DGLA supplementation could effectively inhibit colon tumor proliferation. In addition, while 5-FU alone suppressed tumor proliferation, the combination of DGLA and 5-FU in D5D-*KD* tumor resulted in more reduced Ki-67 than 5-FU treatment only.

Tumor apoptosis was examined by immunofluorescence analysis using cleaved PARP as an apoptotic marker [213-214]. Results showed that, for the mice bearing wt-D5D tumors, DGLA treatment alone could not induce apoptosis, while treatment with 5-FU as well as the combination of 5-FU and DGLA led to similar level of tumor apoptosis (**Fig. 30**). On the other hand, for mice bearing D5D-*KD* tumors, DGLA supplementation was shown to induce apoptosis to a similar level as 5-FU treatment (*e.g.* percentage of apoptotic cells 9.0 ± 0.4% and 11.3 ± 1.0%, respectively). In addition, the combination of DGLA and 5-FU in D5D-*KD* tumor appeared to result in more apoptosis (13.4 ± 0.6%) compared to DGLA alone and 5-FU alone.

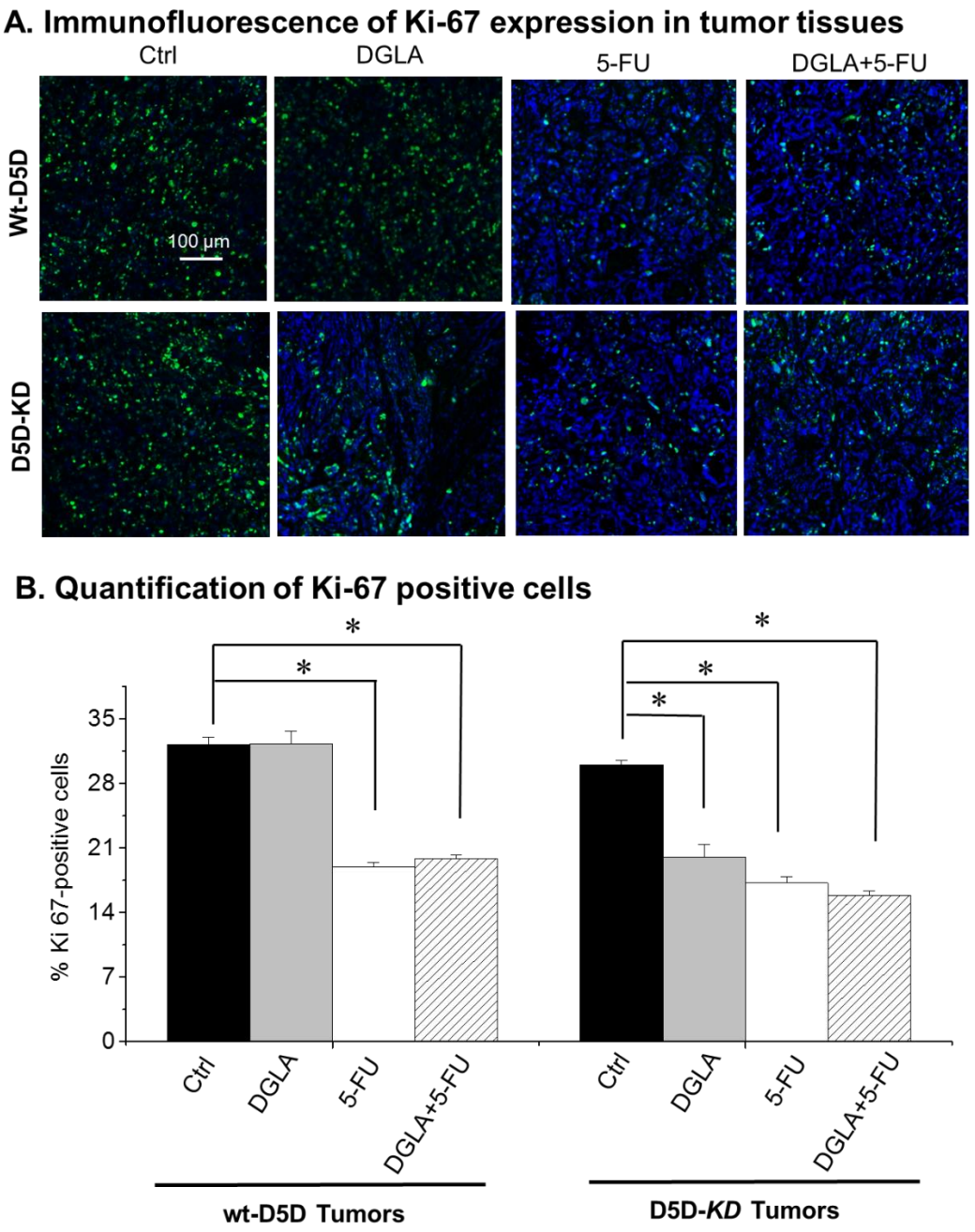

Figure 29. Immunofluorescence analysis of Ki-67 expression in tumor tissues.
A. Representative images for Ki-67expression in tumor tissues. Ki 67 was stained in green, cell nuclei were counter stained with DAPI; **B.** Quantification analysis of Ki-67, the results were presented as percentage of Ki-67 positive events to the total number of events in each image. Data represent mean ± SD (*: significant difference vs. control with $p < 0.05$).

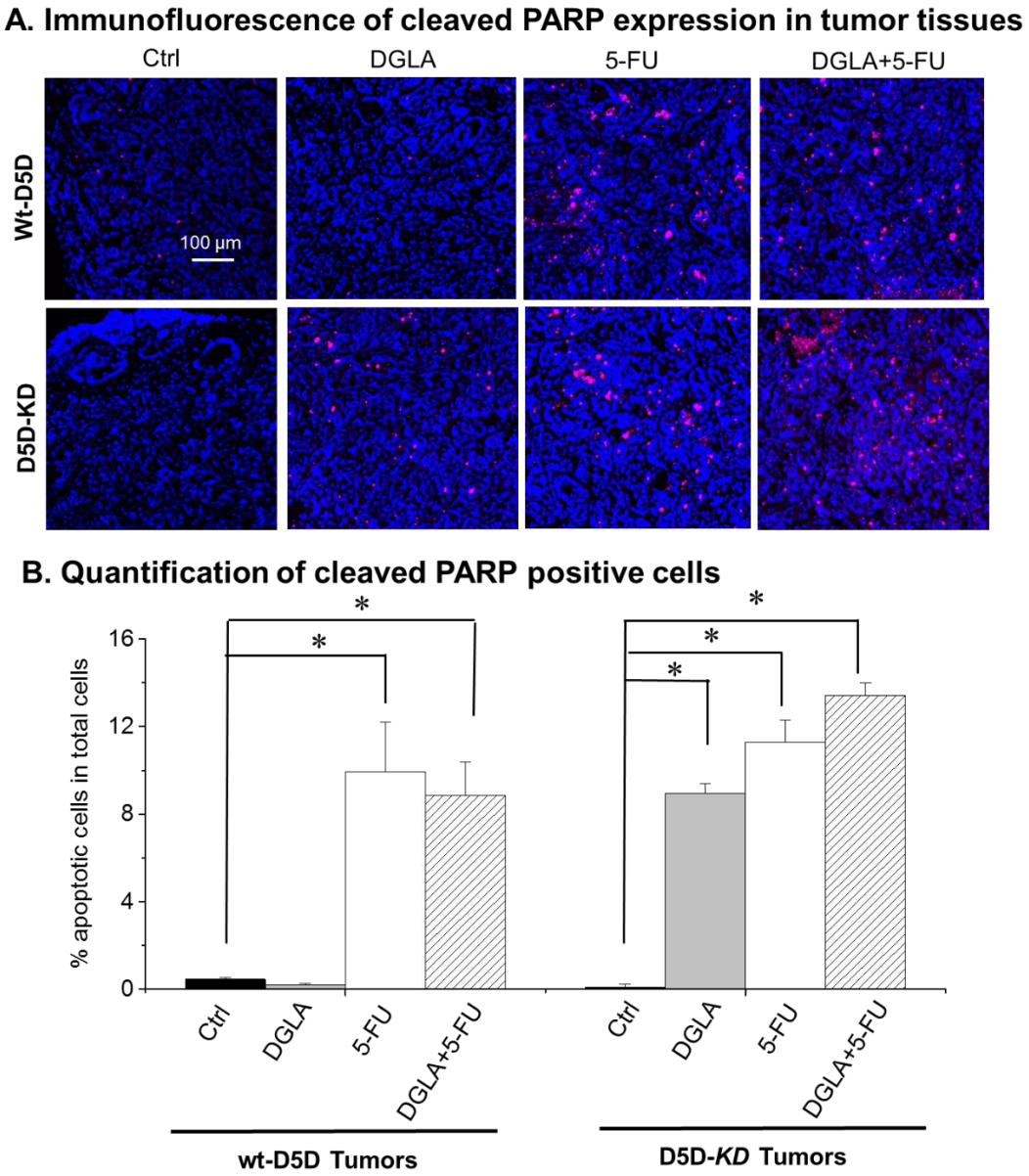

Figure 30. Immunofluorescence analysis for apoptosis in tumor tissues.
A. Representative images for cleaved PARP expression in tumor tissues, Cleaved PARP was stained in red, cell nuclei were counter stained with DAPI; **B.** Quantification analysis of cell apoptosis, the results were presented as percentage of cleaved PARP positive events to the total number of events in each sample. Data represent mean ± SD (*: significant difference vs. control with $p < 0.05$).

Western blotting was then performed to investigate the molecular mechanism of observed tumor growth inhibition and apoptosis in our study. Results showed that, in wt-D5D tumors, DGLA treatment did not affect the expression of cell apoptotic proteins and acetyl histone H3 (**Fig. 31**). However, in D5D-*KD* tumors, DGLA supplementation led to a significant increase of p53 and decrease of procaspase 9, suggesting activation of the cell apoptotic pathway (**Fig. 32**), which is consistent with the results from apoptosis analysis (Fig. 30). We also observed that DGLA supplementation in D5D tumors led to an accumulation of acetyl histone H3 and yH2AX (Fig. 32), which further confirmed our *in vitro* data (Fig. 12) and indicated that the promoted formation of 8-HOA from our treatment could inhibit HDAC and induce DNA damage. These data together suggested that, DGLA supplementation promoted 8-HOA formation in D5D-*KD* tumors, which in turn regulated histone deacetylation and induced DNA damage, thereby triggering the activation of the cell apoptosis pathway, and led to tumor growth inhibition. In comparison, in wt-D5D tumors, DGLA treatment failed to activate apoptosis and had no effect on HDAC activity.

5-FU treatment was shown to up-regulate p53 expression, activate procaspase 9 and induce DNA damage in both wt-D5D and D5D-*KD* tumors (Figs. 31-32), which is consistent with other reports [196-198]. Noteworthy, the effect from 5-FU treatment was comparable to that from the DGLA supplementation in D5D-*KD* tumor, suggesting our novel treatment strategy could achieve similar therapeutic outcome as the front line chemotherapy.

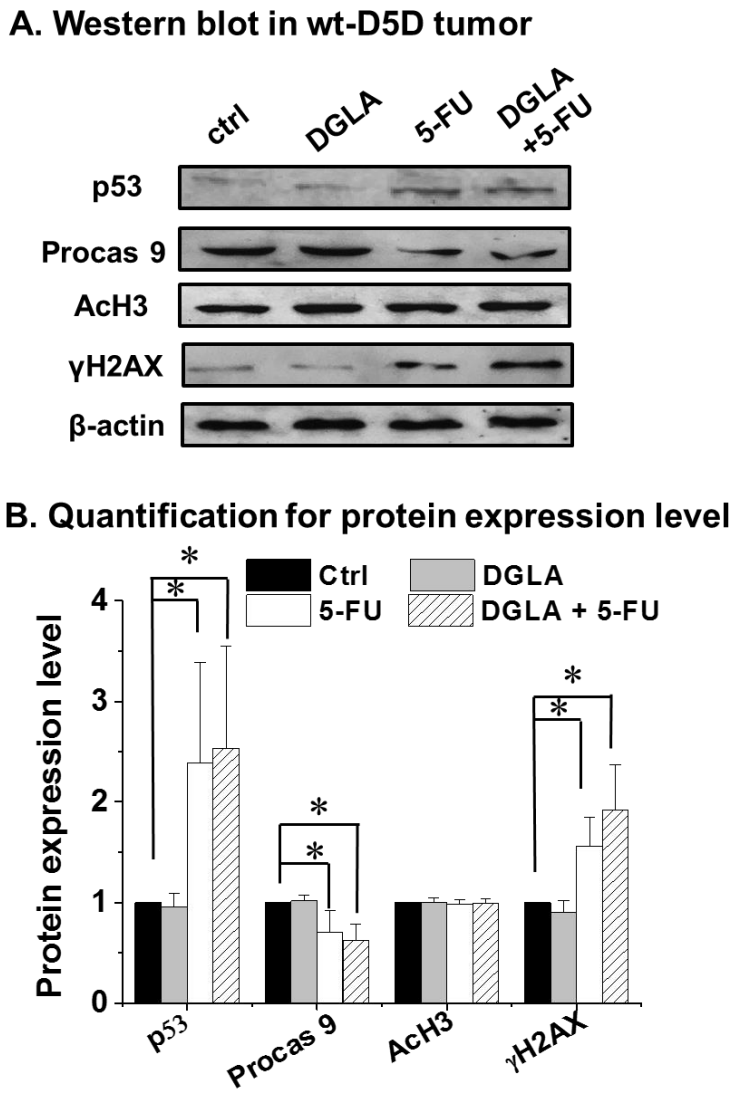

Figure 31. Alteration of apoptotic proteins in wt-D5D tumor tissues.
A. Western blot and **B.** protein expression level of p53, procaspase 9, acetyl histone H3 and γH2AX in wt-D5D tumor tissues. β-actin served as a loading control. The ratio of D5D to β-actin in control was normalized to 1.Data represent mean ± SD (*: significant difference vs. control with $p < 0.05$).

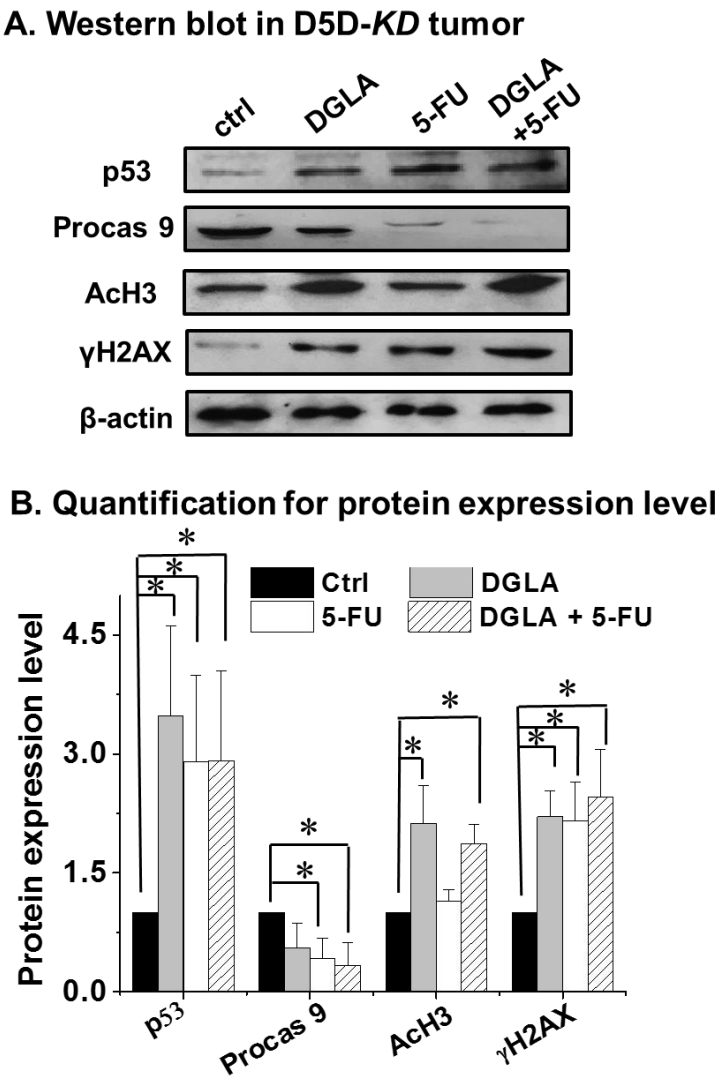

Figure 32. Alteration of apoptotic proteins in D5D-*KD* tumor tissues.
A. western blot and **B.** protein expression level of p53, procaspase 9, acetyl histone H3 and γH2AX in D5D-*KD* tumor tissues. β-actin served as a loading control. The ratio of D5D to β-actin in control was normalized to 1.Data represent mean ± SD (*: significant difference vs. control with $p < 0.05$).

5.5. DGLA Treatment Suppressed Metastasis Potential of D5D-*KD* Tumors

Besides development of a primary tumor, cancer metastasis is also a severe issue for cancer patients and accounts for around 90% of cancer-associated death [167-169]. Data from Chapter 3 showed that 8-HOA could inhibit migration and invasion in human colon cancer cells *in vitro* [170]. Hence we also tested whether promoted formation of 8-HOA from our treatment could inhibit tumor metastasis *in vivo*.

Immunofluorescence study showed that, for the mice bearing wt-D5D tumors, DGLA supplementation led to increased expression of MMP-2, a protein that degrades extracellular matrix and contributes to cancer cell migration/invasion (**Fig. 33**). This is probably because 1) DGLA was converted to AA in wt-D5D tumor, thus unable to produce enough 8-HOA to the threshold level for its anti-cancer activity (Fig. 28), and 2) DGLA supplementation in wt-D5D tumor led to an increased level of PGE2 (Fig. 28), which has been shown to play a role in cancer migration [215-216]. On the other hand, for mice bearing D5D-*KD* tumors, promoted 8-HOA formation from DGLA supplementation significantly decreased the expression of MMP-2 (mean fluorescence intensity 69.33 ± 6.7) compared to vehicle control (mean fluorescence intensity 88.3 ± 8.5%), suggesting endogenous 8-HOA inhibited tumor metastasis potential in D5D-*KD* tumors. In addition, 5-FU treatment alone or in combination of DGLA were able to down-regulate MMP-2 expression in both wt-D5D and D5D-*KD* tumors.

E-cadherin plays an important role in epithelial cell adhesion, thus, is essential for the maintenance of tissue architecture [205]. Down-regulation of E-cadherin expression was observed in the tumor environment which correlates with a strong invasive potential [205]. Our data showed that for the mice bearing wt-D5D tumors, DGLA supplementation did not have influence on the expression of E-cadherin in tumor tissues compared to the control group (**Fig. 34**). On the other

hand, for mice bearing D5D-*KD* tumors, promoted 8-HOA formation from DGLA significantly increased level of E-cadherin compared to vehicle control (mean fluorescence intensity 131.9 ± 5.2% vs. 98.8 ± 7.9%, respectively). In addition, FU treatment alone or in combination of DGLA also up-regulated E-cadherin expression in both wt-D5D and D5D-*KD* tumors.

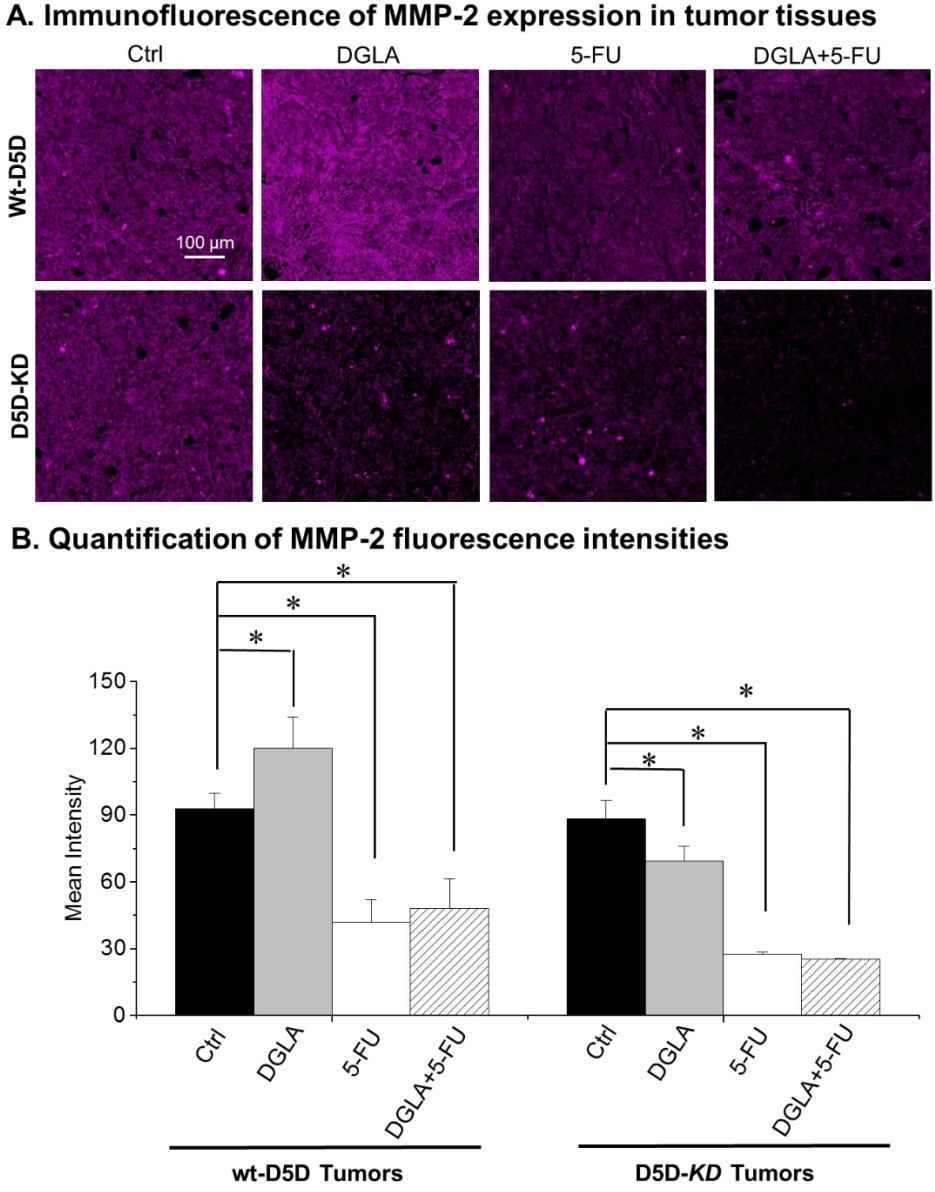

Figure 33. Immunofluorescence analysis of MMP-2 expression in tumor tissues.
A. Representative images for MMP-2 expression in tumor tissues. MMP-2 was stained in red, cell nuclei were counter stained with DAPI; **B.** Mean intensity of MMP-2 in each sample was quantified as an index of its expression level in tumor tissue (*: significant difference vs. control with $p < 0.05$).

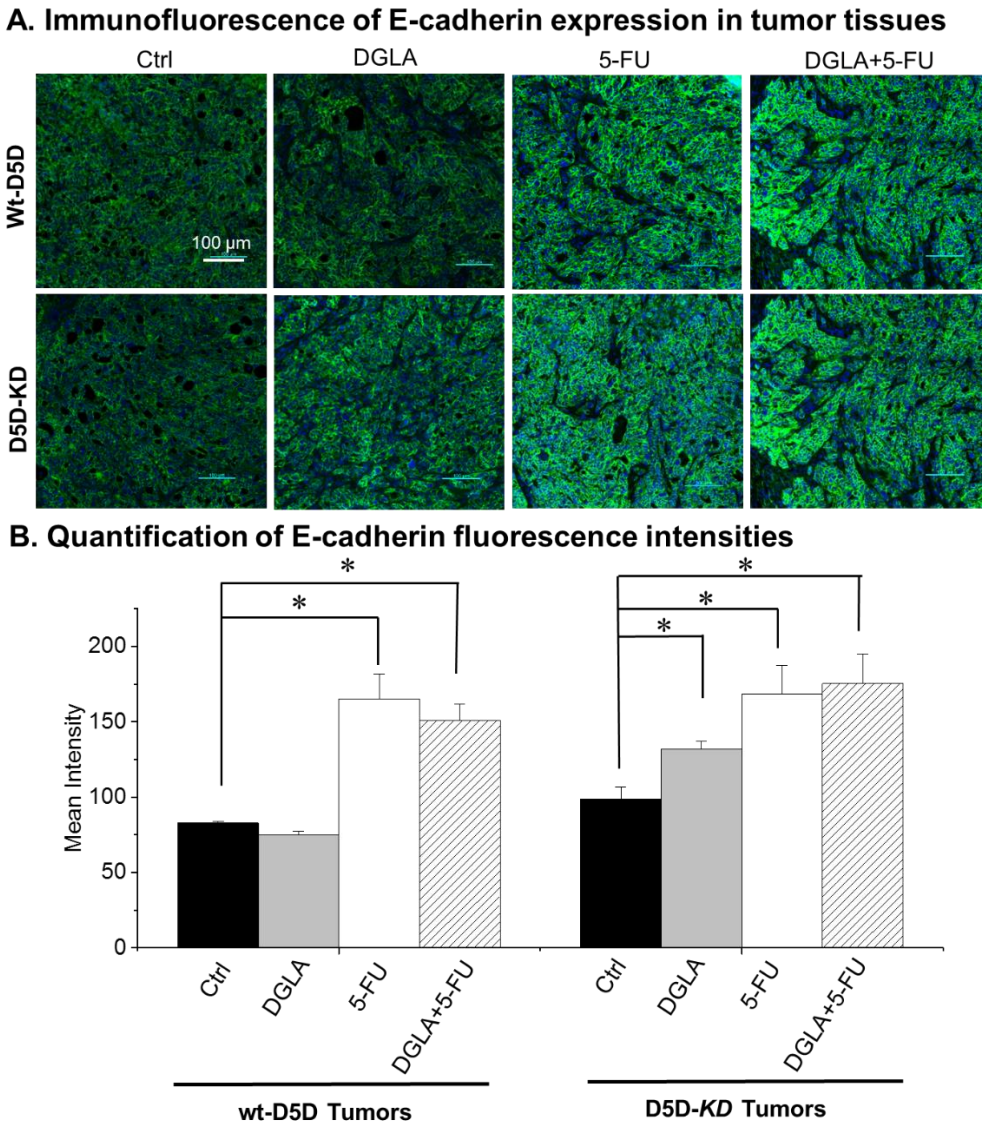

Figure 34. Immunofluorescence analysis of E-cadherin expression in tumor tissues.
A. Representative images for E-cadherin expression in tumor tissues. E-cadherin was stained in green, cell nuclei were counter stained with DAPI; **B.** Mean intensity of E-cadherin in each sample was quantified as an index of its expression level in tumor tissue (*: significant difference vs. control with $p < 0.05$).

5.6. Conclusion and Discussion

In this chapter, we tested and demonstrated that DGLA supplementation could promote the formation of 8-HOA from COX-2 catalyzed DGLA peroxidation to a threshold level in D5D-*KD* xenograft colon tumor tissues, which in turn suppressed tumor growth and metastatic potential.

Consistent with our *in vitro* studies, we observed that promoted 8-HOA formation from COX-2 catalyzed DGLA peroxidation could induce apoptosis in D5D-*KD* HCA-7 xenograft tumors, which is probably mediated through the induction of the cancer suppressor p53 (Fig. 30-32). However, p53 dysregulation is frequently observed in many cancer types including colon cancer [217], which may result in resistance to p53-dependent anti-cancer therapy. In fact, our results showed that 8-HOA could inhibit the growth of HT-29 cells with mutated p53 (Fig. 1), indicating that 8-HOA can also cause cancer cell death *via* p53-independent mechanisms. Therefore, in our future work we also plan to investigate the potential p53-independent mechanisms of 8-HOA's anti-cancer effect by establishing a HT-29 derived xenograft tumor model.

5-FU is a pyrimidine analog which induces cancer cell apoptosis by interfering with DNA replication. Resistance to 5-FU remains a major limitation of 5-FU-based cancer therapy [187]. In this study, we demonstrated that combination of 8-HOA (produced from DGLA peroxidation) and 5-FU led to improved anti-cancer effect compared to 5-FU treatment alone. However, the observed effect is only additive, not synergistic. This is because 8-HOA could not reverse the 5-FU resistance mechanisms including alteration of drug influx and efflux, drug inactivation, high level expression of thymidylate synthase, *etc* [187]. However, it has been reported that HDAC inhibitors could synergistically enhance the anti-cancer activities of various chemo- and targeted-cancer drugs, such as decitabine and sorafenib, through distinct mechanisms [218-219]. Therefore, in our

future study, we will test whether the promoted formation of 8-HOA could also synergistically improve the efficacies of these reagents in different cancers.

We found that 8-HOA could also inhibit migration and invasion in human colon cancer cell lines [170]. Consistently, we observed that promoted formation of 8-HOA from our treatment strategy could suppress the expression of MMP-2 and increase E-cadherin level, suggesting a potential in inhibiting tumor metastasis (Fig. 33-34). Therefore, in our future studies we plan to develop an orthotopic tumor model using nude mice to investigate the effect of D5D-*KD* along with DGLA supplementation on tumor metastasis. In addition, the orthotopic tumor model has similar tumor microenvironment as the original tumors, and will reflect how our strategy would actually perform in cancer patients, thus it is ideal for testing the anti-cancer effect of our strategy.

6. SUMMARY, DISCUSSION AND FUTURE DIRECTION

6.1. Research Summary

6.1.1. Summary for Chapter 3: DGLA's distinct byproduct 8-HOA inhibited colon cancer cell growth and migration

Arachidonic acid, a downstream ω-6, has been shown to promote colon cancer development by producing PGE2 during its COX-catalyzed peroxidation [12-13, 98-99]. On the other hand, DGLA, the immediate precursor of arachidonic acid, may represent an exceptional ω-6 with certain anti-cancer effects [19-20, 22, 24]. However, the mechanisms underlying DGLA's anti-cancer effects are still unclear. Using a novel HPLC/ESR (spin-trapping)/MS combined technique, previous work from our group identified distinct free radical byproduct produced from COX-2-catalyzed DGLA peroxidation, *e.g.* 8-HOA, which shares similar structures as currently known HDAC inhibitors [136-138, 179]. We thus proposed that these distinct DGLA byproducts may be responsible for DGLA's anti-cancer effect by inhibiting HDAC activity and consequently inhibiting cancer growth and migration. Therefore, in Chapter 3, we tested this hypothesis by assessing the potential anti-cancer effect and mechanism from DGLA's byproducts in three human colon cancer cell lines, *e.g.* HCA-7, HT-29 and HCT 116 cells.

Results showed that among all of the tested DGLA's byproducts, 48 h supplementation of 8-HOA, start at 1.0 μM (physiological relevant concentration), could significantly inhibit the growth and colony formation of HCA-7, HT-29 and HCT 116 cells (Fig. 1-2) [163]. In comparison, the other DGLA byproducts from COX-2 peroxidation including PGE1, HTA and HEX did not significantly influence on colon cancer cell growth at same concentration range. It was also found that supplementation of 8-HOA (1.0 μM, 48 h) resulted in cell cycle arrest at G1 phase and induced apoptosis, as well as inhibited migration in HCA-7 cells (Fig. 3-5). Mechanism study showed that

8-HOA could up-regulate cancer suppressor p53 and cyclin-dependent kinase inhibitor p27, while down-regulate MMP-2 and MMP-9, which may be responsible for observed growth and migration inhibition in HCA-7 cells (Fig. 3-5). Further investigation showed that as a short chain fatty acid, 8-HOA could serve as a HDAC inhibitor and induce DNA damage (Fig. 6). These data together indicated that 8-HOA, by inhibiting deacetylation of histone, could regulate gene transcription and induce DNA damage, then subsequently induce cell cycle arrest and apoptosis, eventually resulting in the suppression of cancer cell growth and migration. In addition, results from Chapter 3 also demonstrated that concurrent supplementation of 8-HOA in combination with 5-FU led to a better growth inhibitory effect in human colon cancer cells compared to 5-FU alone.

6.1.2. Summary for Chapter 4: D5D-*KD* and high COX-2 level in colon cancer cells promoted 8-HOA formation and suppressed cancer cell growth and migration

DGLA can produce the distinct byproduct 8-HOA which has anti-cancer effects, however, DGLA can be effectively converted to its downstream ω-6 fatty acid AA by D5D, which greatly restricts DGLA's bioavailability and activity. We proposed that knockdown of D5D could limit the conversion from DGLA to AA, thus promote 8-HOA formation from COX-2 catalyzed DGLA peroxidation to a threshold level which could inhibit colon cancer growth.

COX-2 is overexpressed in 85% of adenocarcinomas, and it can promote colon cancer progression by catalyzing AA peroxidation to produce the deleterious metabolite PGE2 [106-109]. Therefore, COX-2 inhibition, which aims at limiting the COX-2/AA pathway, has been extensively studied as a conventional strategy for the treatment of cancers. However, application of COX-2 inhibitors associated with high risk of GI injury and cardiovascular side effects in patients [30, 32-34]. In our research, instead of inhibiting COX-2, we aimed to take advantage of the high COX-2 expression in cancer cells to produce the DGLA-derived beneficial byproduct 8-

HOA to control cancer cell growth, which is a paradigm shifting concept in COX-2 biology in cancer.

In Chapter 4, in order to limit the conversion of DGLA to AA, we knocked down D5D expression in HCA-7 colony 29 cells by transfecting the cells with D5D targeted siRNA. As expected, we observed that more DGLA was preserved in D5D-*KD* cells compared to Nc-si cells during a 48 h incubation after DGLA supplementation, in association with a decreased level of free AA in D5D-*KD* cells (Fig. 11). More importantly, we found a significant increase of 8-HOA and PGE1, two metabolites from COX-catalyzed DGLA peroxidation, in D5D-*KD* cells compared to those in Nc-si cells. For example, in Nc-si cells, PGE1 retained a stable concentration range (0.35 μM to 0.39 μM) during the 48 h incubation, while PGE1 in D5D-*KD* cells ranged from ~0.5 μM (8 h-12 h) to 0.8 μM in 48 h (Fig. 11). However, we previous demonstrated that PGE1 did not inhibit colon cancer cell growth at a concentration range from 0.1 μM to 10 μM (Fig. 1), suggesting that DGLA's anti-cancer activity is not from PGE1 at physiological relevant concentration. On the other hand, 8-HOA was found to accumulate and reach a plateau at 24 h to 48 h (0.92 ± 0.09 μM at 48 h, Fig. 12) in D5D-*KD* HCA-7 cells treated with DGLA, while in Nc-si HCA-7 cells, the maximal level of 8-HOA only reached ~ 0.5 μM at 24 h. Considering 8-HOA was shown to significantly inhibit HCA-7 cells growth at 1.0 μM (Fig. 1), we propose that 8-HOA is the bioactive metabolite responsible for the anti-cancer effect of DGLA, and maintaining a threshold range of endogenous 8-HOA (~ 0.5 μM to 1.0 μM) is essential for eliciting DGLA's anti-cancer activity.

After confirming D5D-*KD* could limit conversion of DGLA and accumulate 8-HOA, we then investigated whether this strategy could actually inhibit colon cancer cell growth and migration as we observed from direct 8-HOA treatment in Chapter 3. Colony formation assay and

wound healing assay showed that 100 μM of DGLA treatment significantly inhibited the colony formation and migration in D5D-*KD* HCA-7 cells, while no inhibition effect was observed from DGLA treatment on the control siRNA transfected cells (Fig. 9-10). In addition, we also found that DGLA treatment in D5D-*KD* HCA-7 cells resulted in a significant increase of acetyl histone H3 and γH2AX (Fig. 12), which is similar to the effect from direct 8-HOA treatment (Fig. 6), indicating the anti-cancer effect of DGLA is derived from formation of 8-HOA. To further confirm that the observed DGLA's anti-cancer effect is derived from COX-2 catalyzed DGLA peroxidation, we performed a D5D/COX-2 double knockdown experiment using HCA-7 cells. Results showed that DGLA significantly inhibited cell growth in D5D-*KD* cells, however, this inhibitory effect was abolished in D5D/COX-2 double-KD cells (Fig. 13), suggesting that COX-2 is involved in DGLA's anti-cancer effect. This observation provides evidence to further support our hypothesis that 8-HOA from COX-2 catalyzed DGLA peroxidation is responsible for DGLA's anti-cancer activity. Consistently, we observed that 48 h DGLA treatment (100 μM) only led to a minimal growth inhibitory effect in D5D-*KD* HT-29 cells, while no inhibitory effect from DGLA was observed in D5D-*KD* HCT 116 cells (Fig. 14), probably because there is much less 8-HOA generated from DGLA in these two cell lines due to their low/deficient COX-2 levels.

We also found that D5D-*KD* and DGLA treatment in combination with various chemo-drugs led to better inhibitory effects in colon cancer cell growth and migration, compared to drug treatments alone (Figs. 15-21). This observation was associated with promoted cell cycle arrest and apoptosis, as well as further activation of cell apoptosis (Figs. 15-21).

6.1.3. Summary for Chapter 5: DGLA supplementation inhibited D5D-*KD* xenograft tumor grow and migration potential by promoting 8-HOA formation

In Chapters 4, we observed that D5D-*KD* in human colon cancer cell lines could promote 8-HOA formation from DGLA peroxidation to a threshold level, which in turn inhibits cancer cell growth and enhances the efficacy of chemo-drugs. However, the *in vitro* experimental system cannot completely represent the complex tumor environment in patients. Therefore, in Chapter 5, we further tested our novel strategy using a mice xenograft tumor model.

Results showed that for mice bearing D5D-*KD* tumors, DGLA supplementation led to significantly reduced tumor size compared to that in the control group (Fig. 24). In addition, mice receiving the combination of DGLA and 5-FU appeared to have reduced tumor size than mice receiving 5-FU only, although no significant difference was observed. As we expected, in D5D-*KD* tumors with DGLA supplementation, we detected higher level of DGLA, 8-HOA and PGE1 compared to those in wt-D5D tumors with DGLA supplementation, suggesting D5D-*KD* in tumor tissues effectively limited the conversion of DGLA to AA and promoted the formation of 8-HOA (Fig. 27-28). Noteworthy, from our *in vitro* study, we observed a one fold increase of 8-HOA in D5D-*KD* cancer cells compared to wt-D5D cells after 48 h DGLA supplementation (Fig. 12), here we observed a more dramatic increase of 8-HOA in D5D-*KD* tumors compared to wt-D5D tumors, which is very like to be responsible for the observed tumor inhibitory effect.

We also observed that DGLA supplementation in D5D-*KD* tumors significantly inhibited tumor proliferation and induced apoptosis, evidenced by Ki-67 and cleaved PARP staining (Fig. 29-30). This observation was associated with activation of the p53-dependednt apoptotic pathway and inhibition of HDAC, further confirming the tumor suppressive effect was derived from 8-HOA (Fig. 32).

In addition, other work from our group found that 8-HOA could also inhibit migration and invasion in various cancer cell lines [170]. Consistently, we observed that promoted formation of 8-HOA from our treatment strategy could affect the expression of MMP-2 and increase E-cadherin level, suggesting a potential in inhibiting tumor metastasis (Fig. 33-34).

6.1.4. Conclusion and discussion

COX-2 is overexpressed in 85% of adenocarcinomas, and it can promote colon cancer progress by catalyzing AA peroxidation to produce deleterious metabolite PGE2 [106-109]. Therefore, COX-2 inhibition, which aims at limiting COX-2/AA pathway, has been extensively studied as a conventional strategy for the treatment of cancers. However, COX-2, by its nature, can be induced rapidly in cancer environment, resulting in undesirable therapeutic effect from the COX-2 inhibition strategy. In addition, COX-2 inhibitors commonly suffer from high risk of GI injury and cardiovascular side effect in patients [30, 32-34]. Therefore, developing an alternative treatment strategy for colon cancer with safer and better therapeutic outcomes is in urgent need.

For the first time, our research showed that, through COX-2 catalyzed peroxidation, DGLA can produce a distinct byproduct 8-HOA which serves as an HDAC inhibitor and inhibits colon cancer growth and migration [136-139, 163-164]. Based on this novel finding, we proposed and demonstrated that instead of inhibiting COX-2, we can take advantage of the high COX-2 expression in cancer cells to promote the formation of DGLA's beneficial byproduct 8-HOA to control cancer cell growth and migration. We believe this novel strategy will lead to a better therapeutic effect in colon cancer treatment due to its dual anti-cancer mechanisms, *i.e*. promoting anti-cancer effect from DGLA while limiting the pro-cancer effect from AA. On the other hand, our strategy will have less side effect compared to COX inhibition, thus resulting in a safer cancer treatment. In addition, our proposed strategy of making use the hallmark of cancer cell to work

against cancer cell itself would provide an excitingly novel insight into cancer therapy and may challenge the current paradigm of COX biology in cancer treatment.

Although we have demonstrated that COX-2 is essential for eliciting DGLA's anti-cancer effect, results from our study also showed that regardless of the COX-2 expression levels, the growth of HCA-7, HT-29 and HCT 116 cells could all be significantly suppressed by direct treatment of 8-HOA (Fig. 1-2). This observation suggested that even in the cancer cells with a limited level of COX-2, our strategy will also be effective as the tumor surrounding cells with considerable levels of COX-2 could also produce 8-HOA, which may act as paracrine-like manner to trigger anti-cancer effects. In addition, a recent study from Mustafi *et al* established a xenograft colon tumor model using HCT 116 cells, in which they observed an interaction between tumor cells and stromal cells that led to an upregulation of COX-2 levels in both types of cells [210]. This indicates that the COX-2 level in both cancer cells and stromal cells will be upregulated in the tumor environment, which makes the tumor more vulnerable to our strategy.

Prostaglandin E1 is one of the major metabolites from DGLA peroxidation and has been reported to possess certain anti-inflammation and anti-cancer effect [159-162]. Therefore, people generally considered PGE1 the major beneficial bioactive metabolite from DGLA. In this study, we also tested the potential effect of PGE1 on colon cancer cell growth at the concentration range from 0.1 μM to 10 μM. The tested concentration range was selected based on PGE1 production from cells treated with 100 μM of DGLA [164]. However, our data showed that the cell growth of all three tested cell lines was not affected by PGE1 treatment (Fig. 1), probably due to the low (but physiological relevant) concentration employed in our experiment compared to that in other research, [159-162, 195].

Although our results showed that 8-HOA could induce p53-dependent apoptosis in HCA-7 cells, our results also showed that 8-HOA could inhibit the growth of cell lines with different p53 status, *e.g.* HT-29 cells (mutant p53) and HCT 116 (wt-p53) (Fig. 1), indicating that 8-HOA could cause cancer cell death *via* p53-dependent and p53-independent mechanisms. Considering the fact that many cancer cells bear a mutant p53 gene, in our future study we will further investigate the possible p53-independent mechanism by which 8-HOA could deliver anti-cancer effects.

Our results also showed that 8-HOA could act as an HDAC inhibitor and consequently lead to DNA damage, which may explain the observed cell cycle arrest, apoptosis and growth inhibition in colon cancer cells (Fig. 6). However, HDAC consists of a family of proteins which may interact with specific target proteins individually, and HDAC inhibition may lead to various biological consequences through different mechanisms [173-179, 184-185]. Therefore, further mechanistic studies are required to elaborate whether and how 8-HOA could interact with specific HDACs and trigger inhibitory effects on cancer cell growth and migration.

D5D has not been investigated specifically related to cancer. In this study, we demonstrated that genetic knockdown of D5D could effectively reserve more DGLA to promote the formation of DGLA's distinct byproduct to deliver its anti-cancer effect. Therefore, D5D represents a novel drug target for colon cancer treatment and investigation of D5D inhibitors will be a promising direction for cancer research.

As the most abundant essential dietary fatty acids, ω-6s have not received much research attention for their potential health beneficial effects. However, our research showed that, through COX-2 catalyzed peroxidation, DGLA can produce a distinct byproduct 8-HOA which serves as an HDAC inhibitor and inhibits colon cancer growth and migration *in vitro* and *in vivo*. Our

research outcome will guide us to develop a novel ω-6-based diet care strategy in combination with frontline chemotherapy for colon treatment.

6.2. Future Directions

6.2.1. To design and screen for specific and effective D5D inhibitors

In the present study, we knocked down D5D expression in cancer cells *via* siRNA or shRNA transfection. However, direct siRNA and shRNA treatments are not suitable in clinical practice due to stability issues of the siRNA products and safety concerns for shRNA vectors [217]. Therefore, in our future study, we plan to screen and/or design specific and effective D5D inhibitors to be used in patients. In fact, we already selected a lead compound from various candidate compounds which are reported to have D5D inhibitory effects. The protein-ligand interaction between D5D and lead compounds was investigated by using various bioinformatics tools to define the structure-activity relationship of D5D inhibitor. Then we optimized lead compound by modifying the different functional moieties and synthesized a series of new compounds. Our preliminary *in vitro* and *in vivo* data showed that these newly synthesized compounds, along with DGLA treatment, could effectively inhibit colon cancer cell and tumor growth.

6.2.2. Inhibiting D5D expression by innovative RNA nanoparticles

Besides screening D5D inhibitors, we are also planning to employ an innovative RNA nanoparticle for delivering D5D-target siRNA into cancer cells [220-223]. Delivery of therapeutic RNAs has remained a difficult task for a long time, some challenges include specific cancer targeting, tissue penetration, intracellular delivery and unfavorable pharmacological profiles. However, recent study from Dr. Peixuan Guo's group has developed multi-functional, thermodynamically and chemically stable RNA nanoparticles harboring cancer targeting ligand

for specific delivering therapeutic siRNA into cancer cells [220-223]. In collaboration with Dr. Guo's group, we constructed RNA nanoparticles carrying targeting ligand as well as D5D-targeted siRNA to inhibit D5D expression specifically in colon cancer cells. In our preliminary study, the RNA nanoparticles containing D5D-siRNA have been shown to inhibit D5D expression effectively and suppressed colon cancer growth when DGLA was supplemented concurrently.

6.2.3. To investigate tumor metastasis using orthotopic tumor model

We demonstrated that direct treatment of 8-HOA or endogenous formation of 8-HOA from DGLA peroxidation could inhibit cancer cell migration *in vitro* and suppress the expression of proteins involved in tumor metastasis *in vivo* (Fig. 5, 10, 33, 34). However, we cannot test the direct effect of our strategy on tumor metastasis in our study as the subcutaneous xenograft model generally does not lead to spontaneous metastasis [224]. Therefore, in future study, we plan to employ an orthotopic tumor model in which the cancer cells are implanted into the organ of origin. The orthotopic tumor model more closely resembles human cancers and could develop spontaneous metastasis which will enable us to investigate the effect of our strategy on tumor metastasis. The orthotopic tumor model is ideal for our future *in vivo* research also because it has similar tumor microenvironment as the original tumor, thus may provide more reliable data on how our strategy would actually perform in cancer patients. In addition, besides colon cancer, we will extend our study to other types of cancer, including breast cancer, skin cancer and lung cancer, *etc*. In fact, our recent research has already demonstrated that the D5D-*KD* along with DGLA supplementation could inhibit the growth and migration of other types of cancer cells, including pancreatic and breast cancer. We believe our novel ω-6-based treatment strategy will provide a powerful alternative option for clinic cancer therapy.

6.2.4. To synergistically improve the efficacies of chemo- and targeted-cancer therapy

Drug resistance remains a major obstacle for cancer therapy [187]. In this study, we demonstrated that combination of 8-HOA (produced from DGLA peroxidation) and 5-FU led to improved anti-cancer effect compared to 5-FU treatment alone. However, the observed effect is only additive, not synergistic. This is because 8-HOA could not reverse the 5-FU resistance mechanisms including alteration of drug influx and efflux, drug inactivation, high level expression of thymidylate synthase, *etc* [187]. However, it has been reported that HDAC inhibitors could synergistically enhance the anti-cancer activities of various chemo- and targeted-cancer drugs, such as decitabine and sorafenib, through distinct mechanisms [218-219]. We propose that, as an HADC inhibitor, 8-HOA can also synergistically improve these chemo- and targeted-cancer therapy. Therefore, in our future study, we will combine our novel treatment strategy with various anti-cancer reagents to test whether promoted 8-HOA formation from DGLA peroxidation could synergistically improve the efficacies of chemo- and targeted-cancer drugs.

REFERENCES

1. American cancer society. Key statistics for colorectal cancer. Available at https://www.cancer.org/cancer/colon-rectal-cancer/about/key-statistics.html

2. Serini S, Piccioni E, Merendino N, Calviello G. Dietary polyunsaturated fatty acids as inducers of apoptosis: Implications for cancer. *Apoptosis.* 2009, **14:**135-152.

3. Spencer L, Mann C, Metcalfe M, Webb M, Pollard C, Spencer D, Berry D, Steward W, Dennison A. The effect of omega-3 FAs on tumour angiogenesis and their therapeutic potential. *Eur J Cancer*. 2009, **45:**2077-2086.

4. Cockbain AJ, Toogood GJ, Hull MA. Omega-3 polyunsaturated fatty acids for the treatment and prevention of colorectal cancer. *Gut*. 2012, **61:**135-149.

5. Pot GK, Geelen A, van Heijningen EM, Siezen CL, van Kranen HJ, Kampman E. Opposing associations of serum n-3 and n-6 polyunsaturated fatty acids with colorectal adenoma risk: an endoscopy-based case-control study. *Int J Cancer.* 2008, **123:**1974-1977.

6. Kokura S, Nakagawa S, Hara T, Boku Y, Naito Y, Yoshida N, Yoshikawa T. Enhancement of lipid peroxidation and of the antitumor effect of hyperthermia upon combination with oral eicosapentaenoic acid. *Cancer Lett.* 2002, **185:**139-144.

7. Siddiqui RA, Harvey KA, Xu Z, Bammerlin EM, Walker C, Altenburg JD. Docosahexaenoic acid: A natural powerful adjuvant that improves efficacy for anticancer treatment with no adverse effects. *Biofactors*. 2011, **37:**399-412.

8. Sauer LA, Blask DE, Dauchy RT. Dietary factors and growth and metabolism in experimental tumors. *J Nutr Biochem*. 2007, **18:**637-649.

9. Kimura Y, Kono S, Toyomura K, Nagano J, Mizoue T, Moore MA, Mibu R, Tanaka M, Kakeji Y, Maehara Y, Okamura T, Ikejiri K, Futami K, Yasunami Y, Maekawa T, Takenaka K,

Ichimiya H, Imaizumi N. Meat, fish and fat intake in relation to subsite-specific risk of colorectal cancer: The Fukuoka Colorectal Cancer Study. *Cancer Sci.* 2007, **98:**590-597.

10. Wen B, Deutsch E, Opolon P, Auperin A, Frascognal V, Connault E, Bourhis J. n-3 polyunsaturated fatty acids decrease mucosal/epidermal reactions and enhance anti tumour effect of ionising radiation with inhibition of tumour angiogenesis. *Br J Cancer*. 2003, **89:**1102-1107.

11. Huerta-Yépez S, Tirado-Rodriguez AB, Hankinson O. Role of diets rich in omega-3 and omega-6 in the development of cancer. *Boletín Médico del Hospital Infantil de México*. 2016, **73:** 446-456.

12. Li S, Zhao X, Wu Z, Li Y, Zhu L, Cui B, Dong X, Tian S, Hu F, Zhao Y. Polymorphisms in arachidonic acid metabolism-related genes and the risk and prognosis of colorectal cancer. *Fam Cancer*. 2013, **12:**755-765.

13. Sakai M, Kakutani S, Horikawa C, Tokuda H, Kawashima H, Shibata H, Okubo H, Sasaki S. Arachidonic acid and cancer risk: A systematic review of observational studies. *BMC Cancer*. 2012, **12:**606.

14. Brown MD, Hart C, Gazi E, Gardner P, Lockyer N, Clarke N. Influence of omega-6 PUFA arachidonic acid and bone marrow adipocytes on meta- static spread from prostate cancer. *Br J Cancer*. 2010, **102:**403-413.

15. Li Y, Zhao H, Wang Y, Zheng H, Yu W, Chai H, Zhang J, Falck JR, Guo AM, Yue J, Peng R, Yang J. Isoliquiritigenin induces growth inhibition and apoptosis through downregulating arachidonic acid metabolic network and the deactivation of PI3K/Akt in human breast cancer. *Toxicol Appl Pharmacol*. 2013, **272:**37-48.

16. Pender-Cudlip MC, Krag KJ, Martini D, Yu J, Guidi A, Skinner SS, Zhang Y, Qu X, He C, Xu Y, Qian SY, Kang JX. Delta-6-desaturase activity and arachidonic acid synthesis are increased in human breast cancer tissue. *Cancer Sci*. 2013, **104:**760-764.

17. Yang P, Cartwright CA, Li J, Wen S, Prokhorova IN, Shureiqi I, Troncoso P, Navone NM, Newman RA, Kim J. Arachidonic acid metabolism in human prostate cancer. *Int J Oncol*. 2012, **41:**1495-1503.

18. Amirian ES, Ittmann MM, Scheurer ME. Associations between arachidonic acid metabolism gene polymorphisms and prostate cancer risk. *Prostate.* 2011, **71:**1382-1389.

19. Das UN, Madhavi N. Effect of polyunsaturated fatty acids on drug-sensitive and resistant tumor cells in vitro. *Lipids Health Dis*. 2011, **10:**159.

20. Ramchurren N, Karmali R. Effects of gamma-linolenic and dihomo-gamma-linolenic acids on 7,12-dimethylbenz (alpha) anthracene-induced mammary tumors in rats. *Prostaglandins Leukot Essent Fatty Acids.* 1995, **53:**95-101.

21. Berquin IM, Edwards IJ, Kridel SJ, Chen YQ. Polyunsaturated fatty acid metabolism in prostate cancer. *Cancer metastasis reviews*. 2011, **30:**295-309.

22. Sagar PS, Das UN, Koratkar R, Ramesh G, Padma M, Kumar GS. Cytotoxic action of cis-unsaturated fatty-acids on human cervical-carcinoma (Hela) cells - relationship to free-radicals and lipid-peroxidation and its modulation by calmodulin antagonists. *Cancer letters.* 1992, **63:**189-198.

23. Menendez JA, Ropero S, Mehmi I, Atlas E, Colomer R, Lupu R. Overexpression and hyperactivity of breast cancer- associated fatty acid synthase (oncogenic antigen-519) is insensitive to normal arachidonic fatty acid-induced suppression in lipogenic tissues but it is selectively inhibited by tumoricidal alpha-linolenic and gamma-linolenic fatty acids: A novel

mechanism by which dietary fat can alter mammary tumorigenesis. *Int J Oncol*. 2004, **24:**1369-1383.

24. Sagar PS, Das UN. Cytotoxic action of cis-unsaturated fatty-acids on human cervical-carcinoma (Hela) cells in-vitro. *Prostag Leukotr Ess*. 1995, **53:**287-299.

25. Wang D, Dubois RN. The role of COX-2 in intestinal inflammation and colorectal cancer. *Oncogene*. 2010, **29:**781-788.

26. Eberhart CE, Coffey RJ, Radhika A, Giardiello FM, Ferrenbach S, DuBois RN. Up-regulation of cyclooxygenase 2 gene expression in human colorectal adenomas and adenocarcinomas. *Gastroenterology*. 1994, **107:**1183-1188.

27. Dixon DA, Blanco FF, Bruno A, Patrignani P. Chapter 2: Mechanistic Aspects of COX-2 Expression in Colorectal Neoplasia. *Recent results in cancer research. Fortschritte der Krebsforschung Progres dans les recherches sur le cancer*. 2013, **191:**7-37.

28. Ogino S, Kirkner GJ, Nosho K, Irahara N, Kure S, Shima K, Hazra A, Chan AT, Dehari R, Giovannucci EL, Fuchs CS.Cyclooxygenase-2 expression is an independent predictor of poor prognosis in colon cancer. *Clin Cancer Res*. 2008, **14:**8221-8227.

29. Koehne CH, Dubois RN. COX-2 inhibition and colorectal cancer. *Semin Oncol*. 2004, **2 Suppl 7:**12-21.

30. Zarghi A, Arfaei S. Selective COX-2 inhibitors: a review of their structure-activity relationships. *Iran J Pharm Res*. 2011, **10:**655-683.

31. Yokouchi H, Kanazawa K. Revisiting the role of COX-2 inhibitor for non-small cell lung cancer. *Transl Lung Cancer Res*. 2015, **4:**660-664.

32. Bresalier RS, Sandler RS, Quan H, Bolognese JA, Oxenius B, Horgan K, Lines C, Riddell R, Morton D, Lanas A, Konstam MA, Baron JA. Adenomatous Polyp Prevention on Vioxx

(APPROVe) Trial Investigators. Cardiovascular events associated with rofecoxib in a colorectal adenoma chemoprevention trial. *N Engl J Med*. 2005, **352:**1092-1102.

33. Chinese Rheumatism Data Center; Chinese Systemic Lupus Erythematosus Treatment and Research Group. Recommendation for the prevention and treatment of non-steroidal anti-inflammatory drug-induced gastrointestinal ulcers and its complications. *Zhonghua Nei Ke Za Zhi*. 2017, **56:**81-85.

34. Scarpignato C, Hunt RH. Nonsteroidal antiinflammatory drug-related injury to the gastrointestinal tract: clinical picture, pathogenesis, and prevention. *Gastroenterol Clin North Am*. 2010, **39:**433-464.

35. Currie E, Schulze A, Zechner R, Walther TC, Farese RV. Cellular fatty acid metabolism and cancer. *Cell metabolism*. 2013, **18:**153-161.

36. Das UN. Essential fatty acids - a review. *Curr Pharm Biotechnol.* 2006, **7:**467-482.

37. Panickar KS, Bhathena SJ. Fat detection: taste, texture, and post ingestive effects. Chapter 18: Control of fatty acid intake and the role of essential fatty acids in cognitive function and neurological disorders. *CRC Press, Boca Raton (FL)* 2010.

38. Sprecher H, Metabolism of highly unsaturated n-3 and n-6 fatty acids. *Biochim. Biophys. Acta*, 2000, **1486:**219-231.

39. Tapiero H, Ba GN, Couvreur P, Tew KD. Polyunsaturated fatty acids (PUFA) and eicosanoids in human health and pathologies. *Biomed Pharmacother*. 2002, **56:**215-222.

40. Ibarguren M, López DJ, Escribá PV. The effect of natural and synthetic fatty acids on membrane structure, microdomain organization, cellular functions and human health. *Biochim Biophys Acta*. 2014, **1838:**1518-1528.

41. Lapshina EA, Zavodnik IB, Bryszewska M. Effect of free fatty acids on the structure and properties of erythrocyte membrane. *Scand. J. Clin. Lab. Invest*. 1995, **55:**391-397.

42. Berg JM, Tymoczko JL, Stryer L. Biochemistry. 5th edition. Section 22.6, Elongation and Unsaturation of Fatty Acids Are Accomplished by Accessory Enzyme Systems. *New York: W H Freeman*, 2002.

43. US Department of Agriculture, Agricultural Research Service. Nutrient Intakes from Food: Mean Amounts Consumed per Individual, by Gender and Age. Available at: http://www.ars.usda.gov/ba/bhnrc/fsrg. Accessed 4/25/14.

44. Simon D, Eng PA, Borelli S, Kägi R, Zimmermann C, Zahner C, Drewe J, Hess L, Ferrari G, Lautenschlager S, Wüthrich B, Schmid-Grendelmeier P. Gamma-linolenic acid levels correlate with clinical efficacy of evening primrose oil in patients with atopic dermatitis. *Adv Ther*. 2014, **31:**180-188.

45. Bezard, J.; Blond, J. P.; Bernard, A.; Clouet, P. The metabolism and availability of essential fatty acids in animal and human tissues. *Reproduction, nutrition, development.* 1994, **34:**539-568.

46. Ulven SM, Kirkhus B, Lamglait A, Basu S, Elind E, Haider T, Berge K, Vik H, Pedersen JI. Metabolic effects of krill oil are essentially similar to those of fish oil but at lower dose of EPA and DHA, in healthy volunteers. *Lipids*. 2011, **46:**37-46.

47. Sargent JR. Fish oils and human diet. *Br J Nutr*. 1997, **78 Suppl 1:**S5-13.

48. Simopoulos AP, Leaf A, Salem N Jr. Essentiality of and recommended dietary intakes for omega-6 and omega-3 fatty acids. *Annals of nutrition & metabolism*. 1999, **43:**127-130.

49. Calder PC, Yaqoob P. Omega-3 polyunsaturated fatty acids and human health outcomes. *Biofactors.* 2009, **35:**266-272.

50. Woutersen RA, Appel MJ, van Garderen-Hoetmer A, Wijnands MV. Dietary fat and carcinogenesis. *Mutation research*. 1999, **443:**111-127.

51. Calder PC. Dietary modification of inflammation with lipids. *P Nutr Soc*. 2002, **61:**345-358.

52. Nakamura MT, Nara TY. Structure, function, and dietary regulation of delta6, delta5, and delta9 desaturases. *Annu Rev Nutr*. 2004, **24:**345-376.

53. Jump DB, Depner CM, Tripathy S. Omega-3 fatty acid supplementation and cardiovascular disease. *J Lipid Res*. 2012, **53:**2525-2545.

54. Burdge GC, Jones AE, Wootton SA. Eicosapentaenoic and docosapentaenoic acids are the principal products of α-linolenic acid metabolism in young men. *Br J Nutr*. 2002, **88:**355-364.

55. Burdge GC, Wootton SA. Conversion of α-linolenic acid to eicosapentaenoic, docosapentaenoic and docosahexaenoic acids in young women. *Br J Nutr*. 2002, **88:**411-420.

56. Moghadasian MH. Advances in dietary enrichment with n-3 fatty acids. *Crit Rev Food Sci Nutr*. 2008, **48:**402-410.

57. Leaf DA, Hatcher L. The effect of lean fish consumption on triglyceride levels. *Phys Sportsmed*. 2009, **37:**37-43.

58. Ibarguren M, López DJ, Encinar JA, González-Ros JM, Busquets X, Escribá PV. Partitioning of liquid-ordered/liquid-disordered membrane microdomains induced by the fluidifying effect of 2-hydroxylated fatty acid derivatives. *Biochim Biophys Acta*. 2013, **1828:**2553-1863.

59. Igarashi M, Chang L, Ma K, Rapoport SI. Kinetics of eicosapentaenoic acid in brain, heart and liver of conscious rats fed a high n−3 PUFA containing diet. *Prostaglandins Leukot. Essent. Fatty Acids*. 2013, **89:**403-412.

60. Usher JR, Epand RM, Papahadjopoulos D. The effect of free fatty acids on the thermotropic phase transition of dimyristoyl glycerophosphocholine. *Chem. Phys. Lipids*. 1978, **22:**245-253.

61. Karnovsky MJ, Kleinfeld AM, Hoover RL, Klausner RD. The concept of lipid domains in membranes. *J. Cell Biol*. 1982, **94:**1-6.

62. Epand RM, Epand RF, Ahmed N, Chen R. Promotion of hexagonal phase formation and lipid mixing by fatty acids with varying degrees of unsaturation. *Chem. Phys. Lipids*. 1991, **57:**75-80

63. Onuki Y, Morishita M, Chiba Y, Tokiwa S, Takayama K. Docosahexaenoic acid and eicosapentaenoic acid induce changes in the physical properties of a lipid bilayer model membrane *Chem. Pharm. Bull*. 2006, **54:**68-71.

64. Jeffrey BG, Weisingerb HS, Neuringer M, Mitcheli DC. The role of docosahexaenoic acid in retinal function. *Lipids*. 2001, **36:**859-871.

65. SanGiovanni JP, Chew EY. The role of omega-3 long-chain polyunsaturated fatty acids in health and disease of the retina. *Prog Retin Eye Res*. 2005, **24:**87-138.

66. Innis SM. Dietary omega 3 fatty acids and the developing brain. *Brain R*es. 2008, **1237:**35-43.

67. Chalon S, Vancassel S, Zimmer L, Guilloteau D, Durand G. Polyunsaturated fatty acids and cerebral function: focus on monoaminergic neurotransmission. *Lipids*. 2001, **36:**937-944.

68. Price PT, Nelson CM, Clarke SD. Omega-3 polyunsaturated fatty acid regulation of gene expression. *Curr Opin Lipidol*. 2000, **11:**3-7.

69. Sampath H, Ntambi JM. Polyunsaturated fatty acid regulation of gene expression. *Nutr Rev*. 2004, **62:**333-339.

70. Rouzer CA, Marnett LJ. Endocannabinoid oxygenation by cyclooxygenases, lipoxygenases, and cytochromes P450: cross-talk between the eicosanoid and endocannabinoid signaling pathways. *Chemical reviews.* 2011, **111:**5899-5921.

71. Buczynski MW, Dumlao DS, Dennis EA. Thematic review series: proteomics. An integrated omics analysis of eicosanoid biology. *J. Lipid Res.* 2009, **50:**1015-1038.

72. Funk CD. Prostaglandins and leukotrienes: advances in eicosanoid biology. *Science*. 2001, **294:**1871-1875.

73. Granstrom E. The arachidonic acid cascade. The prostaglandins, thromboxanes and leukotrienes. *Inflammation,* 1984, **8:**S15–S25.

74. AOCS. The AOCS Lipid Library. 2014. Available at: http://lipidlibrary.aocs.org/. Accessed 4/25/14.

75. Siegel G, Ermilov E. Omega-3 fatty acids: benefits for cardio-cerebro-vascular diseases *Atherosclerosis*. 2012, **225:**291-295.

76. Horrobin DF. Low prevalences of coronary heart disease (CHD), psoriasis, asthma and rheumatoid arthritis in Eskimos: are they caused by high dietary intake of eicosapentaenoic acid (EPA), a genetic variation of essential fatty acid (EFA) metabolism or a combination of both? Med. *Hypotheses*, 1987, **22:**421-428.

77. Weylandt KH, Chiu CY, Gomolka B, Waechter SF, Wiedenmann B. Omega-3 fatty acids and their lipid mediators: towards an understanding of resolvin and protectin formation *Prostaglandins Other Lipid Mediat*. 2012, **97:**73-82.

78. Mozaffarian D, Wu JH. Omega-3 fatty acids and cardiovascular disease: effects on risk factors, molecular pathways, and clinical events. *J Am Coll Cardiol*. 2011, **58:**2047-2067.

79. Hooper L, Thompson RL, Harrison RA, Summerbell CD, Ness AR, Moore HJ, Worthington HV, Durrington PN, Higgins JP, Capps NE, Riemersma RA, Ebrahim SB, Davey Smith G. Risks and benefits of omega 3 fats for mortality, cardiovascular disease, and cancer: systematic review. *BMJ*. 2006, **332:**752-760.

80. Rangel-Huerta OD, Aguilera CM, Mesa MD, Gil A. Omega-3 long-chain polyunsaturated fatty acids supplementation on inflammatory biomakers: a systematic review of randomised clinical trials. *Br J Nutr*. 2012, **107 Suppl 2:**S159-170.

81. Kromhout D. Omega-3 fatty acids and coronary heart disease. The final verdict? *Curr Opin Lipidol*. 2012, **23:**554-559.

82. Leaf A, Xiao YF, Kang JX, Billman GE. Prevention of sudden cardiac death by n-3 polyunsaturated fatty acids. *Pharmacol Ther*. 2003, **98:**355-377.

83. Chowdhury R, Stevens S, Gorman D, Pan A, Warnakula S, Chowdhury S, Ward H, Johnson L, Crowe F, Hu FB, Franco OH. Association between fish consumption, long chain omega 3 fatty acids, and risk of cerebrovascular disease: systematic review and meta-analysis. *BMJ*. 2012, **345:**e6698.

84. van Marum RJ. Current and future therapy in Alzheimer's disease. *Fundam Clin Pharmacol*. 2008, **22:**265-274.

85. Kyle DJ, Schaefer E, Patton G, Beiser A. Low serum docosahexaenoic acid is a significant risk factor for Alzheimer's dementia. *Lipids*. 1999, **34 Suppl:**S245.

86. Conquer JA, Tierney MC, Zecevic J, Bettger WJ, Fisher RH. Fatty acid analysis of blood plasma of patients with Alzheimer's disease, other types of dementia, and cognitive impairment. *Lipids*. 2000, **35:**1305-1312.

87. Simopoulos AP. Evolutionary aspects of diet, the omega-6/omega-3 ratio and genetic variation: nutritional implications for chronic diseases. *Biomed. Pharmacother*. 2006, **60:**502-507.

88. Kiage JN, Merrill PD, Robinson CJ, Cao Y, Malik TA, Hundley BC, Lao P, Judd SE, Cushman M, Howard VJ, Kabagambe EK. Intake of trans fat and all-cause mortality in the Reasons for Geographical and Racial Differences in Stroke (REGARDS) cohort. *Am. J. Clin. Nutr*. 2013, **97:**1121-1128.

89. Rouzer CA, Marnett LJ. Mechanism of free radical oxygenation of polyunsaturated fatty acids by cyclooxygenases. *Chemical reviews.* 2003, **103:**2239-2304.

90. Garavito RM, Mulichak AM. The structure of mammalian cyclooxygenases. *Annu Rev Bioph Biom*. 2003, **32:**183-206.

91. Smith WL, Song I. The enzymology of prostaglandin endoperoxide H synthases-1 and -2. *Prostaglandins & other lipid mediators.* 2002, **68-69:**115-128.

92. Smith WL, Garavito RM, DeWitt DL. Prostaglandin endoperoxide H synthases (cyclooxygenases)-1 and -2. *J. Biol. Chem*. 1996, **271:**33157-33160.

93. Xiao G, Chen W, Kulmacz RJ. Comparison of structural stabilities of prostaglandin H synthase-1 and -2. *J. Biol. Chem.* 1998, **273:**6801-6811.

94. Smith WL, Urade Y, Jakobsson PJ. Enzymes of the Cyclooxygenase Pathways of Prostanoid Biosynthesis. *Chemical Reviews*. 2011, **111:**5821-5865.

95. Roth GJ, Siok CJ, Ozols J. Structural characteristics of prostaglandin synthetase from sheep vesicular gland. *J Biol Chem*. 1980, **255:**1301-1304.

96. Chen YN, Bienkowski MJ, Marnett LJ. Controlled tryptic digestion of prostaglandin H synthase. Characterization of protein fragments and enhanced rate of proteolysis of oxidatively inactivated enzyme. *J Biol Chem*. 1987, **262:**16892-16899.

97. Sirois J, Richards JS. Purification and characterization of a novel, distinct isoform of prostaglandin endoperoxide synthase induced by human chorionic gonadotropin in granulosa cells of rat preovulatory follicles. *J Biol Chem*. 1992, **267:**6382-6388.

98. Smith WL, DeWitt DL, Garavito RM. Cyclooxygenases: structural, cellular, and molecular biology. *Annu Rev Biochem*. 2000, **69:**145-182.

99. Smith WL. Nutritionally essential fatty acids and biologically indispensable cyclooxygenases. *Trends Biochem Sci*. 2008, **33:**27-37.

100. Mutoh M, Watanabe K, Kitamura T, Shoji Y, Takahashi M, Kawamori T, Tani K, Kobayashi M, Maruyama T, Kobayashi K, Ohuchida S, Sugimoto Y, Narumiya S, Sugimura T, Wakabayashi K. Involvement of prostaglandin E receptor subtype EP(4) in colon carcinogenesis. *Cancer research*. 2002, **62:**28-32.

101. Sonoshita M, Takaku K, Sasaki N, Sugimoto Y, Ushikubi F, Narumiya S, Oshima M, Taketo MM. Acceleration of intestinal polyposis through prostaglandin receptor EP2 in Apc (Delta 716) knockout mice. *Nat Med*. 2001, **7:**1048-1051.

102. Regan JW. EP2 and EP4 prostanoid receptor signaling. *Life sciences*. 2003, **74:**143-153.

103. Han S, Roman J. Suppression of prostaglandin E2 receptor subtype EP2 by PPARgamma ligands inhibits human lung carcinoma cell growth. *Biochem. Biophys. Res. Commun*. 2004, **314:**1093-1099.

104. Wang D, Wang H, Shi Q, Katkuri S, Walhi W, Desvergne B, Das SK, Dey SK, DuBois RN. Prostaglandin E(2) promotes colorectal adenoma growth via transactivation of the nuclear peroxisome proliferator-activated receptor delta. *Cancer Cell*. 2004, **6:**285-295.

105. Castellone MD, Teramoto H, Williams BO, Druey KM, Gutkind JS. Prostaglandin E2 promotes colon cancer cell growth through a Gs-axin-beta-catenin signaling axis. *Science.* 2005, **310:**1504-1510.

106. Brudvik KW, Paulsen JE, Aandahl EM, Roald B, Tasken K. Protein kinase A antagonist inhibits beta-catenin nuclear translocation, c-Myc and COX-2 expression and tumor promotion in Apc(Min/+) mice. *Mol cancer*. 2011, **10:**149.

107. Jansen SR, Holman R, Hedemann I, Frankes E, Elzinga CR, Timens W, Gosens R, de Bont ES, Schmidt M. Prostaglandin E2 promotes MYCN non-amplified neuroblastoma cell survival via beta-catenin stabilization. *J Cell Mol Med*. 2015, **19:**210-226.

108. Jansen SR, Poppinga WJ, de Jager W, Lezoualc'h F, Cheng X, Wieland T, Yarwood SJ, Gosens R, Schmidt M. Epac1 links prostaglandin E2 to β-catenin-dependent transcription during epithelial-to-mesenchymal transition. *Oncotarget*. 2016, **7:**46354-46370.

109. Kim ER, Chang DK. Colorectal cancer in inflammatory bowel disease: the risk, pathogenesis, prevention and diagnosis. *World J Gastroenterol*. 2014, **20:**9872-9881.

110. Xie J, Itzkowitz, SH. Cancer in inflammatory bowel disease. *World J Gastroenterol*. 2008, **14:**378-389.

111. Triantafillidis JK, Nasioulas, G, Kosmidis, PA. Colorectal cancer and inflammatory bowel disease: epidemiology, risk factors, mechanisms of carcinogenesis and prevention strategies. *Anticancer Research*. 2009, **29:**2727-2737.

112. Dommels YE, Haring MM, Keestra NG, Alink GM, van Bladeren PJ, van Ommen B. The role of cyclooxygenase in n-6 and n-3 polyunsaturated fatty acid mediated effects on cell proliferation, PGE2 synthesis and cytotoxicity in human colorectal carcinoma cell lines. *Carcinogenesis.* 2003, **24:**385-392.

113. Ferrández A, Prescott S, Burt RW. COX-2 and colorectal cancer. *Curr Pharm Des*. 2003, **9:**2229-2251.

114. Rahman M, Selvarajan K, Hasan MR, Chan AP, Jin C, Kim J, Chan SK, Le ND, Kim YB, Tai IT. Inhibition of COX-2 in colon cancer modulates tumor growth and MDR-1 expression to enhance tumor regression in therapy-refractory cancers in vivo. *Neoplasia*. 2012, **14:**624-633.

115. Brown JR, DuBois RN. COX-2: A Molecular Target for Colorectal Cancer Prevention. *J. Clin. Oncol*. 2005, **23:**2840-2855.

116. Elder DJE, Paraskeva C. COX-2 inhibitors for colorectal cancer. *Nature Medicine*. 1998, **4:**392-393.

117. Cha YI, DuBois RN. NSAIDs and cancer prevention: targets downstream of COX-2. *Annu Rev Med.* 2007, **58:**239-252.

118. Baron JA. Aspirin and NSAIDs for the prevention of colorectal cancer. *Recent results in cancer research. Fortschritte der Krebsforschung. Progres dans les recherches sur le cancer.* 2009, **181:**223-229.

119. Iwama T. NSAIDs and colorectal cancer prevention. *J gastroenterol*. 2009, **44 Suppl 19:**72-76.

120. North GL. Celecoxib as adjunctive therapy for treatment of colorectal cancer. *Ann Pharmacother*. 2001, **35:**1638-1643.

121. Tanwar L, Vaish V, Sanyal SN. Chemopreventive role of etoricoxib (MK-0663) in experimental colon cancer: induction of mitochondrial proapoptotic factors. *Eur J Cancer Prev*. 2010, **19:**280-287.

122. Ng K, Meyerhardt JA, Chan AT, Sato K, Chan JA, Niedzwiecki D, Saltz LB, Mayer RJ, Benson AB 3rd, Schaefer PL, Whittom R, Hantel A, Goldberg RM, Venook AP, Ogino S,

Giovannucci EL, Fuchs CS. Aspirin and COX-2 inhibitor use in patients with stage III colon cancer. *J Natl Cancer Inst*. 2014, **107:**345.

123. Moss JWE, Ramji DP. Nutraceutical therapies for atherosclerosis. *Nat. Rev. Cardiol*. 2016, **13:**513-532.

124. Takai S, Jin D, Kawashima H, Kimura M, Shiraishi-Tateishi A, Tanaka T, Kakutani S, Tanaka K, Kiso Y, Miyazaki M. Anti-atherosclerotic effects of dihomo-gamma-linolenic acid in ApoE-deficient mice. *J Atheroscler Thromb*. 2009, **16:**480-489.

125. Gardner HW. Oxygen radical chemistry of polyunsaturated fatty acids. *Free Radic. Biol. Med*. 1989, **7:**65-86.

126. Wagner BA, Buettner GR, Burns CP. Free radical-mediated lipid peroxidation in cells: Oxidizability is a function of cell lipid *bis*-allylic hydrogen content. *Biochem*. 1994, **33:**4449-4453.

127. Girotti AW. Mechanisms of lipid peroxidation. *Free Radic. Biol. Med*. 1985, **1:**87-95.

128. North JA, Spector AA, Buettner GR. Detection of lipid radicals by electron paramagnetic resonance spin trapping using intact cells enriched with polyunsaturated fatty acid. *J. Biol. Chem*. 1992, **267:**5743-5746.

129. Qian SY, Tomer KB, Yue GH, Guo Q, Kadiiska MB, Mason RP. Characterization of the initial carbon-centered pentadienyl radical and subsequent radicals in lipid peroxidation: Identification via on-line high performance liquid chromatography/electron spin resonance and mass spectrometry. *Free Radic. Biol. Med*. 2002, **33:**998-1009.

130. Qian SY, Yue GH, Tomer KB, Mason RP. Identification of all classes of spin trapped carbon-centered radicals in soybean lipoxygenase-dependent lipid peroxidation of ω-6 polyunsaturated fatty acids via LC/ESR, LC/MS, and tandem MS. *Free Radic. Biol. Med*. 2003, **34:**1017-1028.

131. Qian SY, Guo Q, Mason RP. Identification of spin trapped carbon-centered radicals in soybean lipoxygenase-dependent peroxidation of ω-3 polyunsaturated fatty acids by LC/ESR, LC/MS, and tandem MS. *Free Radic. Biol. Med*. 2003, **35:**33-44.

132. Yu Q, Shan Z, Ni K, Qian SY. LC/ESR/MS study of spin trapped carbon-centered radicals formed from in vitro lipoxygenase-catalyzed peroxidation of γ-linolenic acid. *Free Radic. Res*. 2008, **42:**442-455.

133. Shan Z, Yu Q, Purwaha P, Guo B, Qian SY. A combination study of spin-trapping, LC/ESR and LC/MS on carbon-centred radicals formed from lipoxygenase-catalysed peroxidation of eicosapentaenoic acid. *Free Radic. Res*. 2008, **43:**1-15.

134. Purwaha P, Gu Y, Kelavkar U, Kang JX, Law B, Wu E, Qian SY. LC/ESR/MS study of pH-dependent radical generation from 15-LOX-catalyzed DPA peroxidation. *Free Radic. Biol. Med*. 2011, **51:**1461-1470.

135. Xu Y, Gu Y, Qian SY. An Advanced Electron Spin Resonance (ESR) Spin-Trapping and LC/(ESR)/MS Technique for the Study of Lipid Peroxidation. *Int. J. Mol. Sci.* 2012, **13:**14648-14666.

136. Yu Q, Purwaha P, Ni K, Sun C, Mallik S, Qian SY. Characterization of novel radicals from COX-catalyzed arachidonic acid peroxidation. *Free Radic. Biol. Med*. 2009, **47:**568-576.

137. Xiao Y, Gu Y, Purwaha P, Ni K, Law B, Mallik S, Qian SY. Characterization of free radicals formed from COX-catalyzed DGLA peroxidation. *Free Radic. Biol. Med*. 2011, **50:**1163-1170.

138. Gu Y, Xu Y, Law B, Qian SY. The first characterization of free radicals formed from cellular COX-catalyzed peroxidation. *Free Radic Biol Med*. 2013, **57:**49-60.

139. Levin G, Duffin KL, Obukowicz MG, Hummert SL, Fujiwara H, Needleman P, Raz A. Differential metabolism of dihomo-gamma-linolenic acid and arachidonic acid by cyclo-oxygenase-1 and cyclo-oxygenase-2: implications for cellular synthesis of prostaglandin E1 and prostaglandin E2. *Biochem Jl*. 2002, **365:**489-496.

140. Fan Y, Chapkin RS. Mouse peritoneal macrophage prostaglandin E1 synthesis is altered by dietary c-linoleic acid. *J. Nutr*. 1992, **122:**1600-1606.

141. Rubin D, Laposata M. Regulation of agonist-induced prostaglandin E1 versus prostaglandin E2 production. *J. Biol. Chem*. 1991, **266:**23618-23623.

142. Behrouzian B, Buist PH. Fatty acid desaturation: variations on an oxidative theme. *Curr Opin Chem Biol*. 2002, **6:**577-582.

143. Los DA, Murata N: Structure and expression of fatty acid desaturases. *Biochim Biophys Acta*. 1998, **1394:**3-15.

144. Sperling P, Heinz E. Desaturases fused to their electron donor. *Eur J Lipid Sci Technol*. 2001, **103:**158-180.

145. Shanklin J, Cahoon EB: Desaturation and related modifications of fatty acids. *Annu Rev Plant Physiol Plant Mol Biol*. 1998, **49:**611-641.

146. Broadwater JA, Fox BG, Haas JA. The fundamental, versatile role of diiron enzymes in lipid metabolism. *Fett Lipid*. 1998, **100:**103-113.

147. Tocher DR, Leaver MJ, Hodgson PA. Recent advances in the biochemistry and molecular biology of fatty acyl desaturases. *Prog Lipid Res*. 1998, **37:**73-117.

148. Sperling P, Ternes P, Zank TK, Heinz E. The evolution of desaturases. *Prostaglandins Leukot Essent Fatty Acids*. 2003, **68:**73-95.

149. Fujiyama-Fujiwara Y, Umeda R, Igarashi O. Effects of sesamin and curcumin on delta 5-desaturation and chain elongation of polyunsaturated fatty acid metabolism in primary cultured rat hepatocytes. *J Nutr Sci Vitaminol (Tokyo)*. 1992, **38:**353-363.

150. Shimizu S, Jareonkitmongkol S, Kawashima H, Akimoto K, Yamada H. Inhibitory effect of curcumin on fatty acid desaturation in Mortierella alpina 1S-4 and rat liver microsomes. *Lipids*. 1992, **27:**509-512.

151. Shimizu S, Akimoto K, Shinmen Y, Kawashima H, Sugano M, Yamada H. Sesamin is a potent and specific inhibitor of delta 5 desaturase in polyunsaturated fatty acid biosynthesis. *Lipids*. 1991, **26:**512-516.

152. Obukowicz MG, Raz A, Pyla PD, Rico JG, Wendling JM, Needleman P. Identification and characterization of a novel delta6/delta5 fatty acid desaturase inhibitor as a potential anti-inflammatory agent. *Biochem Pharmacol*. 1998, **55:**1045-1058.

153. Obukowicz MG, Welsch DJ, Salsgiver WJ, Martin-Berger CL, Chinn KS, Duffin KL, Raz A, Needleman P. Novel, selective delta6 or delta5 fatty acid desaturase inhibitors as antiinflammatory agents in mice. *J Pharmacol Exp Ther*. 1998, **287:**157-166.

154. CellTiter 96® AQueous One Solution Cell Proliferation Assay System Technical Bulletin. Available at https://www.promega.com/resources/protocols/technical-bulletins/0/celltiter-96-aqueous-one-solution-cell-proliferation-assay-system-protocol/

155. Franken NA, Rodermond HM, Stap J, Haveman J, van Bree C. Clonogenic assay of cells in vitro. *Nat Protoc*. 2006, **1:**2315-2319.

156. Pozarowski P, Darzynkiewicz Z. Analysis of cell cycle by flow cytometry. *Methods Mol Biol*. 2004, **281:**301-311.

157. Vermes I, Haanen C, Steffens-Nakken H, Reutelingsperger C. A novel assay for apoptosis. Flow cytometric detection of phosphatidylserine expression on early apoptotic cells using fluorescein labelled Annexin V. *J Immunol Methods*. 1995, **184:**39-51.

158. Quehenberger O, Armando A, Dumlao D, Stephens DL, Dennis EA. Lipidomics analysis of essential fatty acids in macrophages. *Prostaglandins Leukot Essent Fatty Acids*. 2008, **79:**123-129.

159. Fantone JC, Marasco WA, Elgas LJ, Ward PA. Anti-inflammatory effects of prostaglandin E1: in vivo modulation of the formyl peptide chemotactic receptor on the rat neutrophil. *J Immunol*. 1983, **130:**1495-1497.

160. Ellis LM, Copeland EM, Bland KI, Sitren HS. Inhibition of tumor growth and metastasis by chronic intravenous infusion of prostaglandin E1. *Annals of Surgery*. 1990, **212:**45-50.

161. Kornberg A, Witt U, Kornberg J, Friess H, Thrum K. Treating ischaemia-reperfusion injury with prostaglandin E1 reduces the risk of early hepatocellular carcinoma recurrence following liver transplantation. *Aliment Pharmacol Ther*. 2015, **42:**1101-1110.

162. Ikeguchi M, Maeta M, Kaibara N. Cisplatin combined with prostaglandin E1 chemotherapy in rat peritoneal carcinomatosis. *Int J Cancer*. 2000, **88:**474-478.

163. Xu Y, Qi J, Yang XY, Wu E, Qian SY. Free radical derivatives formed from COX-catalyzed DGLA peroxidation can attenuate colon cancer cell growth and enhance 5-FU's cytotoxicity. *Redox Biology*. 2014, **2:**610-618.

164. Xu Y, Yang XY, Zhao PJ, Yang ZY, Yan CH, Guo B, Qian SY. Knockdown of delta-5-desaturase promotes the anti-cancer activity of dihomo-γ-linolenic acid and enhances the efficacy of chemotherapy in colon cancer cells expressing COX-2. *Free Radic Biol Med*. 2016, **96:**67-77.

165. Abukhdeir AM, Park BH. p21 and p27: roles in carcinogenesis and drug resistance. *Expert reviews in molecular medicine*. 2008, **10:**e19.

166. Wong RS. Apoptosis in cancer: from pathogenesis to treatment. *J Exp Clin Cancer Res*. 2011, **30:**87.

167. Mehlen P, Puisieux A. Metastasis: a question of life or death. *Nature Reviews Cancer*, 2006, **6:**449-458.

168. Monteiro J, Fodde R. Cancer stemness and metastasis: therapeutic consequences and perspectives. *Eur. J. Cancer*. 2010, **46:**1198-1203.

169. Nguyen DX, Bos PD, Massague J. Metastasis: from dissemination to organ-specific colonization. *Nat. Rev. Cancer*. 2009, **9:**274-284.

170. Yang X, Xu Y, Wang T, Shu D, Guo P, Miskimins KW, Qian SY. Inhibition of cancer migration and invasion by knocking down delta-5-desaturase in COX-2 overexpressed cancer cells. *Redox Biol*. 2017, **11:**653-662.

171. Dong W, Li H, Zhang Y, Yang H, Guo M, Li L, Liu TG. Matrix metalloproteinase 2 promotes cell growth and invasion in colorectal cancer. *Acta Biochim Biophys Sin (Shanghai).* 2011, **43:**840-848.

172. Burg-Roderfeld M, Roderfeld M, Wagner S, Henkel C, Grötzinger J, Roeb E. MMP-9-hemopexin domain hampers adhesion and migration of colorectal cancer cells. *Int J Oncol*. 2007, **30:**985-992.

173. Mariadason JM. HDACs and HDAC inhibitors in colon cancer. *Epigenetics*. 2008, **3:**28-37.

174. Tampakis A, Tampaki EC, Nebiker CA, Kouraklis G. Histone deacetylase inhibitors and colorectal cancer: what is new? *Anticancer Agents Med Chem*. 2014, **14:**1220-1227.

175. Lee JC, Maa MC, Yu HS, Wang JH, Yen CK, Wang ST, Chen YJ, Liu Y, Jin YT, Leu TH. Butyrate regulates the expression of c-Src and focal adhesion kinase and inhibits cell invasion of human colon cancer cells. *Mol Carcinog*. 2005, **43:**207-214.

176. Steliou K, Boosalis MS, Perrine SP, Sangerman J, Faller DV. Butyrate histone deacetylase inhibitors. *Biores Open Access*. 2012, **1:**192-198.

177. Davie JR. Inhibition of histone deacetylase activity by butyrate. *J Nutr*. 2003, **133(7 Suppl)**:2485S-2493S.

178. Krämer OH, Zhu P, Ostendorff HP, Golebiewski M, Tiefenbach J, Peters MA, Brill B, Groner B, Bach I, Heinzel T, Göttlicher M.. The histone deacetylase inhibitor valproic acid selectively induces proteasomal degradation of HDAC2. *EMBO J*. 2003, **22:**3411-3420.

179. Chen JS, Faller DV, Spanjaard RA. Short-chain fatty acid inhibitors of histone deacetylases: promising anticancer therapeutics? *Curr Cancer Drug Targets*. 2003, **3:**219-236.

180. Venkataramani V, Rossner C, Iffland L, Schweyer S, Tamboli IY, Walter J, Wirths O, Bayer TA. Histone Deacetylase Inhibitor Valproic Acid Inhibits Cancer Cell Proliferation via Down-regulation of the Alzheimer Amyloid Precursor Protein. *J. Biol. Chem*. 2010, **285:**10678-10689.

181. Brodie SA, Brandes JC. Could valproic acid be an effective anticancer agent? The evidence so far. *Expert review of anticancer therapy*. 2014, **14:**1097-1100.

182. Chen X, Wong P, Radany E, Wong JYC. HDAC Inhibitor, valproic acid, induces p53-dependent radiosensitization of colon cancer cells. *Cancer Biotherapy & Radiopharmaceuticals*. 2009, **24:**689-699.

183. Gilbert KM, DeLoose A, Valentine JL, Fifer EK. Structure-activity relationship between carboxylic acids and T cell cycle blockade. *Life Sci*. 2006, **78:**2159-2165.

184. Li Y, Li X Guo B. Chemopreventive agent 3,3'-diindolylmethane selectively induces proteasomal degradation of class I histone deacetylases. *Cancer Res*. 2010, **70:**646-654.

185. Lee JH, Choy ML, Ngo L, Foster SS, Marks PA. Histone deacetylase inhibitor induces DNA damage, which normal but not transformed cells can repair. *PNAS*. 2010, **107:**14639-14644.

186. Longley DB, Johnston PG. Molecular mechanisms of drug resistance. *J. Pathol*. 2005, **205:**275-292.

187. Zhang N, Yin Y, Xu SJ, Chen WS. 5-Fluorouracil: mechanisms of resistance and reversal strategies. *Molecules*. 2008, **13:**1551-1569.

188. Réti A. Application of non-steroidal anti-inflammatory drugs to enhance 5-fluorouracil efficacy in experimental systems. *Magy Onkol*. 2010, **54:**377-381,

189. Gasparini G, Gattuso D, Morabito A, Longo R, Torino F, Sarmiento R, Vitale S, Gamucci T, Mariani L. Combined therapy with weekly irinotecan, infusional 5-fluorouracil and the selective COX-2 inhibitor rofecoxib is a safe and effective second-line treatment in metastatic colorectal cancer. *Oncologist*. 2005, **10:**710-717.

190. Réti A, Barna G, Pap E, Adleff V, L Komlósi V, Jeney A, Kralovánszky J, Budai B. Enhancement of 5-fluorouracil efficacy on high COX-2 expressing HCA-7 cells by low dose indomethacin and NS-398 but not on low COX-2 expressing HT-29 cells. *Pathol Oncol Res*. 2009, **15:**335-344.

191. Adeyemo D, Imtiaz F, Toffa S, Lowdell M, Wickremasinghe RG, Winslet M. Antioxidants enhance the susceptibility of colon carcinoma cells to 5-fluorouracil by augmenting the induction of the bax protein. *Cancer Lett*. 2001, **164:**77-84.

192. Jordan A, Stein J. Effect of an omega-3 fatty acid containing lipid emulsion alone and in combination with 5-fluorouracil (5-FU) on growth of the colon cancer cell line Caco-2. *Eur J Nutr*. 2003, **42:**324-331.

193. Rani I, Sharma B, Kumar S, Kaur S, Agnihotri N. Apoptosis mediated chemosensitization of tumor cells to 5-fluorouracil on supplementation of fish oil in experimental colon carcinoma. *Tumour Biol*. 2017, **39:**1010428317695019.

194. Rani I, Vaiphei K, Agnihotri N. Supplementation of fish oil augments efficacy and attenuates toxicity of 5-fluorouracil in 1,2-dimethylhydrazine dihydrochloride/dextran sulfate sodium-induced colon carcinogenesis. *Cancer Chemother Pharmacol.* 2014, **74:**309-322.

195. Tabolacci C, Lentini A, Provenzano B, Gismondi A, Rossi S, Beninati S. Similar anti neoplastic effects of nimesulide, a selective COX-2 inhibitor, and prostaglandin E1on B16 F10 murine melanoma cells. *MelanomaRes*. 2010, **20:**273-279.

196. Guo X, Goessl E, Jin G, Collie-Duguid ES, Cassidy J, Wang W, O'Brien V. Cell cycle perturbation and acquired 5-fluorouracil chemoresistance. *Anticancer Res*. 2008, **28:**9-14.

197. Sun XX, Dai MS, Lu H. 5-fluorouracil activation of p53 involves an MDM2-ribosomal protein interaction. J. *Biol. Chem*. 2007, **282:** 8052-8059.

198. Thant AA, Wu Y, Lee J, Mishra DK, Garcia H, Koeffler HP, Vadgama JV. Role of caspases in 5-FU and selenium induced growth inhibition of colorectal cancer cells. *Anticancer Res*. 2008, **28:**3579-3592

199. Zhu P, Zhao N, Sheng D, Hou J, Hao C, Yang X, Zhu B, Zhang SS, Han ZP, Wei LX, and Zhang L. Inhibition of Growth and Metastasis of Colon Cancer by Delivering 5-Fluorouracil-loaded Pluronic P85 Copolymer Micelles. *Scientific Reports*. 2016, **6:**20896.

200. Shakibaei M, Kraehe P, Popper B, Shayan P, Goel A, Buhrmann C. Curcumin potentiates antitumor activity of 5-fluorouracil in a 3D alginate tumor microenvironment of colorectal cancer. *BMC Cancer*. 2015, **15:**250.

201. Iovieno A, Lambiase A, Moretti C, Perrella E, Bonini S. Therapeutic effect of topical 5-fluorouracil in conjunctival squamous carcinoma is associated with changes in matrix metalloproteinases and tissue inhibitor of metalloproteinases expression. *Cornea*. 2009, **28:**821-4.

202. Buhrmann C, Shayan P, Kraehe P, Popper B, Goel A, Shakibaei M. Resveratrol induces chemosensitization to 5-fluorouracil through up-regulation of intercellular junctions, Epithelial-to-mesenchymal transition and apoptosis in colorectal cancer. *Biochem Pharmacol*. 2015, **98:**51-68.

203. Liu CY, Lin HH, Tang MJ, Wang YK. Vimentin contributes to epithelial-mesenchymal transition cancer cell mechanics by mediating cytoskeletal organization and focal adhesion maturation. *Oncotarget*. 2015, **6:**15966-15983.

204. Lamouille S, Xu J, Derynck R. Molecular mechanisms of epithelial–mesenchymal transition. *Nat. Rev. Mol. Cell Biol*. 2014, **15:**178-196.

205. Tsanou E, Peschos D, Batistatou A, Charalabopoulos A, Charalabopoulos K. The E-cadherin adhesion molecule and colorectal cancer. A global literature approach. *Anticancer Res*. 2008, **28:**3815-3826.

206. Rudolf E, John S, Cervinka M. Irinotecan induces senescence and apoptosis in colonic cells in vitro. *Toxicol. Lett*. 2012, **214:**1-8

207. Thorn CF, Oshiro C, Marsh S, Hernandez-Boussard T, McLeod H, Klein TE, Altman RB. Doxorubicin pathways: pharmacodynamics and adverse effects. *Pharmacogenetics and Genomics*. 2011, **21:**440-446.

208. Schmieder R, Hoffmann J, Becker M, Bhargava A, Müller T, Kahmann N, Ellinghaus P, Adams R, Rosenthal A, Thierauch KH, Scholz A, Wilhelm SM, Zopf D. Regorafenib (BAY 73-4506): Antitumor and antimetastatic activities in preclinical models of colorectal cancer. *Int. J. Cancer*. 2014, **135:**1487-1496.

209. Mao Y, Keller ET, Garfield DH, Shen K, Wang J. Stroma Cells in Tumor Microenvironment and Breast Cancer. *Cancer Metastasis Rev*. 2013, **32:**303-315.

210. Mustafi R, Dougherty U, Shah H, Dehghan H, Gliksberg A, Wu J, Zhu H, Joseph L, Hart J, Dive C, Fichera A, Threadgill D, Bissonnette M. Both stromal cell and colonocyte epidermal growth factor receptors control HCT116 colon cancer cell growth in tumor xenografts. *Carcinogenesis*. 2012, **33:**1930-1939.

211. Information avaialble at https://www.jax.org/strain/007850

212. Scholzen T, Gerdes J. The Ki-67 protein: from the known and the unknown. *J. Cell Physiol*. 2000, **182:**311-322.

213. Sena P, Roncucci L, Marzona L, Mariani F, Maffei S, Manenti A, De Pol A. Altered expression of apoptosis biomarkers in human colorectal microadenomas. *Cancer Epidemiol Biomarkers Prev*. 2010, **19:**351-357.

214. Bressenot A, Marchal S, Bezdetnaya L, Garrier J, Guillemin F, Plénat F. Assessment of Apoptosis by Immunohistochemistry to Active Caspase-3, Active Caspase-7, or Cleaved PARP in Monolayer Cells and Spheroid and Subcutaneous Xenografts of Human Carcinoma. *J. Histochem. Cytochem*. 2009, **57:**289-300.

215. Nakanishi M, Rosenberg DW. Multifaceted roles of PGE2 in inflammation and cancer. *Semin Immunopathol*. 2013, **35:**123-137.

216. Kim JI, Lakshmikanthan V, Frilot N, Daaka Y. Prostaglandin E2 Promotes Lung Cancer Cell Migration Via EP4-βArrestin1-c-Src Signalsome. Molecular cancer research : *MCR*. 2010, **8:**569-577.

217. Lam JKW, Chow MYT, Zhang Y, Leung SWS. siRNA Versus miRNA as Therapeutics for Gene Silencing. *Mol Ther Nucleic Acids*. 2015, **4:**e252.

218. Kalac M, Scotto L, Marchi E, Amengual J, Seshan VE, Bhagat G, Ulahannan N, Leshchenko VV, Temkin AM, Parekh S, Tycko B, O'Connor OA. HDAC inhibitors and decitabine are highly synergistic and associated with unique gene-expression and epigenetic profiles in models of DLBCL. *Blood*. 2011, **118:**5506-5516.

219. Chen CH, Chen MC, Wang JC, Tsai AC, Chen CS, Liou JP, Pan SL, Teng CM. Synergistic interaction between the HDAC Inhibitor, MPT0E028, and sorafenib in liver cancer cells in vitro and in vivo. *Clin Cancer Res*. 2014, **20:**1274-1287.

220. Shu D, Moll WD, Deng Z, Mao C, Guo P. Bottom-up Assembly of RNA Arrays and Superstructures as Potential Parts in Nanotechnology. *Nano Lett*, 2004, **4:**1717-1723.

221. Jasinski D, Haque F, Binzel DW, Guo P. Advancement of the Emerging Field of RNA Nanotechnology. *ACS Nano*. 2017, **11:**1142-1164.

222. Li H, Lee T, Dziubla T, Pi F, Guo S, Xu J, Li C, Haque F, Liang XJ, Guo P. RNA as a stable polymer to build controllable and defined nanostructures for material and biomedical applications. *Nano Today*. 2015, **10:**631-655.

223. Shu D, Li H, Shu Y, Xiong G, Carson WE, Haque F, Xu R, Guo P. Systemic Delivery of Anti-miRNA for Suppression of Triple Negative Breast Cancer Utilizing RNA Nanotechnology. *ACS Nano*. 2015, **9:**9731-9740.

224. Khanna C, Hunter K. Modeling metastasis in vivo. *Carcinogenesis*, 2005, **26:**513-523.